UNIVERSIDAD NACIONAL AUTÓNOMA DE MÉXICO

FACULTAD DE QUÍMICA

"CARACTERIZACIÓN DE LA VÍA GLUTAMINOLÍTICA EN CÉLULAS TUMORALES AS-30D"

T E S I S

QUE PARA OBTENER EL TÍTULO DE

QUÍMICA FARMACÉUTICA BIÓLOGA

P R E S E N T A:

PAOLA ANGELA VITAL GONZÁLEZ

MÉXICO, D. F **2008**

Agradecimientos

Le doy gracias a mis padres Rocío y Federico porque gracias a su amor, esfuerzos y cuidados tuve la gran oportunidad de terminar este trabajo. Siempre estuvieron y estarán conmigo.

A mi hermano Federico, gracias por tu compañía, tu cariño y por todos los momentos compartidos.

A toda mi familia que en todo momento me apoyan y me impulsan para salir adelante, gracias por su cariño y su preocupación.

A mis compañeros y amigos, su amistad es algo muy valioso que me dejo la Universidad, gracias por su lealtad y su compañía. Agradezco a cada uno por los momentos que hicieron de mi estancia algo bueno y divertido.

Al Instituto Nacional de Cardiología, que me permitió realizar este trabajo en sus instalaciones. Agradezco a mi asesora y a cada una de las personas que colaboraron conmigo en el laboratorio y me ayudaron enormemente para estructurar esta tesis.

A la escuela que me formó como una profesionista, la Universidad Nacional Autónoma de México, gracias a todos los profesores por su dedicación, es un orgullo ser egresada de esta Institución.

A todas las personas que no mencioné pero que de alguna manera me ayudaron a concluir mis estudios y cumplir mis metas, que han estado presentes y mostraron interés a lo largo del camino.

Jurado asignado:

Presidente:	**Dr. Jesús Montiel Aguirre**
Vocal:	**M. en C. Elpidio García Ramírez**
Secretario:	**Dra. Sara Rodríguez Enríquez**
1er suplente	**Dr. Francisco Javier Plasencia de la Parra**
2do suplente	**Dra. Vanessa Maya Ampudia**

El presente trabajo se desarrolló en el Departamento de Bioquímica del Instituto Nacional de Cardiología "Ignacio Chávez"

Asesora:

_____

Dra. Sara Rodríguez Enríquez

Sustentante:

_____

Paola Angela Vital González

RESUMEN

La glutaminólisis es la vía de degradación de glutamina (gln) hasta lactato, en la cual el aminoácido entra a la mitocondria por medio de un transportador y forma glutamato (glut) en una reacción catalizada por la glutaminasa. El glutamato se desamina a α-cetoglutarato por la glutamato deshidrogenasa (GDH) y se transforma a malato el cual al ser expulsado de la mitocondria es utilizado por la enzima málica dependiente de $NADP^+$ para formar piruvato y posteriormente lactato. El transporte mitocondrial de gln y la actividad de la glutaminasa en células tumorales AS-30D es 3.5 y 5-10 veces mayor, respectivamente, que en células normales. Además, se ha demostrado que la glutaminasa tumoral es activada a concentraciones no-fisiológicas de fosfato. Sin embargo, el transportador de gln y la glutaminasa no se han caracterizado cinéticamente en condiciones óptimas y en el mismo tipo tumoral. Nuestro objetivo fue determinar los cambios en las velocidades de oxidación de la gln en mitocondrias de AS-30D medida como consumo de oxigeno y la actividad de las enzimas involucradas en dicha oxidación en presencia y ausencia de sus respectivos activadores en condiciones de velocidad máxima. En paralelo, los estudios se realizaron en un tipo celular no tumorigénico (hígado de rata).

El consumo de oxígeno con gln fue mayor en AS-30D que en hígado (49 ± 3 *vs* 17 ± 1 nanogramo átomo de oxígeno/min/mg de proteína respectivamente, n=3), al igual que la actividad de la glutaminasa (86 ± 8 *vs* 20 ± 4 nmol/min/mg de proteína, n=3). Con glut por el contrario el consumo de oxígeno y la actividad de la GDH fueron mayores en mitocondrias de hígado que en mitocondrias del tumor (124 ± 6 *vs* 28 ± 4 nanogramo átomo de oxígeno/min/mg de proteína y 1.4 ± 0.3 *vs* 0.7 ± 0.1 µmol/min/mg de proteína, respectivamente, n=3). Estos datos sugieren que la glutaminasa y el transportador de gln tumoral podrían ser los que favorecen la rápida oxidación del aminoácido en AS-30D. Se determinó la estimulación por fosfato y ambos tipos mitocondriales fueron sensibles al anión, sin embargo a 100 mM, la enzima de AS-30D aumentó su actividad 2.7 veces (de 29 a 80 nmol/min/mg de proteína), mientras que la de hígado aumentó 2.2 veces (de 5 a 11 nmol/min/mg de proteína). A pesar de que se ha sugerido una posible

estimulación de la glutaminasa por calcio (de 0.1 a 1 μM), la actividad no se modificó en ambos tipos de mitocondrias por el catión.

La aspartato aminotransferasa es otra enzima altamente activa en tumores cuyo sustrato es el glut. La actividad resultó ser 30% mayor en AS-30D que en hígado (4.5 y 3.3 μmol/min/mg de proteína respectivamente) lo cual sugiere que la síntesis de aspartato es mayor que la oxidación de glutamato por el ciclo de Krebs.

Con la intención de estimular al máximo el flujo del ciclo de Krebs, y por lo tanto la oxidación de gln, se midió el consumo de oxígeno mitocondrial en presencia de malato (0.3 mM), un sustrato poco oxidado por las mitocondrias no tumorales pero que impulsa la oxidación de intermediarios del ciclo de Krebs. Sin embargo, la respiración mitocondrial de AS-30D fue similar en presencia y en ausencia de malato exógeno (36 ± 2.5 y 34 ± 11 nanogramo átomo de oxígeno/min/mg de proteína, n=4).

Se descartó que la estimulación de la respiración sostenida por gln se debiera a que en AS-30D fuera mayor la cantidad de componentes de la fosforilación oxidativa, determinando la actividad de la citocromo c oxidasa y del complejo II de la cadena respiratoria (succinato deshidrogenasa). La actividad de la citocromo c oxidasa, fue 2 veces mayor en AS-30D (625 ± 33 y 362 ± 50 nanogramo átomo de oxígeno/min/mg proteína, respectivamente). La respiración sostenida por succinato, no fue diferente entre ambos tipos mitocondriales en el estado de máxima activación mitocondrial (estado 3) (264 ± 61 *vs* 243 ± 19 nanogramo átomo de oxígeno/min/mg de proteína en AS-30D e hígado, respectivamente, n=3), sugiriendo que la estimulación mitocondrial no se debe al complejo II.

El transporte de gln se midió por hinchamiento mitocondrial y resultó ser mayor en mitocondrias de hígado (0.78 vs. 0.34 UA/min/mg de proteína). Esta diferencia se puede explicar por el hecho de que las mitocondrias de AS-30D contienen más colesterol en la membrana mitocondrial aumentando su rigidez y por lo tanto limitando la actividad del transportador. Como conclusiones, el consumo de gln y la actividad de la glutaminasa se encuentran incrementadas en AS-30D. La actividad de la glutaminasa en AS-30D e hígado se activa a altas concentraciones de Pi, sin embargo, la glutaminasa de hígado no alcanza las velocidades máximas

obtenidas en AS-30D. Las mitocondrias de hígado oxidan preferentemente glut comparado con gln. Estos resultados confirman que las células tumorales de AS-30D requieren metabolitos mitocondriales para su acelerada duplicación celular.

ABREVIATURAS

ADP Adenin difosfato
AAT Aspartato Amino Transferasa
ATP Adenin trifosfato
COX Citocromo c oxidasa
CTRC Células tumorales de rápido crecimiento
DNA Ácido desoxirribonucleico
EM Enzima Málica
FMN Flavín-mononucleótido
Glut Glutamato
GDH Glutamato deshidrogenasa
Gln Glutamina
HK Hexocinasa
LDH Lactato deshidrogenasa
MDH Malato deshidrogenasa
PEP Fosfoenolpiruvato
PGM Fosfoglicerato mutasa
PFK-1 Fosfofructocinasa tipo 1
Pi Fosfato inorgánico
RNA Ácido ribonucleico
TMPD Tetrametilfenilendiamino

CARACTERIZACIÓN DE LA VÍA GLUTAMINOLÍTICA EN CÉLULAS TUMORALES AS-30D

CONTENIDO

CAPITULO IV. RESULTADOS

CAPÍTULO I
INTRODUCCIÓN

1.1 Metabolismo atípico de las células tumorales de rápido crecimiento.

Las células tumorales presentan modificaciones metabólicas importantes en comparación con las células normales de las cuales proceden (Tabla 1). Entre las células tumorales de rápido crecimiento (CTRC), llamadas así porque su desarrollo se lleva a cabo en horas o días, se encuentran los hepatomas de AS-30D, Ehrlich, Morris y Novikoff que se desarrollan en la cavidad peritoneal de roedor [1]. Los tumores considerados de bajo o mediano crecimiento se desarrollan en meses o años, como son algunos tumores sólidos. Como característica particular, las CTRC mantienen una actividad incrementada de glucólisis aún en presencia de altas concentraciones de oxígeno [2].

Los tumores humanos altamente metastásicos como el carcinoma mamario (MCF-7), el carcinoma cervicouterino y de ovario (HeLa, SiKa, SW756, 2774), el melanoma (Colo 829BL, HMCB), y el carcinoma de pulmón (DMS53), también son clasificadas como CTRC [1].

En la tabla 1 se comparan algunas de las vías metabólicas más relevantes en CTRC y células normales.

Tabla 1. Cambios en el metabolismo intermediario de las Células Tumorales de Rápido Crecimiento en comparación con las células normales.

Vías Metabólicas	**Célula normal** Hígado de rata	**Célula tumoral** AS-30D	**Ref**
Glucólisis (nmol/min/mg prot)	**2**	**21**	[3]
Respiración con glutamato	**54**	**62**	[4]
Respiración con β-hidroxibutirato	**25**	**18**	[5]
Respiración con acetoacetato	**12**	**44**	[5]
Cantidad de colesterol libre (µg/mg prot)	**1.9**	**8**	[6]
Actividad Enzimática (nmol/min/mg prot)			
Enzima málica citosólica	**4.8** Corazón de humano	**6.2** C 261*	[7]
Enzima málica mitocondrial	**<1**	**32**	[8]
Succinil CoA acetoacetil CoA transferasa	**8**	**334**	[4]
Transportadores (nmol/min/mg prot)			
Transporte de piruvato	**21**	**12** Ehrlich	[9]
Transporte mitocondrial de glutamina	**33** Hígado de rata **15** Riñón de rata	**52** Ehrlich	[10] [11]

Glutaminasa	**1** Hígado de rata **39** Linfocitos de humano	**73** MCF-7** **892** T24/83 **264** Ehrlich	[12-15]
Glutamato deshidrogenasa	**368**	**750** Ehrlich	[16]

*carcinoma humano de colon; **carcinoma humano de mama.

Las velocidades de respiración se reportan en (nanogramo atomo de oxigeno/min/mg proteina)

1.2 Metabolismo glicolítico en células tumorales

Las CTRC mantienen un flujo glicolítico elevado comparado con células normales (Tabla 1). Sin embargo, esta no es una característica exclusiva de las células tumorales ya que también las células de la mucosa intestinal, la médula renal y la retina presentan altas velocidades de glicólisis [1,17]. En células HeLa las 10 enzimas de la glucólisis se sobreexpresan de 2 a 7 veces, con excepción de la PGM y la LDH cuya sobreexpresión es 2 a 7 veces menor que en hepatocitos de rata [18]. Esta sobreexpresión enzimática puede ser inducida por oncogenes o factores de transcripción como son HIF-1α o Myc [18].

En el hepatoma AS-30D todas las enzimas glicolíticas se encuentran sobreexpresadas comparadas con hígado de rata, de dos a cuatro veces se sobreexpresan la hexosa-6-fosfato isomerasa, la aldolasa, la triosa-fosfato isomerasa, la gliceraldehído-3-fosfato deshidrogenasa, la fosfoglicerato cinasa, la fosfoglicerato mutasa, la enolasa y la lactato deshidrogenasa, de ocho a diez veces la piruvato cinasa y de 17 a 300 veces la hexocinasa (HK) y la fosfofructocinasa tipo 1 (PFK-1). Debido a esta diferencia en la sobreexpresión, no todos los tipos celulares se deben comparar de igual manera, en el caso de HeLa

la comparación con el tipo celular de origen (células epiteliales cervicouterinas) debe ser más riguroso con respecto al que se realice con AS-30D y hepatocitos [18].

En células normales la HK y la PFK-1 mantienen el control de la vía, a través de los activadores e inhibidores alostéricos, y precisamente en estas dos enzimas se ha demostrado la presencia de isoenzimas en células tumorales.

En células de mamífero existen 4 isoformas de la HK (HK-I, HK-II, HK-III y HK-IV o glucocinasa), la HK-I es la isoforma predominante en cerebro, glándula mamaria, riñón y retina [18], mientras que en tumores, músculo esquelético y adipocitos predomina la HK-II [19]. Esta isoforma se localiza adosada a la membrana externa mitocondrial y se le ha asociado funcionalmente al translocador ATP/ADP, lo cual sugiere que el ATP utilizado por la primera reacción de la glucólisis deriva de la fosforilación oxidativa [1].
En células de mamífero, la PFK-1 tiene 3 subunidades diferentes. En hígado y riñón, la subunidad L (liver) es la más abundante, en músculo esquelético predomina la subunidad M (muscle), las plaquetas tienen subunidades C y en cerebro están presentes los 3 tipos de subunidades. En diferentes tipos tumorales prevalecen las subunidades C y L [20]. Cada subunidad muestra diferentes propiedades cinéticas, la subunidad C tiene una baja sensibilidad al fosfoenolpiruvato (PEP), uno de sus inhibidores alostéricos [21].

En células normales la inhibición de la glicólisis por oxígeno (efecto Pasteur) es el resultado de la modulación de la hexocinasa, la PFK-I y la piruvato cinasa, por el aumento de inhibidores alostéricos productos de la fosforilación oxidativa (ATP, citrato). En células tumorales el efecto Pasteur esta disminuido en comparación con células normales porque algunas enzimas clave en el flujo glicolítico son poco sensibles a sus inhibidores fisiológicos, por ejemplo, el citrato no inhibe a la PFK-1 [18].

Otra razón por la cual los tumores presentan una glicólisis elevada es la inhibición parcial de la fosforilación oxidativa por la glucosa y otras hexosas exógenas. En AS-30D la glucosa fisiológica aumenta el flujo glicolítico y la concentración de hexosas fosforiladas mientras la concentración de ATP y Pi disminuyen; y el pH en el citosol se acidifica de 7.2 a 6.8, a este fenómeno se le conoce como efecto Crabtree [22]. La baja disponibilidad de Pi por el aumento en hexosas fosforiladas es limitante para que la mitocondria sintetice ATP y el medio ácido disminuye la actividad de enzimas sensibles al pH como la α-cetoglutarato deshidrogenasa [23] y el citocromo bc_1 (Complejo III de la cadena respiratoria) [24].

Aunque se ha propuesto que la velocidad de oxidación de metabolitos en células tumorales depende la disponibilidad de sustratos exógenos, es posible pensar que las alteraciones en las vías metabólicas sean el resultado de cambios transcripcionales, tal como sucede con la glucólisis. En varias CTRC la glutaminólisis es una vía altamente activa, lo cual coincide con la alta concentración de glutamina determinada en el líquido de ascítis. Sin embargo, no se ha determinado con precisión cual es, o son, los mecanismos involucrados en la estimulación de la biosíntesis de las enzimas glutaminolíticas.

1.3 Metabolismo oxidativo mitocondrial.

En células normales la síntesis de ATP ocurre por un mecanismo acoplado a la transferencia de electrones a través de la cadena respiratoria en un proceso llamado fosforilación oxidativa (figura 1). El piruvato que proviene de la glucólisis entra a la mitocondria y se oxida a acetil CoA, ácidos grasos y aminoácidos.

En algunos tipos tumorales (AS-30D y Ehrlich), el piruvato se descarboxila por la piruvato dehidrogenasa (PDH) para formar acetil-CoA, una fracción del acetil-CoA formado reacciona con un acetaldehído activado presente en tumores para producir diacetil, que al ser reducido utilizando NADH forma acetoina, este producto inhibe a la PDH, sin embargo la PDH no se encuentra permanentemente inhibida porque no todo el acetil-CoA se transforma en acetoina, la otra fracción se oxida en el ciclo de Krebs, por lo tanto la PDH también se activa por el AMP

mitocondrial. En tumores, la PDH se activa por AMP (0.5-1.0 mM), en AS-30D la concentración de este metabolito es de 0.6 a 3.3 mM, lo cual sugiere que la enzima se encuentra activa y cuenta con un mecanismo de regulación debido a que la síntesis de acetoina también se encuentra incrementada [26].

Dependiendo del metabolismo de cada tipo de célula tumoral, el ATP celular puede provenir de la glicólisis o de la fosforilación oxidativa. En la tabla 2 se muestran los valores del porcentaje de ATP que proviene de la mitocondria en diferentes tipos celulares [27].

Como se aprecia en la tabla 2, varios tipos tumorales dependen de la fosforilación oxidativa para realizar sus procesos celulares de alta demanda energética como síntesis de proteínas, ácidos nucleicos, fenómenos de transporte, etc. En nuestro grupo de trabajo se determinó que las células AS-30D producen más del 95% del ATP total a través de esta vía [5]. Por lo tanto estas células obtienen la mayor parte de su energía oxidando metabolitos mitocondriales [28].

Tabla 2. Contribución de ATP mitocondrial en células normales y tumorales.

	Producción de ATP (nmol/min/mg prot)		
	Fosforilación oxidativa	**Ghlucólisis**	**% ATP fosorilación oxidativa**
Células normales			
Hígado de ratón	4700	40	>99
Macrofagos de ratón	0.24	0.05	82
Eritrocitos de conejo	2*	2.74*	42
Células tumorales			
Morris 7793	3.6	0.02	99
AS-30D	36.1	0.75	98
Carcinoma de ovario	9.16	0.29	97
Melanoma	14.8	0.50	97
Carcinoma mamario	9.25	0.45	95
Ehrlich	2.75	1.30	68
Novikoff	0.36	0.64	36

* mmol/h/cel

Aunque se demostró por Parlo y Coleman que el hepatoma Morris 3924A expulsa el citrato formado a partir de piruvato hacia fuera de la mitocondria 4 veces más rápido que en mitocondrias de hígado, proponiendo un ciclo de Krebs incompleto y no funcional [9], en AS-30D Dietzen y Davis demostraron que las enzimas del ciclo de Krebs son funcionales y activas y oxidan al citrato de manera eficiente. Aunque el citrato si es oxidado por la mitocondria una fracción se expulsa al citosol (Figura 1), estimulando la síntesis de colesterol, triacilgliceridos y fosfolípidos [29].

La producción de ácidos grasos y colesterol en el hepatoma es mayor que en hígado (Tabla 1), en AS-30D la membrana mitocondrial tiene 4 veces más colesterol que las mitocondrias de hígado [6]. En Ehrlich también se determinó la

cantidad de equivalentes reductores transferidos desde el citosol a la matriz mitocondrial y fue similar a la observada en hepatocitos [30]. Por lo tanto, estos resultados sugieren que el hepatoma AS-30D depende del metabolismo mitocondrial para duplicarse.

1.4 Oxidación mitocondrial de glutamina.

La glutamina es un aminoácido que puede sintetizarse en el organismo a partir de valina, isoleucina o el ácido glutámico. La glutamina sintetasa cataliza la reacción de formación de glutamina a partir de glutamato [21]. Se le considera un aminoácido semi-esencial, ya que no se encuentra en el grupo de los esenciales, pero se convierte en esencial bajo ciertas condiciones como estrés, traumatismo, infección, entrenamiento intenso o cuando su consumo celular es mayor a su velocidad de síntesis [31].

La glutamina es un sustrato de la gluconeogénesis en hígado y riñón. En el ciclo de la urea, la glutamina provee del primer átomo de nitrógeno para la síntesis de urea a través de la glutaminasa. Además, en adipocitos la glutamina se utiliza como un precursor para la síntesis de lípidos y participa en la síntesis de proteínas como el resto de los aminoácidos [21].

La concentración de glutamina en el líquido de ascitis (fracción libre de células) en AS-30D es 4 mM y de 0.3 mM dentro de la célula lo cual sugiere que el metabolito es activamente degradado [5]. No se ha medido la concentración de glutamina dentro de la mitocondria en AS-30D.

La glutaminólisis se define como la degradación de glutamina hasta lactato (Figura 1) en células normales y tumorales, que involucra la participación de la mitocondria. Se ha reportado que en células tumorales esta vía se encuentra incrementada y la glutamina es el sustrato preferencial al igual que la glucosa en tumores. Nuestro grupo de trabajo ha encontrado que la proliferación de células tumorales AS-30D es mayor en un medio suplementado con glutamina (4 mM) comparado con un medio que solo contiene glucosa (25 mM) [5]. Como se

muestra en la tabla 1, se han reportado diferentes actividades para las enzimas que participan en la vía glutaminolítica que parece ser importante en el metabolismo energético del tumor. Por lo tanto nuestro objetivo fue caracterizar la parte inicial de la vía, la cual se compone por el transportador de glutamina, la glutaminasa y la glutamato deshidrogenasa.

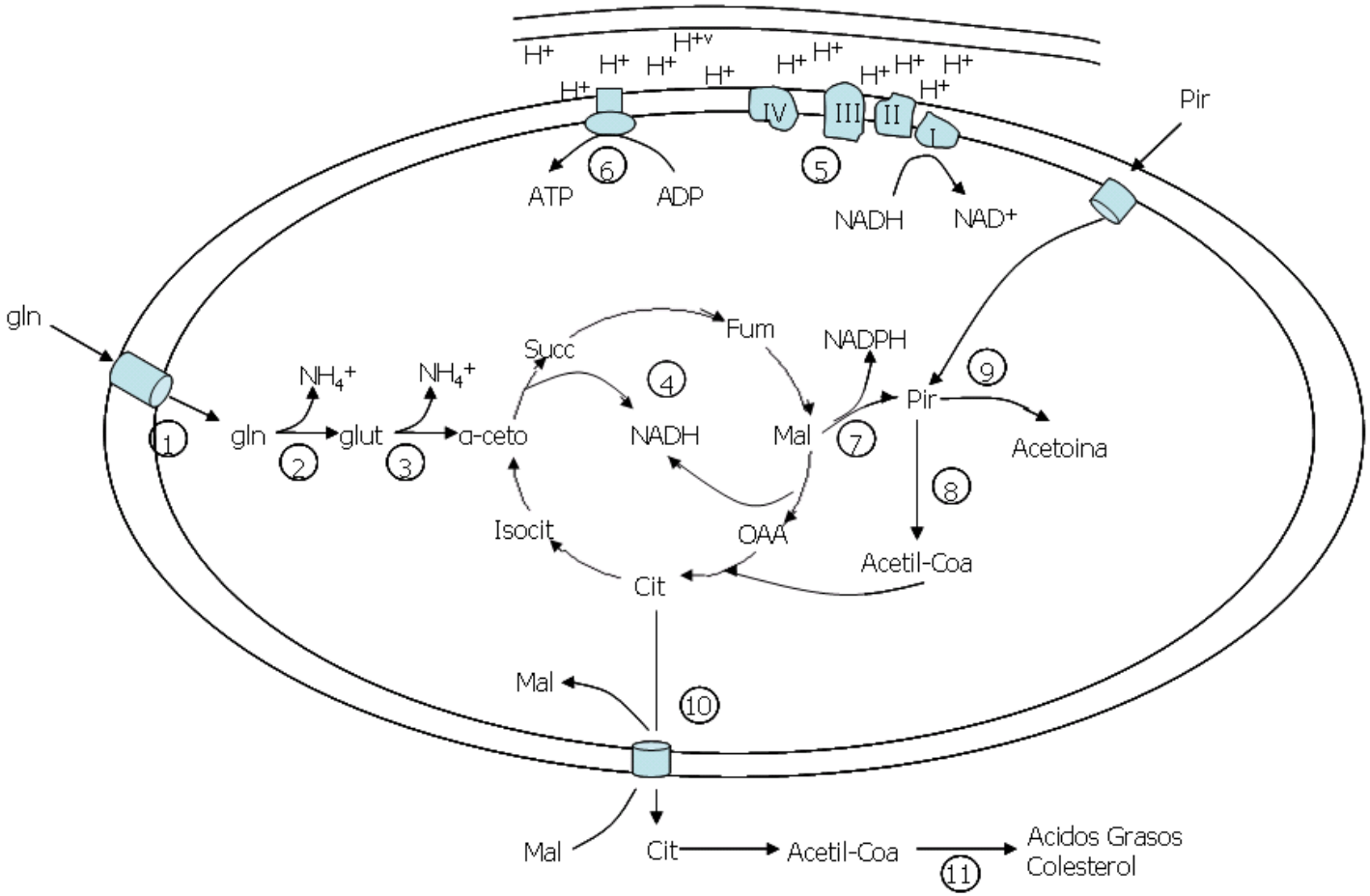

Figura 1. La glutamina (gln) entra a la mitocondria a través de su transportador; 2. Dentro de la mitocondria la glutaminasa cataliza la reacción de desaminación de la gln para formar glutamato (glut) y amonio; 3. El glut se desamina a α-cetoglutarato (α-ceto) por la glutamato deshidorgenasa (GDH); 4. El α-ceto es oxidado en el ciclo de Krebs para formar NADH; 5. El NADH se oxida a través de la cadena respiratoria y genera el gradiente de protones; 6. El complejo ATP sintasa genera ATP con el gradiente de protones, el ADP y el fosfato; 7. La enzima málica mitocondrial produce piruvato (Pir) a partir de malato (Mal); 8. El Pir como sustrato de la piruvato deshidrogenasa (PDH) genera Acetil-CoA y 9. posteriormente acetoina que inhibe a la PDH; 10. Una fracción del citrato generado en el ciclo de Krebs es expulsado de la mitocondria a través de un transportador que lo intercambia por malato; 11. El citrato expulsado de la mitocondria se utiliza para la síntesis de ácidos grasos y colesterol.

En células tumorales se ha descrito que la formación de piruvato a partir de glutamina por la glutaminólisis (Figura 1) requiere de algunas reacciones que no se reportan en mitocondrias de células normales, por ejemplo, la participación de la enzima málica dependiente de $NAD(P)^+$ mitocondrial tumoral que cataliza la oxidación de malato a piruvato. Por ello se ha determinado que la respiración en AS-30D aumenta cuando las células crecen en un medio enriquecido con 5mM de glutamina [16].

Analizando la velocidad de degradación de glutamina en hígado, se ha propuesto que el control de la vía lo ejerce la glutaminasa y el transportador de glutamina [32]. Por lo tanto la relevancia de llevar a cabo esta caracterización es que se propone que las diferencias en las enzimas que participan en la vía en mitocondrias tumorales y normales son significativas y esclarecen cuales vías energéticas son predominantes en el tumor. Sin embargo, los estudios son escasos donde las actividades de las enzimas tumorales se realicen en paralelo con las células normales.

1.5 Transporte citosólico y mitocondrial de glutamina.

Las células tumorales compiten con el hospedero por diversos sustratos. Cuando éstas compiten por glucosa, resulta una hipoglucemia progresiva para el hospedero. De la misma manera, las células tumorales compiten por compuestos nitrogenados, la alanina y la glutamina son ejemplos de los aminoácidos que utilizan las células tumorales para la síntesis de novo de metabolitos y para generar ATP.

Para ser utilizada, la glutamina debe ser transportada dentro de la célula y después al interior de la mitocondria. El primer proceso de transporte es a través de la membrana plasmática. La glutamina es un aminoácido neutro, el cual es transportado por los sistemas de transporte de aminoácidos: el dependiente de sodio (A) y el independiente de sodio (L) [33]. En algunos tejidos como hígado y riñón existe otro sistema específico para transportar glutamina, asparagina e histidina llamado sistema N, el cual pertenece al tipo acoplado a sodio [34]. En las

células tumorales por análisis cinético, se ha propuesto que predomina el transportador de gln acoplado a sodio [35, 36].

El transporte mitocondrial de gln es 1 o 2 veces más rápido que su transporte a través de la membrana plasmática [36]. El transportador mitocondrial de glutamina transporta al aminoácido por un mecanismo uniporte neutro. En mitocondrias de riñón se ha reportado que la velocidad máxima es de 300 nmol/min/mg de proteína [37]. En otro reporte se midió el transporte mitocondrial de glutamina en hígado y se encontró que el transporte es 5 veces mayor que la actividad de la glutaminasa [38].

En otro trabajo fue investigado el efecto del mersalil, un inhibidor del transporte de Pi, sobre la respiración desacoplada en mitocondrias de riñón de cerdo en presencia de glutamina y sobre la actividad de la glutaminasa [39]. Se encontró que el mersalil inhibe completamente la respiración desacoplada en presencia de glutamina, mientras que con glutamato no fue afectada. El mersalil también inhibió la activación de la glutaminasa en mitocondrias intactas solo en presencia de un desacoplante. Estos resultados sugieren que la activación de la enzima por Pi en mitocondrias ocurre sólo si el activador se mueve a través de la membrana interna mitocondrial.

1.6 La glutaminasa.

La glutaminasa cataliza la reacción de desaminación de la glutamina para formar glutamato y NH_4^+ como productos finales (Figura 2). La reacción llevada a cabo por la enzima consiste en la hidrólisis del enlace amida y la producción de amonio.

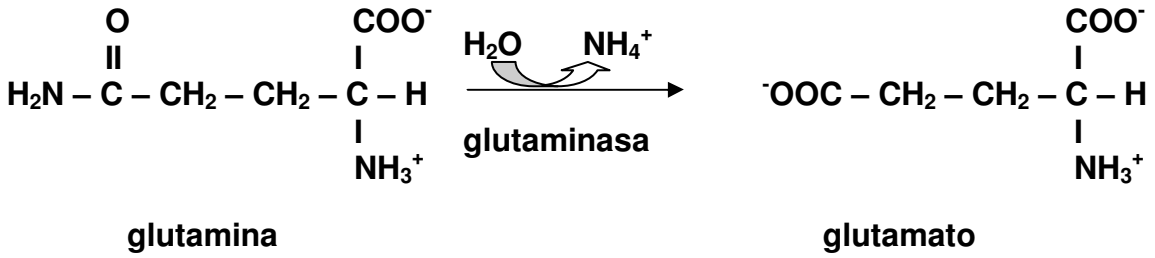

Figura 2. Reacción catalizada por la glutaminasa.

La actividad de la glutaminasa se ha cuantificado en diferentes tipos celulares tumorales y normales. Algunos de los valores reportados se muestran en la tabla 1. Los valores de la actividad de la glutaminasa para diferentes líneas tumorales oscilan de 80 hasta 800 nmol/min/mg proteína [12].

En células normales existen 2 isoformas para la glutaminasa: la tipo hígado y la tipo riñón. La isoenzima tipo hígado solo se expresa en tejido hepático adulto y la isoenzima tipo riñón en el resto de los tejidos. La glutaminasa puede encontrarse en forma de dímero o tetrámero, sin embargo hay una forma polimérica que contiene de diez a veinte subunidades. La forma dimérica es inactiva o tiene muy baja actividad en ausencia de Pi. Se ha sugerido que se requiere la tetramerización de la enzima para que esta sea activa, pero también se ha propuesto que la dimerización es secundaria a la activación. Los activadores que se conocen son el Pi, intermediarios del ciclo de Krebs (malato y citrato) y grupos acilo derivados de lípidos. Los principales inhibidores son los protones y el glutamato. El amonio, que es producto de la reacción, estimula la actividad de la enzima en cerebro e hígado de cerdo [13].

En Ehrlich la glutaminasa tumoral es muy sensible al tratamiento con detergentes como la digitonina/lubrol o el tritón X-100. También resultó ser inhibida por fosfolipasa A o C, lo que sugiere que la hidrólisis fosfolípidica puede modificar algunas interacciones lípido-proteína importantes para la función enzimática. Lo anterior puede explicarse debido a que la glutaminasa es una proteína periférica de la membrana interna mitocondrial, cuyo dominio funcional está orientado hacia la matriz y en donde residen algunos grupos tioles esenciales para su actividad [40].

El grupo de Nelson [41] demostró que la glutaminasa mitocondrial de corazón de rata aumenta su actividad enzimática en presencia de altas concentraciones de Pi exógeno (mayores a 20 mM) a pH 8. La disminución en el pH de 8.0 a 6.0 en las mismas condiciones anteriores disminuye 40% la actividad de la enzima. Otros cationes como Na^+ y K^+ no tuvieron efecto sobre la actividad de la enzima. Sin embargo el Ca^{2+} estimula la actividad de la glutaminasa a concentraciones entre 0.2 y 2.0 mM, pero inhibe a concentraciones más altas [21].

1.7 La glutamato deshidrogenasa (GDH).

La GDH cataliza la reacción de desaminación oxidativa de glutamato (glut) para formar α-cetoglutarato. La enzima utiliza como sustrato al NAD^+ o al $NADP^+$ (figura 3). La oxidación de glut ocurre con la transferencia de un ion hidruro del carbono-α del glutamato al $NAD(P)^+$ formando el α-iminoglutarato, que es hidrolizado a α-cetoglutarato y amonio.

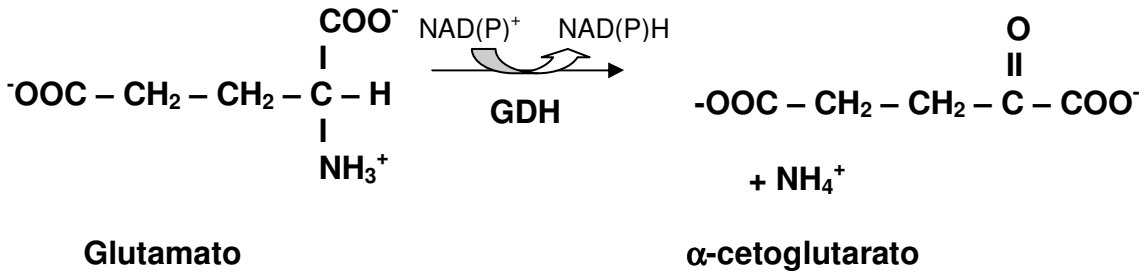

Figura 3. Reacción catalizada por la GDH.

El glutamato formado a partir de glutamina por la glutaminasa tiene dos vías de degradación, una de ellas consiste en formar aspartato y α-cetoglutarato a través de la aspartato aminotransferasa y la otra es producir α-cetoglutarato y NAD(P)H por la GDH (figura 1).

La adición de malato (2 mM) a mitocondrias aisladas de AS-30D y Ehrlich en presencia de glutamato o glutamina inhibe la formación de aspartato un 80%, sugiriendo que la oxidación de malato estimula el ciclo de Krebs a través de la activación de la GDH [42].

En mitocondrias de Ehrlich, se reportó que el glutamato se oxida preferentemente vía transaminación por isoenzimas mitocondriales de alanina y aspartato aminotransferasas, a pesar de que la glutamato deshidrogenasa presentó una actividad significativa. Cuando la glutamina o el glutamato fueron los únicos sustratos, la enzima málica mitocondrial no llevó a cabo la descarboxilación oxidativa del malato producido, mientras que el malato externo fue transportado dentro de la mitocondria y convertido principalmente en piruvato y CO_2 por la enzima málica [16].

Con estos antecedentes, se plantea que la glutamina es un sustrato importante en la célula tumoral y las enzimas involucradas en su metabolismo pueden considerarse blancos terapéuticos.

CAPÍTULO II

2.1 JUSTIFICACIÓN.

En presencia de glutamina más glucosa las células de AS-30D presentan una mayor proliferación comparada con glucosa. Se ha reportado una correlación entre un elevado consumo de oxígeno sensible a oligomicina y la actividad de proliferación tumoral en células crecidas en presencia de glutamina exógena. El hepatoma AS-30D depende 80% del ATP que proviene de la fosforilación oxidativa [7] por lo que requieren de una alta demanda de metabolitos mitocondriales para abastecer la energía requerida para su duplicación. Nosotros proponemos que la vía glutaminolítica provee gran parte de esta energía. A pesar de que se han realizado numerosos estudios sobre las enzimas que participan en la vía glutaminolítica, estos estudios no se han realizado en las mismas condiciones de estado estacionario y tampoco se realizaron de forma paralela en un tipo celular no tumorigénico.

2.2 HIPÓTESIS.

La vía glutaminolítica es más activa en mitocondrias de AS-30D comparada con hígado, debido a que el fenotipo tumoral induce aumento en la velocidad del transportador de glutamina, de la glutaminasa y de la glutamato deshidrogenasa.

2.3 OBJETIVO.

Determinar la velocidad de fosforilación oxidativa en presencia de glutamina en mitocondrias aisladas de AS-30D e hígado de rata y determinar la actividad enzimática del transportador de glutamina, la glutaminasa y la glutamato deshidrogenasa.

1. Determinar las variaciones en las actividades respiratorias (estado 3, estado 4, control respiratorio y ADP/O) en mitocondrias aisladas de AS-30D e hígado de rata a diferentes concentraciones de glutamina, glutamato y glutamina más malato.
2. Medir las velocidades máximas de la glutaminasa, la GDH, la aspartato aminotransferasa, el citocromo bC1 y la citocromo c oxidasa. Evaluar el efecto de activadores fisiológicos como Ca^{2+} y Pi sobre la glutaminasa.
3. Medir el transporte de glutamina en mitocondrias aisladas de AS-30D e hígado de rata con el método de hinchamiento mitocondrial.

CAPÍTULO III
MATERIAL Y MÉTODOS

Nuestro modelo experimental es el hepatoma de roedor AS-30D, catalogado en el grupo de las CTRC. Con este tipo de tumor se obtiene una alta biomasa en poco tiempo (7 días).

3.1 Obtención de células AS-30D por centrifugación diferencial.

Las células tumorales AS-30D (4-6 x 10^8 células/ml) se propagaron por inoculación intraperitoneal en ratas hembras cepa *Wistar* de 200-250 g de peso. Las ratas fueron alimentadas *ad libitum*. Los animales se sacrificaron por dislocación cervical para extraer el hepatoma cuyo volumen aumenta en la cavidad peritoneal como resultado del crecimiento del tumor, de 2mL hasta 40-60 mL totales.

3.2 Aislamiento de mitocondrias tumorales.

El hepatoma (células y líquido de ascitis) se centrifugó diferencialmente a 1600 rpm por 2 minutos a 4°C. El botón celular se resuspendió en medio NKT (NaCl 150 mM, KCl 5 mM, Tris/HCl 10 mM, pH 7.5) y se centrifugó a 1000-1200 rpm por 2 minutos a 4°C. Este procedimiento se repitió 3-4 veces hasta disminuir el contenido de eritrocitos a menos del 10%. Posteriormente, el botón celular se resuspendió en 25 ml de medio SHE (Sacarosa 220 mM, Hepes 10 mM, EGTA 1 mM, pH 7.3), y se centrifugó a 1600 rpm por 2 minutos más. El botón celular (30 mg/ml) se incubó en medio SHE con albúmina deslipidada (Calbiochem) a una concentración de 0.4% en hielo con agitación constante. La permeabilización de las células se realizó agregando digitonina (ICN) gota a gota a una concentración final de 12 µg/mg de proteína y se incubó en agitación constante durante 5 minutos a 4°C. El extracto celular se resuspendió con el mismo volumen de incubación de medio SHE frío y se centrifugó inmediatamente a 2500 rpm durante 5 minutos a 4°C para neutralizar el efecto de la digitonina. El botón celular se homogenizó suavemente con SHE recolectando el sobrenadante (SN) para

obtener las mitocondrias. Este mismo procedimiento se realizó 3 veces más, obteniéndose los SNs en cada centrifugación. Finalmente los SN se centrifugaron a 9500 rpm por 10 minutos a 4°C para recuperar el botón mitocondrial, el cual se incubó en 2 ml de SHE, albúmina (0.1%) y 1 mM de ADP por 10 minutos a 4°C [43]. Después de una centrifugación adicional a 9500 rpm, las mitocondrias se resuspendieron en SHE fresco y se determinó proteína por el método de biuret.

3.3 Aislamiento de mitocondrias de hígado de rata.

El hígado se extrajo de ratas hembras cepa *Wistar* de 250-300 g de peso. El tejido se homogenizó en 25 ml de medio SHE a 4°C y se centrifugó a 2500 rpm por 5 minutos a 4°C. El sobrenadante se centrifugó a 9500 rpm por 10 minutos a 4°C. El botón mitocondrial obtenido se resuspendió en 2 ml de SHE con 0.1% de albúmina deslipidada y 1 mM de ADP, se incubó por 10 minutos a 4°C y posteriormente se centrifugó a 9500 rpm por 10 minutos a 4°C [44]. El botón se resuspendió en 1 mL de SHE y se midió la cantidad de proteína por el método de biuret.

3.4 Consumo de oxígeno mitocondrial.

El consumo de oxígeno se determinó por método polarográfico con un electrodo tipo Clark. El medio de reacción fue 1.9 ml de KME (KCl 120 mM, Mops 20 mM, EGTA 0.5 mM, pH 7.2), 2 mg de proteína totales, K_2HPO_4 5 mM, sustrato (glutamina, malato, glutamina + malato, glutamato) a diferentes concentraciones (0.5-10 mM). Cuando se estableció la línea basal, se añadió 400-600 nmol de ADP para estimular el consumo de oxígeno y se calcularon los parámetros correspondientes (estado 3, estado 4, control respiratorio y ADP/O). El Estado 3 corresponde al consumo de oxígeno en presencia de ADP exógeno; el Estado 4 corresponde al consumo de oxígeno en ausencia de ADP. La relación Edo3/Edo4 corresponde al control respiratorio y el ADP/O corresponde a la cantidad de ATP sintetizada por molécula de oxígeno consumida.

3.5 Determinación de actividades enzimáticas.

Las mitocondrias se sometieron a un ciclo de congelamiento/descongelamiento con nitrógeno líquido para obtener extractos mitocondriales y medir las actividades enzimáticas.

3.5.1 Determinación de la glutaminasa.

La actividad de la glutaminasa se determinó en un medio con hidroxilamina 250 mM pH 8.0 más 1 mM de NAD^+, 0.5-30 mM de glutamina, GDH (1U), 2 µM de rotenona. En experimentos paralelos se evaluó el Pi (5-100 mM) y el Ca^{2+} (0.1-1 mM). La reacción se inició por la adición de mitocondrias (0.1 mg de proteína total). La actividad de la enzima se cuantificó midiendo la generación de NADH en un espectrofotómetro a 340 nm a 37°C.

3.5.2 Determinación de la glutamato deshidrogenasa.

La actividad de la GDH se determinó en un medio con trietanolamina pH 7.5 más 20 mM de NADH, 100 mM de sulfato de amonio, 10 mM de ADP, mitocondrias (0.1 mg de proteína total), 2 µM de rotenona y se inició la reacción con 20 mM de α-cetoglutarato. La actividad de la enzima se cuantificó midiendo la desaparición de NADH en un espectrofotómetro a 340 nm a 37°C.

3.5.3 Determinación de la aspartato aminotransferasa.

La actividad de la AAT se determinó en un medio con trietanolamina pH 7.4 más 20 mM de NADH, 50 mM de aspartato, malato deshidrogenasa (MDH, 17U), mitocondrias (0.03 mg proteína total), 2 µM de rotenona y se inició la reacción con 10 mM de □-cetoglutarato. La actividad de la enzima se cuantificó midiendo la desaparición de NADH en un espectrofotómetro a 340 nm a 37°C.

3.5.4 Determinación de la citocromo c oxidasa.

La actividad de la citocromo c oxidasa se determinó con un electrodo tipo Clark midiendo el consumo de oxígeno en KME a 30 ^{o}C y 37^{o}C. Como donador artificial de electrones se utilizó 3 mM de TMPD (Tetrametilfenilendiamino). La reacción se llevo a cabo en presencia de 5 mM de ascorbato, 0.5 µM de antimicina, 150 µg/ml de citocromo c de caballo y mitocondrias (0.25 mg de proteína total).

3.5.5 Determinación de la succinato deshidrogenasa (Complejo II).

La actividad del Complejo II se determinó midiendo el consumo de oxígeno con un electrodo tipo Clark en 1.9 ml de medio KME, adicionando como sustrato succinato 10 mM y rotenona 2µM, mitocondrias 1 mg, K_2HPO_4 5 mM y 200-400 nmol de ADP. La velocidad de respiración en presencia de succinato se interpretó como actividad del complejo II.

3.5.6 Determinación del transporte de glutamina.

El transporte de glutamina se determinó por la técnica espectrofotométrica de hinchamiento mitocondrial a 540 nm. El hinchamiento se realizó exponiendo a las mitocondrias (0.3 mM) a un medio isotónico preparado con gln (120 mM), a pH 7.3. El transporte se cuantificó como el cambió en la absorbancia por unidad de tiempo por mg de proteína.

CAPÍTULO IV
RESULTADOS

4.1 Determinación de la integridad mitocondrial del ascítis AS-30D e hígado.

En la tabla 3 se muestran los resultados de la integridad mitocondrial en células AS-30D e hígado de rata, la cual se comparó midiendo la respiración de las mitocondrias con sustratos endógenos y con sustratos cuya oxidación es muy eficiente en ambos tipos mitocondriales.

Las mitocondrias de hígado contienen mayor cantidad de sustratos endógenos debido a que su respiración fue 2 veces mayor comparada con AS-30D (Tabla 3).

Aunque el α-cetoglutarato estimuló al doble la respiración en estado 3 de AS-30D *vs* hígado, en ambos tipos mitocondriales se observó un aumento importante en el consumo de oxígeno (12 veces en AS-30D y 13 veces en hígado). Los controles respiratorios y el ADP/O obtenidos con el α-cetoglutarato fueron más altos que los obtenidos con glutamato y glutamina en ambas mitocondrias.

Tabla 3. Integridad de las preparaciones mitocondriales de AS-30D e hígado.

	Estado 3 (ngAO/min/mg)		Control Respiratorio	
	AS-30D	Hígado	AS-30D	Hígado
Sustratos endógenos	5.5 ± 2.6	10 ± 3.1*		
α-cetoglutarato	66	129	5.3	19
Glutamato	35	120	3.0	17
Glutamina	66	19	4.0	2

α-cetoglutarato 10 mM (AS-30D), 5 mM (hígado); Glutamato 10 mM; Glutamina 10 mM.

* *P < 0.5 versus AS-30D (n=3)*

4.2 Oxidación de glutamina en mitocondrias de tumor e hígado.

La glutamina exógena solo estimuló la actividad en Estado 3 en las mitocondrias de AS-30D manteniendo un control respiratorio alto. Mientras que en hígado no hubo una estimulación aparente inducida por este aminoácido. Sugiriendo que AS-30D tiene más activa la vía de oxidación de gln que hígado (Figura 4).

Este acelerado consumo de oxígeno en AS-30D fue el resultado de la elevada actividad de la glutaminasa tumoral ya que la velocidad máxima de la oxidación de glutamina fue 3 veces mayor en AS-30D que en hígado (49 ± 3 y 17 ± 1 ngAO/min/mg respectivamente). Sin embargo la Km por gln resultó ser mayor en mitocondrias de AS-30D (0.25 ± 0.01 *vs* 0.11 ± 0.01 mM), indicando que las mitocondrias de hígado tienen mayor afinidad a la glutamina (Tabla 3). El Estado 4, el control respiratorio y el ADP/O se mantienen constantes (Tabla 4), indicando que los cambios importantes se llevaron a cabo durante la activación del Estado 3 mitocondrial.

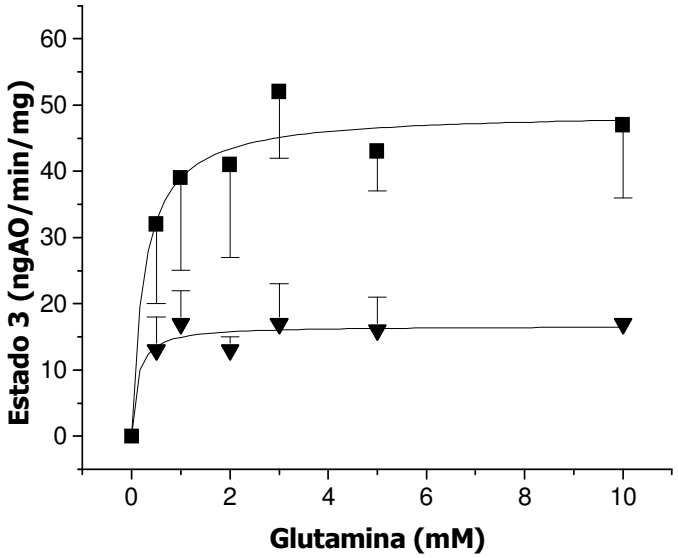

Figura 4. Estimulación de la respiración en estado 3 con glutamina en mitocondrias aisladas. ■ AS-30D ▼ hígado de rata (n = 3). Los datos representan la media ± D.E.

Tabla 4. Estimulación de la respiración en estado 4, control respiratorio y ADP/O con glutamina en mitocondrias aisladas de AS-30D e hígado de rata.

Glutamina (mM)	Estado 4 (ngAO/min/mg)		Control respiratorio		ADP/O	
	AS-30D	Hígado	AS-30D	Hígado	AS-30D	Hígado
0.5	17 ± 4	10 ± 1	1.8 ± 0.4	1.7 ± 0.4	2.7 ± 0.7	2.7 (2)
1.0	16 ± 5	11 ± 2	2.6±1.3	2 ± 0.2	2.6 ±0.7	2.9 ± 0.1
2.0	21 ± 5	11 (2)	1.9 ± 0.3	1.5 (2)	2.7 ± 0.9	2.7 ± 0.2
3.0	22 ± 9	10 ± 3	2.2 ± 0.6	1.3 ± 1.5	2.9 ± 0.3	3 ± 0.1
5.0	24 ± 6	13 ± 3	2 ± 0.1	1.5 ± 0.05	2.6 ± 0.7	2.6 ± 0.2
10.0	17 (2)	11 ± 4	2.5 (2)	2.1 (2)	2.6 (2)	2.5 (2)

Los valores representan el promedio ± D.E., n=3, excepto donde está indicado

4.3 Oxidación de glutamina en presencia de malato exógeno.

El malato es un sustrato fuertemente consumido por las mitocondrias tumorales debido a una alta actividad de glutaminasa, pero para garantizar la completa oxidación de glutamina a glutamato y posteriormente a α-cetoglutarato se empleo malato a bajas concentraciones para estimular el flujo de la glutamina y donde la activación de la enzima málica no fuera significativa (Figura 5).

En comparación con hígado, concentraciones mayores de 0.5 mM de malato estimularon la respiración mitocondrial de AS-30D indicando que la enzima málica se activa por su sustrato (Figura 5).

Por lo tanto para disminuir la participación de la enzima málica y garantizar la completa oxidación de glutamina, los experimentos se realizaron utilizando la concentración de malato de 0.3 mM.

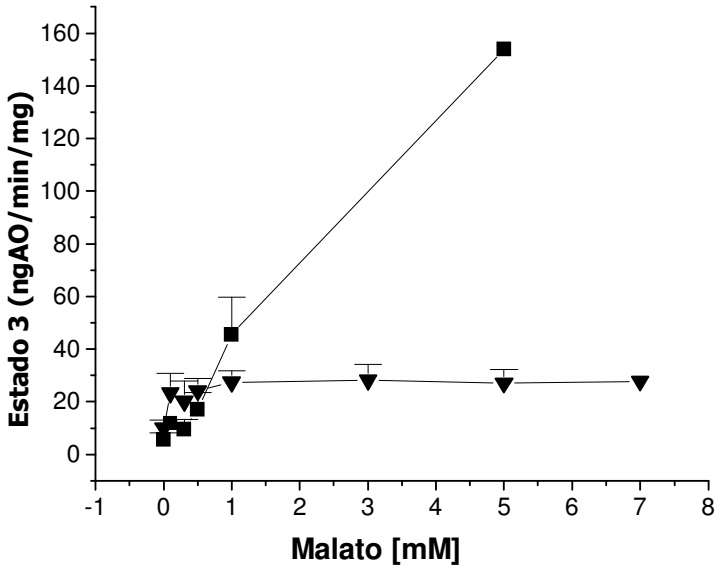

Figura 5. Aumento de la respiración en estado 3 con malato en mitocondrias aisladas de AS-30D e hígado de rata. ■ AS-30D (n = 3). ▼ Hígado (n = 4). Los datos representan la media ± D.E.

Cuando las mitocondrias de ambos tipos celulares se incubaron con glutamina más malato (0.3 mM), en AS-30D e hígado la velocidad máxima de respiración se mantuvo constante (Figura 6).

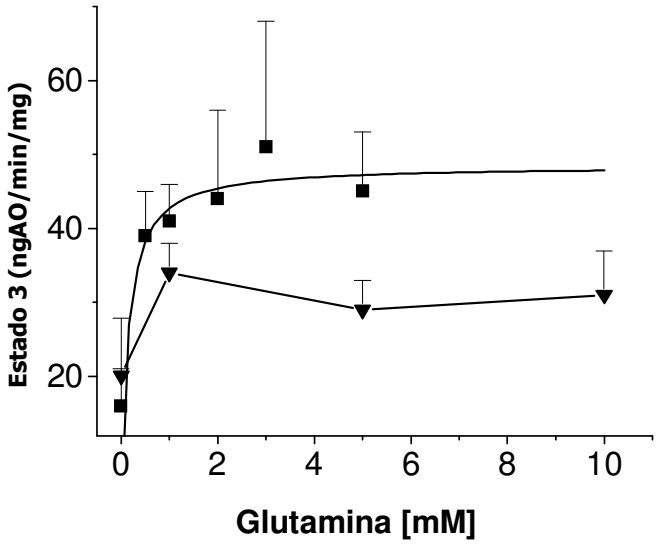

Figura 6. Aumento de la respiración en estado 3 con glutamina + malato 0.3 mM en mitocondrias aisladas.
■ AS-30D (n = 4) ▼ Hígado (n=3). Los datos representan la media ± D.E.

La parte inicial de la vía de oxidación de glutamina puede analizarse mejor si se disecta en cada uno de sus componentes. La oxidación de glutamina en mitocondrias aisladas de tumor o hígado implica la activación del transportador de glutamina, la glutaminasa y la GDH. Para determinar solo la participación de la GDH y del transportador de glutamato, las mitocondrias de ambos tipos celulares se expusieron a concentraciones crecientes de glutamato.

La respiración de mitocondrias de AS-30D en presencia de glutamato fue menor (57%) que la oxidación de glutamina. Al contrario, las mitocondrias de hígado oxidaron glutamato con mayor eficacia (7 veces) que con glutamina (Figura 7).

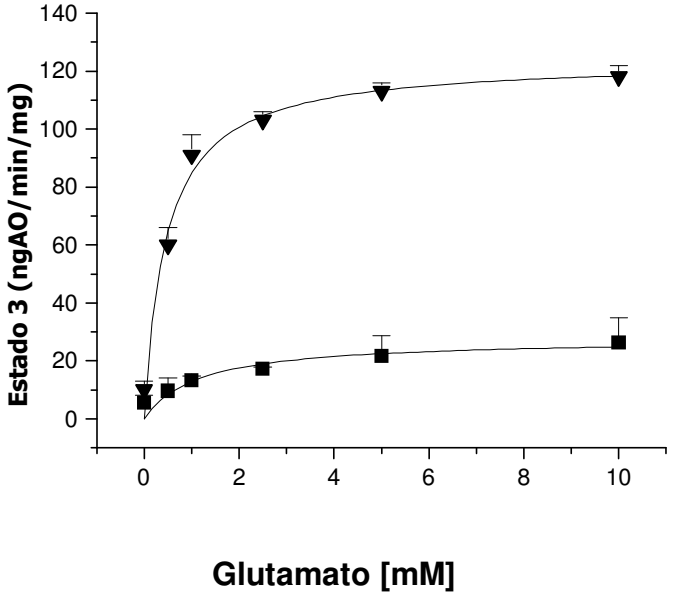

Figura 7. Aumento de la respiración en estado 3 con glutamato en mitocondrias aisladas de ■ AS-30D (n=3) e ▼ hígado de rata (n=3). Los datos representan la media ± D.E.

4.4 Determinación de actividad de citocoromo c oxidasa.

Para descartar que el aumento en la respiración se debe a que en mitocondrias tumorales hay mayor cantidad de complejos de la cadena respiratoria, se midió la actividad de la citocromo c oxidasa (COX) a temperatura fisiológica 37ºC. La actividad es mayor (1.7 veces) en AS-30D comparada con hígado (Tabla 5). A condiciones menos adversas para la preparación mitocondrial (30ºC), la COX fue más activa (1.3 veces) que hígado.

Tabla 5. Actividad de la citocromo c oxidasa en mitocondrias aisladas de AS-30D e hígado de rata.

Temperatura (ºC)	AS-30D (nmol/min/mg)	Hígado (nmol/min/mg)
30	390 ± 42*	281 ± 34
37	625 ± 33**	362 ± 50

** P < 0.05 versus hígado*

** P < 0.005 versus hígado*

Actividad sensible a azida mayor al 90%. n=3. Los datos representan la media ± D.E.

4.5 Determinación de la actividad de la Succinato deshidrogenasa.

Se midió la respiración mitocondrial con succinato (10 mM) más rotenona (2 µM) como indicativo indirecto de la actividad del complejo II o succinato deshidrogenasa (Tabla 6). La respiración mitocondrial en estado 3 y estado 4 estimulada por succinato resultó ser similar en ambos tipos celulares, por lo tanto, bajo estas condiciones los cambios en la actividad respiratoria no se deben a modificaciones en las actividades de otras enzimas mitocondriales.

Tabla 6. Respiración con succinato 10 mM en mitocondrias aisladas de AS-30D e hígado de rata.

	Estado 3 (ngAO/min/mg)	Estado 4 (ngAO/min/mg)	Control respiratorio	ADP/O
AS-30D	264 ± 61	108 ± 42	2.6 ± 0.5*	1.1 ± 0.1
Hígado	243 ± 19	18 ± 8	16 ± 10	1.3 ± 0.2

* *P < 0.025 versus hígado (n=3).* Los datos representan la media ± D.E.

4.6 Determinación de la actividad de la glutaminasa.

Los resultados obtenidos con glutamina, sugirieron que la glutaminasa podría ser la enzima clave en la oxidación de este sustrato. Por lo anterior, se comparó la actividad de la enzima en ambos tipos de mitocondrias. La glutaminasa del tumor resultó ser más rápida (4 veces) comparada con la enzima hepática (Figura 8). La gráfica se ajustó a un modelo Michaelis Menten con el programa Origin 5.0. La velocidad máxima para AS-30D fue de 86 ± 8 y en hígado 20 ± 4 nmol/min/mg y la Km fue 7 ± 2 y 5.8 ± 4 para AS-30D e hígado respectivamente. Lo cual significa que la enzima tumoral realiza su catálisis a mayor velocidad que la de hígado.

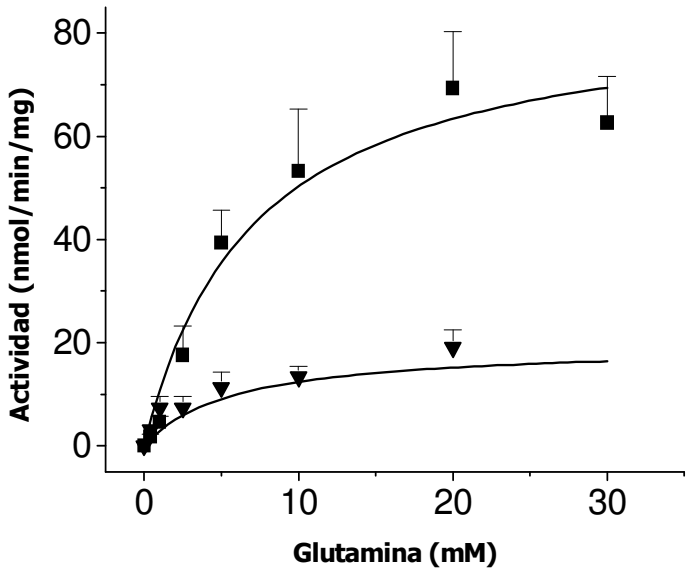

Figura 8. Actividad de la glutaminasa en mitocondrias aisladas de ■ AS-30D (n = 3) ▼ hígado de rata (n = 4). Los datos representan la media ± D.E.

En mitocondrias de corazón de rata, el calcio, el fosfato y el amonio son activadores de la glutaminasa. Para evaluar el efecto de estos activadores sobre la enzima tumoral y hepática medimos la actividad de la enzima a diferentes concentraciones de los mismos.

El efecto de Ca^{2+} a nivel fisiológico se evaluó incubando a las mitocondrias con diferentes buffers de Ca^{2+}/EGTA [45]. Las concentraciones de Ca^{2+} empleadas para la determinación de la activación fueron menores a 0.2 mM debido a que enzimas del ciclo de Krebs se activan a concentraciones micromolares. Sin embargo el Ca^{2+} no estimuló la actividad de la glutaminasa ni la respiración con glutamina en ambos tipos mitocondriales (Tabla 7). Por lo tanto se adicionaron concentraciones de Ca^{2+} mayores a 1 mM, para lo cual se prepararon buffers de Ca^{2+}/HEDTA, pero tampoco se observó un incremento en la actividad de la enzima.

Tabla 7. Efecto del Ca^{2+} sobre la respiración mitocondrial y actividad de glutaminasa en AS-30D.

	Estado 3 (ngAO/min/mg prot)	
Ca^{2+} (mM)	AS-30D	Hígado
0	33	35
0.063	42	28
0.072	38	36
0.087	42	36
0.115	45	35

	Actividad de la glutaminasa (nmol/min/mg prot)	
Ca^{2+} (mM)	AS-30D	Hígado
0	9.2 ± 3.1	2
0.18	8.5 ± 1.3	2
0.32	8.5 ± 2.3	2
0.52	7.8 ± 1.9	4
0.87	8.5 ± 2.9	0
1.1	5.2 ± 4.5	n.d.

Respiración mitocondrial AS-30D (n=2) e hígado (n=1) y glutaminasa AS-30D (n=3) e hígado (n=1).

El Ca^{2+} no estimuló la actividad de la glutaminasa bajo estas condiciones. Sin embargo, se ensayó el efecto del fosfato (Pi). Se ha reportado que 50 mM de Pi aumenta la actividad de la glutaminasa de corazón de rata. El fosfato fue un potente activador de la enzima tumoral y hepática. En el tumor la actividad de la glutaminasa aumentó 3 veces (de 29 ± 14 hasta 67 ± 9 nmol/min/mg prot) mientras que en hígado aumentó 2 veces (de 5 ± 1.7 hasta 11.6 ± 1.9 nmol/min/mg prot), a pesar de que ambos tipos mitocondriales fueron sensibles a Pi la actividad de la glutaminasa en hígado no llegó a la misma velocidad máxima que AS-30D (Figura 9).

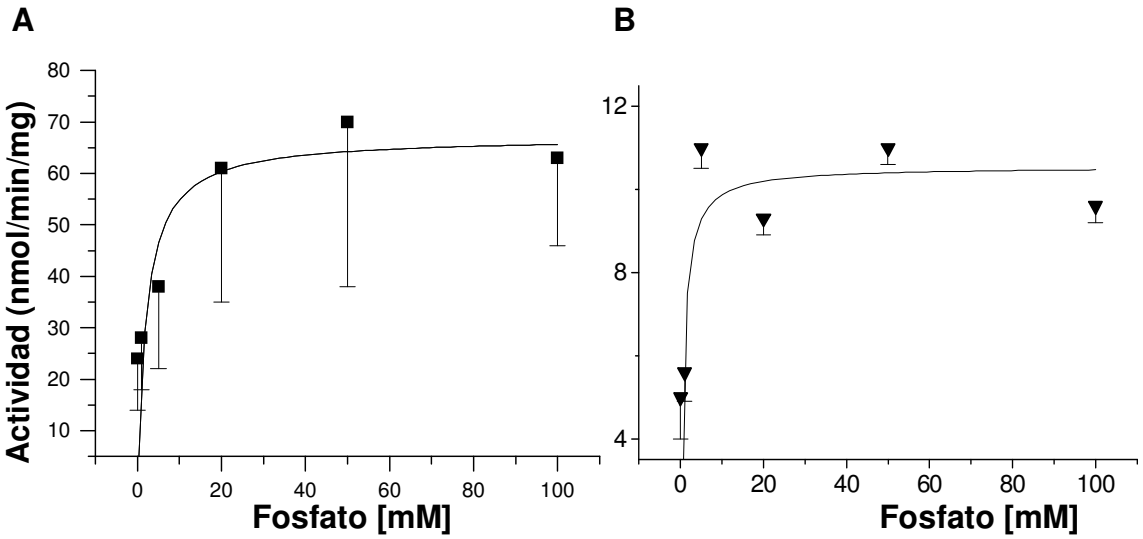

Figura 9. Estimulación de la glutaminasa por fosfato en mitocondrias aisladas. **A)** Actividad de la glutaminasa en AS-30D con glutamina 2.5 mM (n = 4) **B)** actividad de la glutaminasa en hígado con glutamina 5 mM (n = 4). Los datos representan la media ± D.E.

Para determinar si el Pi aumenta aún más la actividad de la enzima, se realizó la curva de activación a diferentes concentraciones de Pi en presencia de glutamina. La Km fue similar (7 mM con 100 mM de Pi y 4 mM en ausencia de Pi) pero la Vmax aumenta 2 veces de 86 a 155 nmol/min/mg con 100 mM de Pi (figura 10). Debido a que 100 mM de Pi no es una concentración fisiológica, se realizó el experimento con 3 mM de Pi que es la concentración fisiológica determinada en el citosol de AS-30D y a 20 mM de Pi, la concentración máxima de Pi que se puede encontrar fisiológicamente en un tejido. En la figura 10 se muestra que la velocidad máxima resultó ser la misma con 3 mM de Pi (133 y 144 nmol/min/mg con 3 mM de Pi y en ausencia de Pi respectivamente) y se incrementa un 28% con 20 mM de Pi (de 92 a 127 nmol/min/mg).

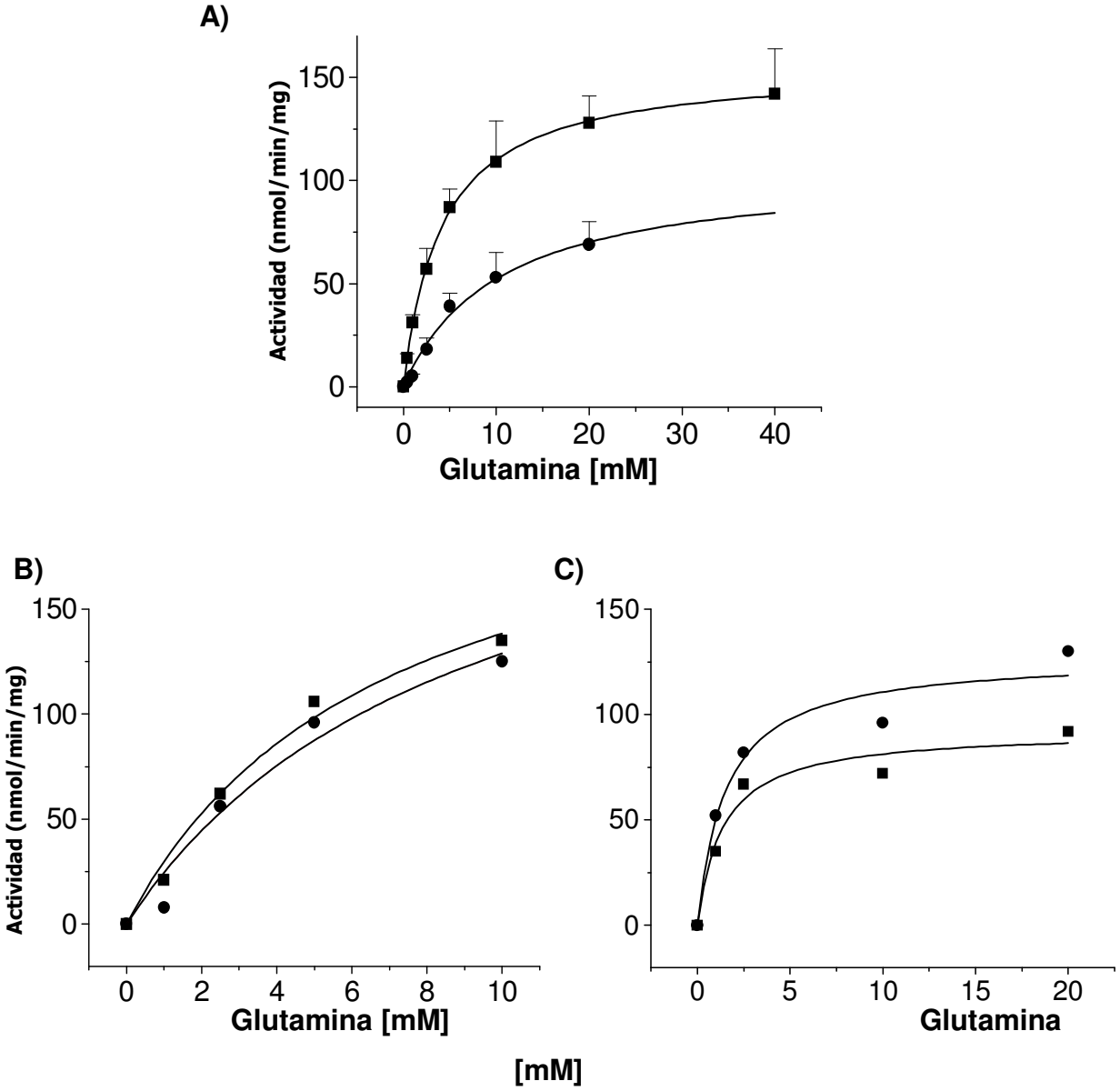

Figura 10. Estimulación de la glutaminasa por fosfato en mitocondrias de AS-30D. **A)** ● Pi 0 mM (n = 3) ■ Pi 100 mM(n = 3) **B)** ■ Pi 0 mM (n = 1) ● Pi 3 mM (n = 1) **C)** ■ Pi 0 mM (n = 1) ● Pi 20 mM (n = 1). Los datos representan la media ± D.E.

Por último se determinó el cambio en la actividad de la glutaminasa en función del pH de la glutaminasa en AS-30D e hígado. Para ambas el pH óptimo resulto ser alrededor de 9. La actividad de la enzima disminuyó 2.5 veces cuando el pH cambia a 7. La glutaminasa de hígado permanece inactiva a pH 7-8.7 (Figura 11).

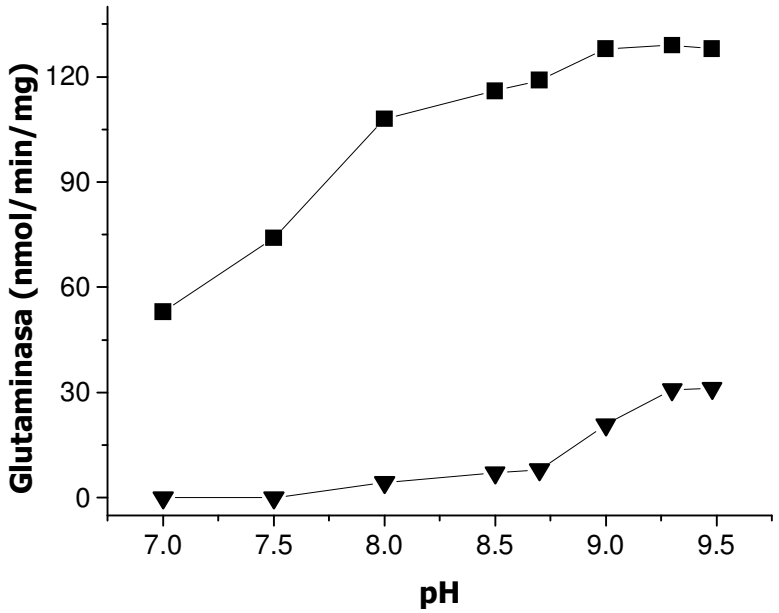

Figura 11. Cambio en la actividad de la glutaminasa en función del pH en mitocondrias aisladas de AS-30D (■) e hígado de rata (▼) (n = 1).

4.7 Determinación de la actividad de la glutamato deshidrogenasa.

Una vez caracterizada la glutaminasa, se determinó la actividad de la GDH en condiciones de estado estacionario en ambos tipos mitocondriales. La GDH mitocondrial de hígado fue 2 veces más rápida que la de AS-30D, como se muestra en la tabla 8. Estos resultados explican porqué las mitocondrias de hígado son más eficientes para consumir oxígeno con glutamato que AS-30D.

Tabla 8. Actividad de la glutamato deshidrogenasa en mitocondrias aisladas de AS-30D e hígado de rata.

	AS-30D	Hígado
GDH	0.73 ± 0.13*	1.37 ± 0.32

** P < 0.05 versus hígado (n=3).*

Actividad en µmol/min/mg prot.

Los datos representan la media ± D.E.

4.8 Determinación de la actividad de la aspartato aminotransferasa.

La respiración con glutamato fue menor que la obtenida con glutamina en AS-30D. Lo anterior sugirió que parte del glutamato puede ser oxidado a otro nivel, por lo tanto medimos la actividad de la aspartato aminotransferasa (AAT). La actividad de la enzima fue mayor en AS-30D (Tabla 9). En ambos tipos mitocondriales la AAT fue más rápida que la GDH.

Tabla 9. Actividad de la aspartato aminotransferasa (AAT) en mitocondrias aisladas de AS-30D e hígado de rata.

	AS-30D	Hígado
AAT	4.5 ± 0.9	3.3 ± 0.3

(n=3). Actividad medida en µmol/min/mg prot.

Los datos representan la media ± D.E.

4.9 Transporte mitocondrial de glutamina.

Se determinó el transporte de glutamina con la técnica de hinchamiento mitocondrial. El transporte de glutamina fue 2 veces más rápido en mitocondrias de hígado comparado con AS-30D, como se muestra en la figura 12.

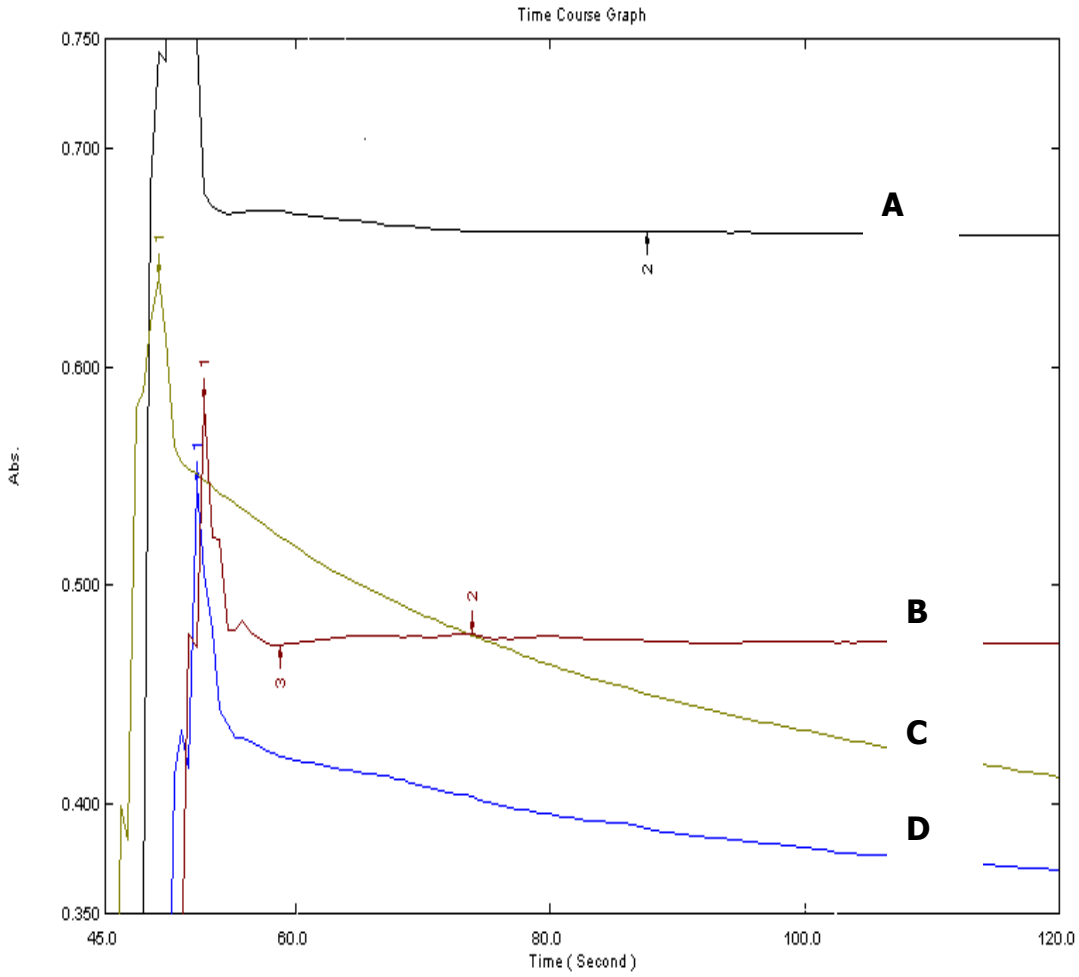

Figura 12. Hinchamiento mitocondrial con glutamina en mitocondrias aisladas de AS-30D e hígado de rata. **A)** mitocondrias de hígado. **B)** mitocondrias de AS-30D. **C)** mitocondrias de hígado + glutamina 120 mM. **D)** mitocondrias de AS-30D + glutamina 120 mM.

CAPÍTULO V
DISCUSIÓN

Ambos tipos mitocondriales son capaces de catabolizar la glutamina y otros sustratos mitocondriales como α-cetoglutarato, succinato y glutamato a alta velocidad. Estos resultados son muy similares a los reportados en mitocondrias de hígado por otros autores [12].

Observamos que en mitocondrias de hígado la respiración con glutamato aumenta con respecto a la de glutamina, y al medir las actividades enzimaticas, la velocidad máxima de la GDH es 7 veces mayor que la actividad de la glutaminasa, por lo tanto las mitocondrias de hígado oxidan preferentemente glutamato que glutamina.

La actividad de citocromo c oxidasa es 2 veces mayor en AS-30D a 37ºC y la actividad del complejo II resultó ser semejante en ambos tipos mitocondriales, de esta manera comprobamos que el aumento en la respiración con glutamina, que llega a ser hasta 3 veces mayor no se debe a que haya mayor cantidad de complejos de la cadena respiratoria.

La oxidación de malato permite que el ciclo de Krebs continúe y el α-cetoglutarato no alimente otra vía, incrementando el consumo de glutamina, sin embargo la adición de malato en hígado no alcanzó la velocidad máxima observada en AS-30D. Las mitocondrias de AS-30D oxidan completamente la glutamina hacia el ciclo de Krebs con o sin malato exógeno.

La respiración con glutamato en AS-30D resultó ser muy baja con respecto a la de glutamina, posiblemente por la insuficiencia en el transporte de glutamato o a una elevada actividad de la aspartato aminotransferasa, la cual produce α-cetoglutarato y aspartato a partir de glutamato y oxaloacetato. Al medir la

actividad de esta enzima, observamos que en ambos tipos mitocondriales la actividad es alta comparada con el resto de las enzimas medidas, por lo tanto el consumo de glutamato hacia la GDH o la AAT depende de la disponibilidad del oxaloacetato, que es otro de los sustratos de la AAT o a la actividad en el transporte de glutamato.

La adición de calcio exógeno no estimuló la actividad de la glutaminasa en ambos tipos mitocondriales, posiblemente se observe la activación a concentraciones más altas o en la enzima aislada.

El fosfato estimuló la actividad de la enzima en mitocondrias tumorales y de hígado, sin embargo la activación fue menor en hígado comparada con AS-30D a las mismas concentraciones de Pi (100 mM). Probablemente en AS-30D se favorece la estabilidad de la forma tetramérica de la enzima, la cual se ha propuesto que presenta mayor actividad en presencia del anión.

El transporte de glutamina es muy importante en tumores ya que la mayor parte del aminoácido proviene del hospedero, se midió el transporte de glutamina como hinchamiento mitocondrial, que es una manera indirecta de medir la entrada de glutamina en mitocondrias intactas, con esta técnica se mide el cambio en el tamaño de las mitocondrias como reflejo de la cantidad de sustrato que esta entrando. Obtuvimos un resultado diferente al que se esperaba, ya que el transporte resultó ser mayor en hígado que en AS-30D, atribuimos este resultado a diferencias en la composición de la membrana mitocondrial entre ambos tipos celulares, se ha reportado que las mitocondrias de AS-30D contienen más colesterol que las de hígado (8 y 1.9 µg/mg de proteína respectivamente), por lo tanto en AS-30D hay mayor rigidez en la membrana y eso puede afectar los resultados empleando este tipo de técnica, es necesario medir el transporte específicamente con glutamina radiactiva y descartando la actividad de la glutaminasa.

CAPÍTULO VI
CONCLUSIONES

- Las mitocondrias de AS-30D oxidan preferentemente glutamina, mientras que las de hígado oxidan glutamato.

- El consumo de glutamina y la actividad de la glutaminasa se encuentran incrementadas en AS-30D comparadas con hígado.

- La glutaminasa de AS-30D e hígado se activa a altas concentraciones de fosfato (20-100 mM), sin embargo la actividad de la enzima en hígado no alcanza las velocidades máximas obtenidas en AS-30D.

- La glutaminasa de AS-30D e hígado no se activó con calcio a concentraciones entre 0.1-1.0 mM.

- El transporte de glutamina resultó ser mayor en hígado comparado con AS-30D empleando la técnica de hinchamiento mitocondrial.

- Las actividades de todas las enzimas medidas son parecidas a las reportadas por otros grupos de trabajo.

REFERENCIAS

1. Pedersen PL. Tumor Mitochondria and the Bioenergetics of Cancer Cells. Prog. Exp. Tumor Res. (1978) 22, 190-274.
2. Rodríguez-Enríquez S. and Moreno-Sánchez R. Intermediary Metabolism of Fast-Growth Tumor Cells. Arch Med Res.(1997) 29, 1-12.
3. Marín-Hernández A., Rodríguez-Enríquez S., Vital-González P., Flores-Rodríguez F., Macías-Silva M., Sosa-Garrocho M. and Moreno-Sánchez. R. Determining and understanding the control of glycolysis in fast-growth tumor cells. FEBS J. (2006) 273, 1975-1988.
4. Briscoe DA., Fiskum G., Holleran AL. and Kelleher JK. Acetoacetate metabolism in AS-30D hepatoma cells. Mol. Cell. Biochem. (1994) 136, 131-137.
5. Rodríguez-Enríquez S., Torres-Márquez ME. and Moreno-Sánchez R. Substrate Oxidation and ATP Supply in AS-30D Hepatoma Cells. Arch of Biochem and Biophys. (2000). 375, 21-30.
6. Dietzen DJ. and Davis EJ. Excess Membrane Cholesterol Is Not Responsible for Metabolic and Bioenergetic Changes in AS-30D Hepatoma Mitochondria. Arch. Biochem. Biophys. (1994). 309, 341-347.
7. Loeber G., Dworkin MB., Infante A., Ahorn H. Characterization of cytosolic malic enzyme in human tumor cells. FEBS Lett. (1994). 344, 181-186.
8. Moreadith RW. and Lehninger AL. Purification, Kinetic Behavior and Regulation of $NADP(P)^+$ Malic Enzyme of Tumor Mitochondria. Biol. Chem. J. (1984). 259, 6222-6227.
9. Parlo RA. and Coleman PS. Continuous pyruvate carbon flux to newly synthesized cholesterol and the suppressed evolution of pyruvate-generated CO_2 in tumors further evidence for a persistent truncated Krebs cycle in hepatomas. Biochem. Biophys. Acta. (1986). 886, 169-176.

10. Molina M., Segura JA., Aledo JC., Medina MA., Nuñez de Castro I., Márquez J. Glutamine transport by vesicles isolated from tumor-cell mitochondrial inner membrane. Biochem. J. (1995). 308, 629-633.
11. Soboll S., Lenzen C., Rettich D., Gründel S. and Ziegler B. Characterization of glutamine uptake in rat liver mitochondria. Eur. J. Biochem. (1991). 197, 113-117.
12. McGivan JD., Lacey JH. and Joseph Suresh K. Localization and some properties of phosphate-dependent glutaminase in disrupted liver mitochondria. Biochem. J. (1980). 192, 537-542.
13. Colquhoun A. and Newsholme EA. Aspects of glutamine metabolism in human tumor-cells. Biochem. Mol. Biol. Int. (1997). 41, 583-596.
14. Kvamme E., Torgner IA. and Roberg B. Kinetics and Localization of brain phosphate activated glutaminase. (2001). 66, 951-958.
15. Quesada AR., Sánchez-Jímenez F., Pérez-Rodríguez J., Márquez J., Medina MA. and Nuñez de Castro I. Purification of phosphate-dependent glutaminase from isolated mitochondria of Ehrlich ascites-tumor cells. Biochem. J. (1988). 255, 1031-1036.
16. Randall WM. And Lenhinger AL. The Pathways of Glutamate and Glutamine Oxidation by Tumor Cell Mitochondria. Biol. Chem. J. (1984). 259:10 6215-6221.
17. Paradies G, Capuano F, Palombini G, Galeotti T, Papa S. Regulation of Carbohydrate Metabolism. Volume II. Pag 142.. Cancer Resch. (1983) 43, 5068.
18. Wilson JE. Isozymes of mammalian hexokinase: structure, subcellular localization and metabolic function. J. Exp. Biol. (2003) 206, 2049-2057.
19. Pedersen PL., Mathupala S., Rempel A., Geschwind JF. and Ko YH. Mitochondrial bound type II hexokinase. Biochem. Biophys. Acta (2002) 1555, 14-20.
20. Sánchez-Martinez C. and Aragón JJ. Analysis of phosphofructokinase subunits and isozymes in ascites tumor cells and its original tissue, murine mammary gland. FEBS Lett. (1997). 409, 86-90.

21. Sánchez-Martínez C., Estévez AM. and Aragón JJ. Phosphoructoknase c isozyme from ascites tumor cells: cloning, expression, and properties. Biochem. Biophys. Res. Commun. (2000). 271, 635-640.
22. Rodríguez-Enríquez S., Juárez O., Rodríguez-Zavala JS. and Moreno-Sánchez R. Multisite control of the Crabtree effect in ascites hepatoma cells. Eur. J. Biochem. (2001). 268, 2512-2519.
23. Rodríguez-Zavala JS. and Moreno-Sánchez R. Modulation of oxidative phosphorylation by Mg^{2+} in rat heart mitochondria. J. Biol. Chem. (1998). 273, 7850-7855.
24. Covian R. and Moreno-Sanchez R. Role of protonatable groups of bovine heart bc(1) complex in ubiquinol binding and oxidation. Eur. J. Biochem. (2001) 268, 5783-5790.
25. Rossignol R., Gilkerson R., Aggeler R., Yamagata K., Remington SJ. and Capaldi RA. Energy substrate modulates mitochondrial structure and oxidative capacity in cancer cells. Cancer Res. (2004). 64, 985-993.
26. Baggeto LG. and Lehninger AL. Formation and utilization of acetoin, an unusual product of pyruvate metabolism by Ehrlich and AS-30D tumor mitochondria. J. Biol. Chem. (1987). 262, 9535-9541.
27. Zu XL and Guppy M. Cancer metabolism: facts, fantasy, and fiction. BBRC. (2004). 313, 459-465.
28. Nakashima RA., Paggi MG. and Pedersen PL. Contributions of glycolysis and oxidative phosphorylation to adenosine 5´-triphosphate production in AS-30D hepatoma cells. Cancer Res. (1984). 44, 5702-5706.
29. Dietzen DJ. and Davis EJ. (1993) Oxidation of pyruvate, malate, citrate, and cytosolic reducing equivalents by AS-30D hepatoma mitochondria. Aech. Biochem. Biophys. (1993). 305, 91-102.
30. Grivell AR., Korpelainen EI., Williams CJ. and Berry MN. Substrate-dependent utilization of the glycerol 3-phosphate or malate/aspartate redox shuttles by Ehrlich ascites cells. Biochem. J. (1995). 310, 665-671.

31. Curi R., Lagranha CJ., Doi SQ., Sellitti DF., Procopio J., Pithon-Curi TC., Corless M. and Newsholme P. Molecular mechanism of glutamine action. J. Cell. Physiol. (2005). 204, 392-401.
32. Haussinger DE. Hepatic Glutamine metabolism. Beitr Infusionther Klin Ernahr. (1987). 17, 144.
33. Low SY., Taylor PM., Ahmed A., Pogson CI. and Rennie MJ. Substrate-specificity of glutamine transporters in membrane vesicles from rat liver and skeletal muscle investigated using amino acid analogues. Biochem. J. (1991). 278, 105-111.
34. Oxender DL. and Christensen HN. Distinct mediating systems for the transport of neutral amino acids by the Ehrlich cell. J. Biol. Chem. (1963). 238, 3686-3699.
35. Christensen HN., Liang M. and Archer EG. A distinct Na^+- requiring transport system for alanine, serine, cysteine, and similar amino acids. J. Biol. Chem. (1967). 242, 5237-5246.
36. Klingenberg M. Overview on mitochondrial metabolite transport systems. Methods Enzymol. (1979) 56, 245-252.
37. Goldstein L., Botlan JM. Renal mitochondrial glutamine transport and metabolism. Studies with rapid-mixing, rapid filtration technique. Amer J Physiol (1978). 234, 514-521.
38. Kovacevic Z, Bajin K. Kinetics of glutamine efflux from liver mitochondria loaded with the ^{14}C-labeled substrate. Biochem. Biophys. Acta. (1982) 687, 291-195.
39. Kovacevic Z. Importance of the flux of phosphate across the inner membrane of kidney mitochondria for the activation of glutaminase and the transport of glutamine. Biochem. Biophys. Acta. (1976). 430, 399-412.
40. Aledo JC., Eva de Pedro, Gómez-Fabre PM, Nuñez de Castro I and Márquez J. Submitochondrial localization and membrane topography of Ehrlich ascitic tumor cell glutaminase. Biochem. Biophys. Acta. (1997). 1323, 173-184.

41. Nelson D., Rumey WL., Erecinska M. Glutamine catabolism by heart muscle. Proprieties of phosphate-activated glutaminase. Biochem. J. (1992). 282, 559-564.
42. Randall WM. And Lenhinger AL. The Pathways of Glutamate and Glutamine Oxidation by Tumor Cell Mitochondria. Biol. Chem. J. (1984) 259:10 6215-6221.
43. Moreadith RW. and Fiskum G. Isolation of mitochondria from ascites tumor cells permeabilized with digitonin. Analytical Biochem. (1984). 137, 360-367.
44. Moreno-Sánchez R. Regulation of oxidative phosphorylation in mitochondria by external free Ca^{2+} concentration. J. Biol. Chem. (1985) 260, 4020-4034.
45. Moreno-Sánchez R, Torres-Márquez y López-Gómez FJ. La determinación de la concentración libre en células y mitocondrias con indicadores fluorescentes. Ciencia (1983). 44, 383-396.
46. Baggetto LG. Deviant energetic metabolism of glycolytic cancer cells. Biochimie. (1992) 74, 959-974.

Available online at www.sciencedirect.com
ScienceDirect
Toxicology and Applied Pharmacology 215 (2006) 208–217
Toxicology and Applied Pharmacology
www.elsevier.com/locate/ytaap

Control of cellular proliferation by modulation of oxidative phosphorylation in human and rodent fast-growing tumor cells

Sara Rodríguez-Enríquez [a,*], Paola A. Vital-González [a], Fanny L. Flores-Rodríguez [a], Alvaro Marín-Hernández [a], Lena Ruiz-Azuara [b], Rafael Moreno-Sánchez [a]

[a] *Departamento de Bioquímica, Instituto Nacional de Cardiología, México*
[b] *Departamento de Quimica Inorgánica, Facultad de Quimica, UNAM, México*

Received 18 October 2005; revised 27 January 2006; accepted 13 February 2006
Available online 31 March 2006

Abstract

The relationship between cell proliferation and the rates of glycolysis and oxidative phosphorylation in HeLa (human) and AS-30D (rodent) tumor cells was evaluated. In glutamine plus glucose medium, both tumor lines grew optimally. Mitochondria were the predominant source of ATP in both cell types (66–75%), despite an active glycolysis. In glucose-free medium with glutamine, proliferation of both lines diminished by 30% but oxidative phosphorylation and the cytosolic ATP level increased by 50%. In glutamine-free medium with glucose, proliferation, oxidative phosphorylation and ATP concentration diminished drastically, although the cells were viable. Oligomycin, in medium with glutamine plus glucose, abolished growth of both tumor lines, indicating an essential role of mitochondrial ATP for tumor progression. The presumed mitochondrial inhibitors rhodamines 123 and 6G, and casiopeina II-gly, inhibited tumor cell proliferation and oxidative phosphorylation, but also glycolysis. In contrast, gossypol, iodoacetate and arsenite strongly blocked glycolysis; however, they did not affect tumor proliferation or mitochondrial metabolism. Growth of both tumor lines was highly sensitive to rhodamines and casiopeina II-gly, with IC_{50} values for HeLa cells lower than 0.5 μM, whereas viability and proliferation of human lymphocytes were not affected by these drugs (IC_{50} > 30 μM). Moreover, rhodamine 6G and casiopeina II-gly, at micromolar doses, prolonged the survival of animals bearing i.p. implanted AS-30D hepatoma. It is concluded that fast-growing tumor cells have a predominantly oxidative type of metabolism, which might be a potential therapeutic target.

Keywords: Antineoplastic drugs; AS-30D hepatoma cells; HeLa cells; Glycolysis; Metabolic therapy; Oxidative phosphorylation

Introduction

Fast-growing tumor cells exhibit increased rates of glycolysis due to enhanced mRNA transcription, enzyme overexpression (Shim et al., 1997; Osthus et al., 2000) and the absence of an efficient oxidative phosphorylation pathway (OxPhos) (Pedersen, 1978; Eigenbrodt et al., 1985; Baggetto, 1992). These observations imply that the blocking of the glycolysis pathway should arrest tumor progression. Consequently, research into the intermediary metabolism for treatment of cancer has been governed by this notion.

In this regard, drugs that inhibit glycolysis such as 2-deoxyglucose, 3-mercaptopicolinic acid, lonidamine, clotrimazole and cyclophosphamide have been used to diminish growth of several carcinomas (HeLa, Walker-256, MCF-7, Lewis, CT-26) and fibrosarcomas (RF-1) (Lampidis et al., 1983; Fearon et al., 1987; Fanciulli et al., 1996; Penso and Beitner, 2002; Poptani et al., 2003; Izyumov et al., 2004). However, few encouraging results have been obtained from these studies due to the low drug efficiency and the severe side effects observed in the host (De Martino et al., 1987; Pulselli et al., 1996; Vivi et al., 1997).

OxPhos may also play an important role in the ATP supply for cellular proliferation. Thus, the tumor energy metabolism has been proposed as a target for antineoplastic therapy, through simultaneous inhibition of glycolysis and OxPhos (Lampidis et al., 1983; Fearon et al., 1987; Jaroszewski et al., 1990; Izyumov et al., 2004). Interestingly, the addition of both glycolytic (2-

* Corresponding author. Departamento de Bioquímica, Instituto Nacional de Cardiología, Juan Badiano No. 1, Colonia Sección XVI, Tlalpan, CP 14080, México. Fax: +52 5 55 5730926.
E-mail address: rodsar@mail.cardiologia.org.mx (S. Rodríguez-Enríquez).

0041-008X/$ - see front matter © 2006 Elsevier Inc. All rights reserved.
doi:10.1016/j.taap.2006.02.005

deoxyglucose, gossypol, 3-mercaptopicolinic acid) and oxidative inhibitors (rhodamines 123 and 6G) suppresses the growth of several carcinomas (Walker 256, MCF-7 cells) and liver-implanted VX2 tumors, by 50–100% (Fearon et al., 1987; Jaroszewski et al., 1990; Geschwind et al., 2002).

Other metabolic drugs such as clofazimine, MKT-077, F16, emodin and ceramide (Sri-Pathmanathan et al., 1994; Weisberg et al., 1996; Gudz et al., 1997; Fantin et al., 2002; Jing et al., 2002) have shown potent uncoupling or inhibitory effect on OxPhos in isolated mitochondria, culture cells and in vivo models, together with inhibition of tumor cell proliferation. Furthermore, the antineoplastic effect of taxol, methoxyestradiol, mofarotene and salsolinol may also involve diminution of the mitochondrial membrane potential in culture cells (Storch et al., 2000; Cariati et al., 2003; Park et al., 2004) and isolated mitochondria (Hagen et al., 2004). Non-steroidal anti-inflammatory drugs such as meloxicam and nimesulide (Moreno-Sánchez et al., 1999), and copper-based antineoplastic drugs such as casiopeinas (Marín-Hernández et al., 2003) also exhibit potent inhibitory effect on the oxidative metabolism of fast-growing hepatoma AS-30D. Unfortunately, assessment of the inhibitory ability of some of these metabolic inhibitors on the oxidative pathways of the tumor cell lines has not been evaluated in parallel with their effects on cell growth.

In this regard, in AS-30D hepatoma cells (Rodríguez-Enríquez et al., 2000), a tumor line previously described as of the glycolytic type (Nakashima et al., 1984), we have shown that OxPhos provides most of the ATP (>98%) required for the cellular processes during the onset of tumor proliferation. Then, it may be hypothesized that inhibition of OxPhos in AS-30D hepatoma could be a complementary strategy for lowering its active cellular proliferation. Energy metabolism of rodent fast-growing tumor cells might be different from that of human origin. However, growth of HeLa cells, a fast-growing human cancer cell line, seems mainly supported by glutamine (Reitzer et al., 1979), a mitochondrial oxidizable substrate. Therefore, the aim of the present work was to determine the extent to which the growth of AS-30D hepatoma and HeLa cells depended upon the ATP supply from glycolysis and mitochondrial function. Once the prevalent energy metabolism was established in both tumor cells, the following step was to modulate the ATP supply and cellular growth by changing substrates (glucose, glutamine or both) or by using inhibitors of glycolysis or OxPhos. Finally, this approach was upgraded to the tumor-bearing animal model to evaluate whether the inhibition of the predominant ATP-producing pathway could be a strategy to inhibit the accelerated proliferation of fast-growing tumor cells.

Materials and methods

Cell types. AS-30D hepatoma cells were propagated by intraperitoneal inoculation in 250 g female Wistar rats as described elsewhere (Rodríguez-Enríquez et al., 2000). The cells were preserved under sterile conditions at −72 °C in the presence of 10% dimethyl sulfoxide. Analysis of oxygen consumption, phosphometabolite content and glycolysis revealed that hepatoma cells remained unaltered in their metabolic characteristics after 300–350 passages in vivo. Lymphocytes were isolated from non-smoking blood donor volunteers, who were informed about the aim of this study and the experimental details. Blood was obtained by venopuncture; lymphocytes were isolated by using a centrifugation step with Histopaque (ICN, Aurora, Ohio), according to the procedure described by the manufacturer. Immediately after isolation, the cells were suspended in RPMI 1640 medium (GIBCO Life Technologies, Rockville, MD).

Cell culture conditions. Primary cultures of AS-30D tumor cells were established from cells isolated from freshly extracted AS-30D ascites tumor. Cells were isolated by differential centrifugation under sterile conditions as previously described (Rodríguez-Enríquez et al., 2000). Aliquots of AS-30D cells and HeLa cells were grown in glucose- and glutamine-free Dulbecco's minimal essential medium (GIBCO), supplemented with 10% fetal bovine serum (GIBCO), 10,000 U streptomycin/penicillin and fungizone (amphotericin B; GIBCO). Glucose (25 mM), glutamine (5 mM) or glutamate (10 mM) (GIBCO), plus 2.5 μM oligomycin (Sigma Chem.) were added to the media at the final concentrations indicated under Results.

For cell proliferation, AS-30D hepatoma cells were cultured in 50 ml-conic centrifuge tubes by using an initial inoculum of 1×10^6 cells/ml. HeLa cells were cultured in 25 or 75 cm^2-flasks or in 24-multiwell plates (both from Corning, NY), and the experiments were started with an inoculum of 1.5×10^4 cells/ml. AS-30D hepatoma cells were cultured at 37 °C in 5% CO_2, 95%O_2, under gentle constant agitation (12–20 oscillations per min), whereas HeLa cells were cultured under similar conditions without agitation. Human primary lymphocytes were cultured in 24-multiwell plates at 2×10^4 cells/ml in the presence of lectin (250 μg/ml) in 5% CO_2, 95% O_2, at 37 °C. To avoid depletion of nutrients and growth factors, fresh medium was replenished every day.

Determination of oxidative and glycolytic fluxes and cellular ATP concentration. HeLa cells were removed from each flask with trypsin/EDTA (GIBCO) after 72 or 96 h of culture, whereas AS-30D hepatoma cells were collected after 24 or 48 h of culture. Both tumor lines were washed with cold Krebs–Ringer buffer (125 mM NaCl, 5 mM KCl, 1 mM $MgCl_2$, 1.4 mM $CaCl_2$, 1 mM H_2PO_4, 25 mM HEPES, pH 7.4).

For glycolytic flux under near-physiological conditions, tumor cells ($3–5 \times 10^6$ cells/ml) were incubated for 1 and 10–11 min at 37 °C in the presence of 0.6 mM glutamine, 5 mM glucose and the indicated concentration of a metabolic inhibitor. Afterwards, the reaction was stopped with 3% perchloric acid (Rodríguez-Enríquez et al., 2000). The glycolytic flux was determined by measuring the increase in lactate, using a standard enzymatic assay (Bergmeyer and Bernt, 1974). For OxPhos flux, tumor cells (1×10^7 cells/ml) were incubated under orbital shaking of 150 rpm for 10 min at 37 °C in the same medium with 0.6 mM glutamine, 5 mM glucose and the indicated concentration of a metabolic inhibitor. Then an aliquot of $3–5 \times 10^6$ cells/ml was transferred to the oxymeter chamber which contained air-saturated fresh Krebs–Ringer medium with 0.6 mM glutamine, 5 mM glucose and the indicated concentration of a metabolic inhibitor (to avoid dilution). The rate of OxPhos was determined by measuring the oligomycin-sensitive O_2 uptake with a Clark-type electrode at 37 °C (Rodríguez-Enríquez et al., 2000). Under these conditions, a linear correlation between rate of O_2 uptake and cellular density (from 3×10^6 up to 15×10^6 cells/ml) was attained.

For the extraction of the intracellular ATP, the cells were mixed with cold 3% perchloric acid and neutralized with 3 M KOH–0.1 M Tris. The ATP content was determined by using the hexokinase/glucose 6-phosphate dehydrogenase assay (Bergmeyer, 1983).

Proliferation rates and toxicity indexes of metabolic inhibitors. The OxPhos inhibitors (rhodamine 123, rhodamine 6G, nimesulide, rotenone, oligomycin, casiopeina II-gly, casiopeina III-i) or glycolytic inhibitors (iodoacetate, gossypol or arsenite) were added to the glutamine + glucose medium at the beginning of the primary culture of AS-30D cells. For HeLa cells and lymphocytes, inhibitors were added 3 h after the beginning of each passage to allow the cells to become attached to the bottom of the well. Cellular densities were determined by using a hematocytometer. The viability of both tumor lines was estimated by 0.5% trypan blue exclusion. The drug toxicity indexes (IC_{50}) on proliferation of HeLa, AS-30D hepatoma cells and human lymphocytes were determined by measuring the cellular density and viability after 48 h (AS-30D), 72 h (human lymphocytes) or 96 h (HeLa) of culture in the presence of different concentrations of inhibitor.

Effect of rhodamine 6G and casiopeina II-gly on in vivo AS-30D tumor progression. AS-30D tumor cells (6×10^8 cells) were implanted i.p. in 250 g female Wistar rats. Drug administration (day 0) was initiated 5–10 min after tumor implantation. Rhodamine 6G and casiopeina II-gly were dissolved in 5 ml sterile PBS (phosphate buffer saline) at a final concentration of 15 μM (30 μg/kg). The total volume injected was 1 ml. The drugs were also administered on days 2, 4 and 6 after tumor implantation. The i.p. ascites liquid generated after 7 days was removed for determination of tumor cell density.

Statistical analysis. Data are presented as mean ± standard deviation (SD) with the number of different preparations assayed between parentheses. Differences were considered as significant when at least a $P < 0.05$ value was obtained by the Student's *t* test for non-paired samples.

Results

Effect of the carbon source on the proliferation of AS-30D hepatoma and HeLa cells

The highest cellular density of both tumor lines was attained in the glucose plus glutamine (gln + gluc) medium (Fig. 1). Under this condition, AS-30D cells reached the stationary phase after 34 h and remained stable for at least 14 h, whereas cellular viability was maintained up to 98% (data not shown); the generation time was 7.2 ± 2 h ($n = 3$). HeLa cells reached the stationary phase after 90 h of culture in the gln + gluc medium with a generation time of 20 ± 6 h ($n = 3$), keeping a viability up to 98% (data not shown).

In the gln or glutamate rich-medium without glucose, AS-30D cellular density diminished by 30 and 50% ($P < 0.005$), respectively (Fig. 1A). Similarly, HeLa cell proliferation decreased by 23% in the gln-rich medium without glucose although cell viability was high (97%, $n = 2$) (Fig. 1B). In contrast, it was only in the glucose-rich medium that both tumor lines were unable to grow, although a high cellular viability was maintained (83 ± 3% for AS-30D cell, $n = 3$; and 97% for HeLa cells, $n = 2$). The mitochondrial ATP synthase inhibitor oligomycin (2.5–5 μM) allowed HeLa cells to adhere to the bottom of the well. It has been reported that 5 μM oligomycin arrests the cellular cycle progression in Jurkat T cells and diminishes viability, without affecting non-tumorigenic cells (Ferrari et al., 1998). In AS-30D and HeLa cells, oligomycin abolished growth (Fig. 1), indicating that mitochondrial ATP was essential for tumor progression. This last observation discounted the possibility that the low proliferation rate observed in the cells grown in the gln-free medium with glucose was due to nitrogen shortage.

Effect of glucose and glutamine on oxidative phosphorylation and intracellular ATP concentration in AS-30D hepatoma cells

AS-30D cells grown in the gln + gluc medium and harvested during the logarithmic or stationary phases showed a relatively high and similar cellular respiration, which was 85–90% oligomycin-sensitive, i.e., respiration exclusively destined to ATP synthesis (Table 1). A similar pattern of cellular respiration was established for freshly obtained AS-30D cells (Rodríguez-Enríquez et al., 2000). These control rates of respiration of both tumor lines were similar to values reported by other authors for

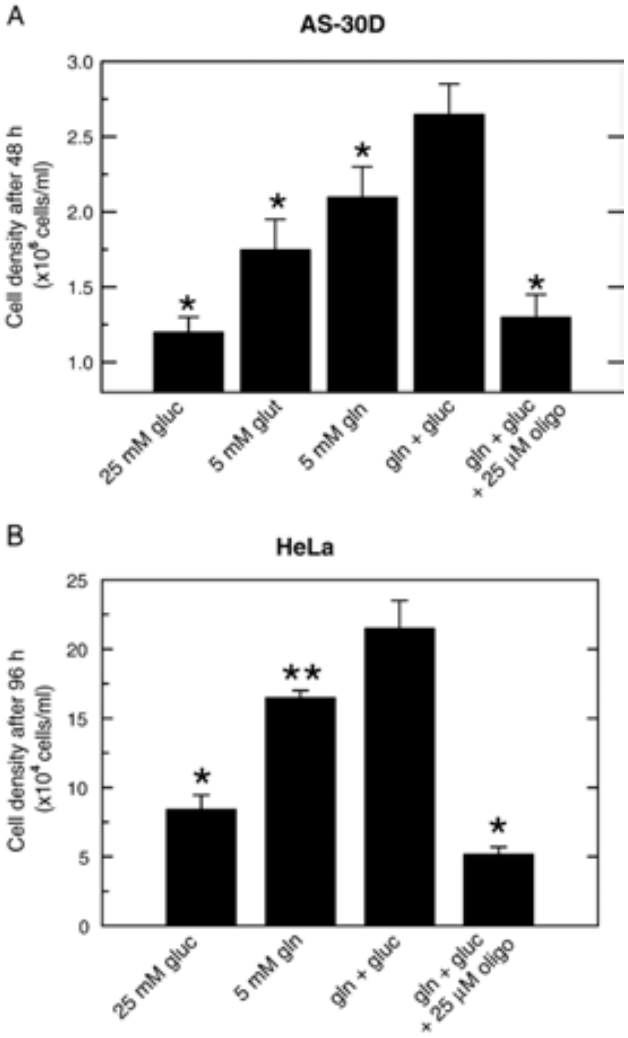

Fig. 1. Effect of different carbon sources on cell proliferation of AS-30D hepatoma (A) and HeLa cells (B). For AS-30D hepatoma cells, the cultures were started with 1×10^6 cells per ml. Cell density is given as the mean of three different experiments ± SD, except for that with glutamate ($n = 2$). For HeLa cells, the cultures were started with 1.5×10^4 cells per well. Cell density is given as the mean of 2 different experiments ± SD (8 wells per condition). The substrate concentrations used are indicated below the bars. For AS-30D cells, the viability under each experimental condition was 98 ± 1%, except for that with glucose in which viability was 83 ± 3%. For HeLa cells, the viability was higher than 95%. Abbreviations: glucose (gluc), glutamine (gln), glutamate (glut), oligomycin (oligo). *$P < 0.005$ vs. gln + gluc. **$P < 0.01$ vs. gln + gluc. Care was taken to maintain the pH of the culture medium above 7.0.

AS-30D or other tumor cell lines using the same methodology (Medina et al., 1988; Rossignol et al., 2004). In cells cultured in a gln-rich medium, oligomycin-sensitive respiration increased by 50%, suggesting de-inhibition of OxPhos due to the absence of glucose. Indeed, exogenous glucose inhibited respiration of both AS-30D and HeLa cells cultured in gln + gluc medium by 60 ± 15 ($n = 3$) and 20 ± 5 ($n = 3$)%, respectively, indicating the presence of the Crabtree effect, a common phenomenon in tumor cells (Rodríguez-Enríquez et al., 2001). Increased respiration correlated well with elevation in the intracellular content of ATP (Table 1).

In contrast, AS-30D cells cultured in the glucose-rich medium maintained a low respiratory activity, which was

Table 1
Relationship between oxidative phosphorylation and ATP concentration in primary cultures of AS-30D hepatoma cells

Carbon source	Cellular respiration (nanogram atoms oxygen/min/10^7 cells)		ATP concentration	
	A	B	nmol ATP/10^7 cells	mM
gln + gluc	91 ± 5 (4)	12 ± 0.6 (4)	1.7 ± 0.4	0.7 ± 0.2 (5)
gln + gluc**	86 (2)	18 (2)	1.5	0.6 (2)
gln	138 ± 20 * (4)	21 ± 3 * (4)	2.8 ± 1 *	1.2 ± 0.4 *(4)
gluc	0 ± 0 * (4)	21 ± 7 * (4)	0.4 ± 0.1 *	0.2 ± 0.04* (4)

AS-30D hepatoma cells were harvested after 24** or 48 h of culture and washed with cold Krebs–Ringer solution as described under Materials and methods. The rates of oligomycin-sensitive (A) and oligomycin-resistant (B) respiration were determined in the absence of added substrates. The values represent the mean ± SD, with the number of different preparations used shown between parentheses. Estimation of molar concentrations was made by assuming an intracellular volume of 2.28 μl/10^7 cells in AS-30D hepatoma (Rodríguez-Enríquez et al., 2000). Abbreviations: glutamine + glucose (gln + gluc); glutamine (gln); glucose (gluc).
* $P < 0.05$ vs. gln + gluc.

completely insensitive to oligomycin, i.e., respiration was not associated with mitochondrial ATP synthesis (Table 1). This behavior was accompanied by a significant lowering of 70% in the ATP concentration. These findings indicated an essential role of OxPhos for the cell supply of ATP, with glycolysis playing a minor role (see Table 2 for additional supporting evidence on negligible glycolysis role). When the cells were cultured in gln + gluc plus oligomycin, the OxPhos rate and ATP concentration were undetectable (data not shown). This last result correlated with the lower cellular density attained in the presence of oligomycin (Fig. 1).

Table 2
Effect of several drugs on oxidative phosphorylation and glycolysis in AS-30D hepatoma and HeLa cells

	AS-30D hepatoma (nmol ATP/min/10^7cells)		HeLa cells (nmol ATP/min/10^7cells)	
	Oxidative phosphorylation	Glycolysis	Oxidative phosphorylation	Glycolysis
Control				
Stationary	106 ± 11 (4)	51 ± 1 (3)	230 ± 39 (6)	67 ± 12 (4)
Exponential	100 (2)	42 (2)	201 (2)	47 ± 8 (3)
Rhod 123				
Stationary	38 ± 12 **	5 ± 5 ** (3)	94 ± 34 ** (6)	12.5 ± 5 ** (3)
Exponential	46 (1)	16 (2)	127 (2)	18 ± 7 (3)
Rhod 6G				
Stationary	37 ± 11 ** (4)	27 ± 10 ** (3)	95 ± 12 ** (6)	4 ± 4 ** (3)
Exponential	49 (2)	18 (2)	118 (2)	
Casio II				
Stationary	65 ± 10 ** (4)	25 ± 6 ** (3)	57 ± 4 ** (6)	39 ± 6 ** (3)
Exponential	76 (2)	26 (2)	62 (2)	31 ± 24 (3)
Casio III				
Stationary	110 ± 28 [a] (3)	50 ± 5 [a] (3)	210 ± 13 [a] (6)	79 ± 8 [a] (3)
Arsenite				
Stationary	111 ± 13 [a] (4)	25 ± 5 ** (3)	214 ± 13 [a] (3)	20 ± 13 ** (3)
Exponential	93 (2)	12 (2)	207 (2)	12 (2)
IAA				
Stationary	103 ± 19 [a] (3)	25 ± 4 ** (3)	183 ± 46 [a] (5)	10 ± 3 ** (3)
Exponential	101 (2)	15 (2)	206 (2)	11 ± 2 (3)
Goss				
Stationary	111 ± 12 [a] (4)	21 ± 5 ** (3)	203 ± 55 [a] (5)	28 ± 17 *(3)

Tumor cells were grown in gln + gluc medium. The indicated inhibitors were added as described under Materials and methods. Cells were harvested in the exponential (24 h for AS-30D; 72 h for HeLa) and stationary (48 h for AS-30D; 96 h for HeLa) growth phases and washed with cold Krebs–Ringer. Respiration and glycolysis of both tumor cells were determined as described under Materials and methods. The inhibitor concentrations used for AS-30D cells were 100 μM each of IAA, goss or arsenite and 10 μM each of rhod 123, rhod 6G, casio II or casio III. For HeLa cells, the concentrations used were 10 μM each of IAA, arsenite, goss or casio III, and 1 μM each of rhod 123, rhod 6G or casio II. Oxidative phosphorylation was estimated from the rate of olygomycin-sensitive respiration and assuming a P/O ratio of 2.5 (Nakashima et al., 1984). In the absence of exogenous oxidizable substrates, the respiratory rates of HeLa cells (with or without inhibitor) reached similar values than those of cells incubated with glucose plus glutamine. Each value represents the mean ± SD, with the number of experiments assayed shown in parentheses. For each experimental condition, 0.1 ml aliquots were taken before, during and after starting the reaction for viability determination by staining with trypan blue. For both tumor lines, the viability was higher than 95% in control; for + goss and + IAA viability was up to 90%; for + casio III viability was up to 60%; for rhod 123, rhod 6G and casio II viability was lower than 10%. Abbreviations: iodoacetate (IAA), gossypol (goss), rhodamine 123 (rhod 123), rhodamine 6G (rhod 6G), casiopeina II-gly (casio II), casiopeina III-i (casio III).
[a] Not significantly different from control value.
* $P < 0.01$ vs. control.
** $P < 0.005$ vs. control.

Effect of metabolic inhibitors on tumor cellular proliferation, glycolysis and OxPhos

To prove the hypothesis that proliferation of fast-growing tumor cells is highly sensitive to OxPhos inhibitors and uncouplers, but not to glycolytic inhibitors, the effect of several drugs was tested on the growth of AS-30D and HeLa cells during the exponential and stationary phases. To determine the rates of OxPhos and glycolysis under near-physiological conditions, HeLa and hepatoma cells were incubated for 10 min in the Krebs–Ringer medium supplemented with 0.6 mM glutamine and 5 mM glucose (Table 2), concentrations found for these oxidizable substrates in rat and human blood (Stahl and Frick, 1978). For both tumor cells, the fluxes of glycolysis and OxPhos in the absence, or in the presence of metabolic inhibitors, were similar during the exponential or stationary phases (Table 2). As HeLa cells were more sensitive to OxPhos and glycolytic inhibitors, these cells were cultured with inhibitor concentrations one order of magnitude lower than that used for hepatoma cells (Fig. 1B; Table 2).

To ensure interaction of drugs with their specific sites, the tumor cells were incubated with the drugs for 10 min. Short-term incubation (1–2 min) of both tumor cells with the drugs reached the same inhibition percentages of OxPhos as those determined with longer incubation times (see Table 2).

Low concentrations of rhodamines and casiopeina II-gly drastically reduced the cellular proliferation and OxPhos of HeLa (nanomolar) and AS-30D cells (micromolar), respectively (Table 3). Nimesulide, at micromolar concentrations, also affected AS-30D cell proliferation (data not shown). The rate of oligomycin-sensitive respiration in HeLa cells and AS-30D hepatoma was similar in the absence of added exogenous substrates (80 ± 15, n = 3 and 91, n = 2 ngAO/min/10^7 cells, respectively). However, the presence of exogenous glucose promoted a drastic diminution in AS-30D OxPhos (from 80 ± 15, n = 3, to 43, n = 2, ng atoms oxygen/min/10^7 cells) and, therefore, in the contribution of the pathway to the content of cellular ATP (Table 2). The OxPhos inhibition together with the glycolysis stimulation by exogenous glucose caused the OxPhos contribution to the ATP supply to diminish to 67–70% in AS-30D cells during the exponential and stationary growth phases (see Table 2).

HeLa cells exhibited a lower sensitivity to exogenous glucose; therefore, ATP supply from OxPhos was slightly higher (77–81%). In spite of the increased glycolytic rate and diminution of mitochondrial function induced by the presence of external glucose, the highest ATP contribution came from mitochondria, suggesting that both tumor lines mostly depended on oxidative metabolism. Thus, OxPhos contribution to the cellular ATP supply predominated both in the absence and in the presence of external glucose. The values of OxPhos and glycolysis rates shown in Table 2 were very similar to those found in other fast-growing tumor lines, such as hepatoma Reuber H-35, hepatoma Morris 7793 or mouse fibrosarcoma 1929 (Rossignol et al., 2004; Zu and Guppy, 2004).

Gossypol, a polyphenolic aldehyde from cotton seed, inhibits NAD(P)$^+$-dependent enzymes, particularly lactate and glyceraldehyde 3-P (GAPDH) dehydrogenases (Qian and Wang, 1984). Arsenite and iodoacetic acid inhibit GAPDH (Ikehara et al., 1984; Dixon, 1997). These three glycolytic inhibitors drastically diminished the glycolytic flux in HeLa cells (>70%), whereas AS-30D hepatoma was somewhat resistant (only 50% inhibition) (Table 2). However, neither gossypol, iodoacetate nor arsenite severely affected cellular viability, proliferation and oligomycin-sensitive respiration of AS-30D hepatoma and HeLa cells (Fig. 2), indicating a negligible part played by glycolysis on the ATP supply for cell proliferation. The cationic lipophilic molecules, rhodamines and casiopeina II-gly, blocked both OxPhos and glycolytic activities in AS-30D hepatoma and HeLa cells (Table 2), suggesting that glycolysis depended on mitochondrial function (i.e., ATP for glucose phosphorylation) or that these drugs could also directly affect some glycolytic enzymes. As these drugs also affected viability and proliferation of tumor cells, the data suggested a strong correlation between OxPhos and cell proliferation.

The potency of the glycolytic and mitochondrial drugs on proliferation and ATP availability of HeLa and AS-30D cells was evaluated (Table 3). Rotenone, oligomycin, rhodamine 6G and rhodamine 123 were the most potent drugs in both tumor

Table 3
Toxicity index (IC_{50}) of several drugs affecting energy metabolism on cellular proliferation and ATP content of AS-30D hepatoma and HeLa cells

	Cellular density IC_{50} μM			Decrease in the ATP content by IC_{50} doses (%)	
	AS-30D	HeLa	Lymphocytes	AS-30D	HeLa
goss	198 ± 60 (3)	6 ± 3 (3)	44.5 (2)		
IAA	99 ± 21(3)	24 ± 8 (3)			
rhod 123	2 ± 1 (3)	0.09 ± 0.03 (3)	35 ± 10 (4)	53 ± 17 * (3)	39 ± 7 * (3)
rhod 6G	0.9 ± 0.7 (3)	0.13 ± 0.05 (4)	34 ± 7 (4)	47 ± 23 * (3)	65 ± 6 * (3)
nime	28.5 ± 10 (3)	30.8 (2)			
rote	0.3 ± 0.02 (3)	0.35 ± 0.13 (5)		47 ± 6 * (3)	64 ± 20 * (3)
oligo	0.6 ± 0.1 (3)	2.5 (2)			
casio II	3.5 ± 1.3 (3)	0.4 ± 0.2 (5)	34 ± 12 (4)	41 ± 12 * (3)	60 ± 9 * (3)
casio III	21.4 ± 6 (3)	6 ± 3 (4)			

For AS-30D hepatoma, the cellular ATP content was normalized vs. the ATP content determined without inhibitor (see Table 1: 1.7 ± 0.4 nmol/10^7cells). For HeLa cells, the ATP content without inhibitor was 8.3 ± 1 nmol/10^7cells (n = 4). Abbreviations: iodoacetate (IAA), gossypol (goss), rhodamine 123 (rhod 123), rhodamine 6G (rhod 6G), nimesulide (nime), rotenone (rote), oligomycin (oligo), casiopeina II-gly (casio II), casiopeina III-i (casio III).

* $P < 0.005$ vs. control.

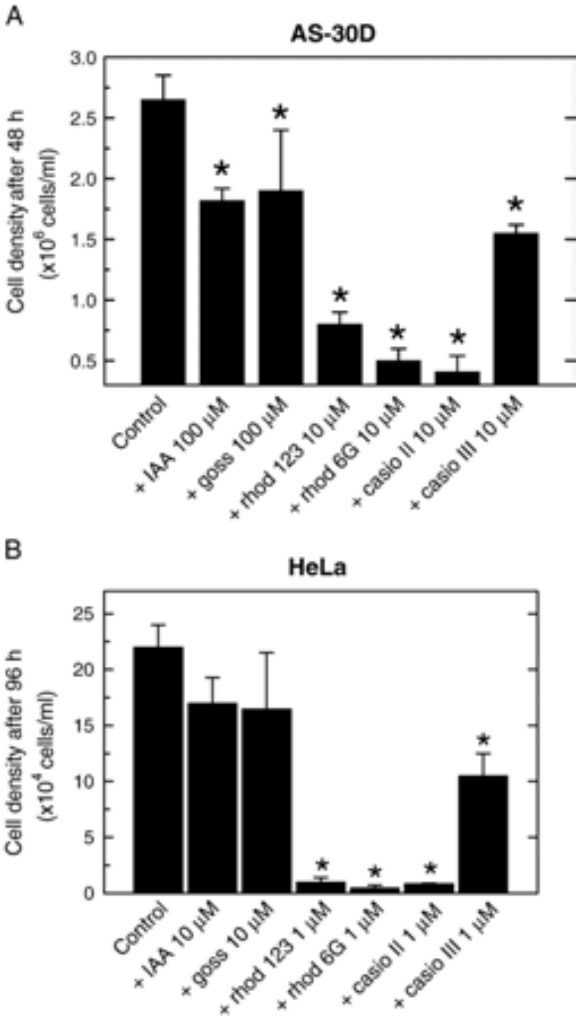

Fig. 2. Effect of different oxidative and glycolytic inhibitors on cell proliferation of AS-30D hepatoma and HeLa cells. AS-30D tumor cells (1×10^6 cells/ml) and HeLa cells (1.5×10^4 cells/ml) were grown in gln + gluc medium without inhibitor (control) or in the presence of different drugs. The concentration of each inhibitor is indicated below the bars. The cellular density was determined after 48 h (AS-30D hepatoma) or 96 h (HeLa cells). For AS-30D, cell densities are given as the mean of at least three independent experiments ± SD. The viability was higher than 95% in control, and + goss conditions; for + IAA and + casio III, viability was 86 ± 4 and 50 ± 8%, respectively; for rhod 123, rhod 6G and casio II, viability was lower than 10%. For HeLa cells, densities are given as the mean of two experiments (8 wells per condition) ± SD; except gossipol ($n = 3$ experiments or 9 well per condition). The viability was higher than 97% in control, + IAA and + goss, 53% with casio III and less than 5% with casio II and rhod 123 and 6G. Abbreviations: iodoacetate (IAA), gossypol (goss), rhodamine 123 (rhod 123), rhodamine 6G (rhod 6G), casiopeina II-gly (casio II) and casiopeina III-i (casio III). *$P < 0.005$ vs. control.

cell lines, followed by casiopeina II-gly. The IC_{50} values for rhodamine 123 and gossypol were in the same range as that reported for other oxidative tumor lines such as A-2780 (a human ovarian carcinoma), human melanoma and MCF-7 cells (Jaroszewski et al., 1990). The diminution in the proliferation rate of both tumor cells induced by these drugs correlated with the lowering in the ATP content (≥50%). The ATP level determined in HeLa cells (3.5 mM) was in the same range as that reported by Ikehara et al. for the same tumor type (3–4 mM). These data indicated that low doses of either rotenone, rhodamines or casiopeina II-gly may suffice to promote a significant diminution in the total ATP, and in consequence a diminution in the tumor growth. HeLa cells showed a higher sensitivity to gossypol than AS-30D hepatoma cells (Table 3).

Likewise, the IC_{50} values determined on cellular viability for several drugs were in the same range as that calculated for cellular proliferation. Thus, rhodamine 123 (IC_{50} = 0.43 ± 0.26 µM, $n = 4$), rhodamine 6G ($IC_{50} = 0.24 \pm 0.2$ µM, $n = 4$) and casiopeina II-gly ($IC_{50} = 0.53 \pm 0.7$ µM, $n = 4$) severely affected HeLa cells viability at low doses in comparison with glycolytic drugs such as IAA ($IC_{50} = 19 \pm 7$, $n = 4$).

Rhodamine 123, rhodamine 6G and casiopeina II-gly did not affect cellular proliferation or viability of human lymphocytes. The IC_{50} values for these drugs were higher than 30 µM (Table 3). A similar IC_{50} value for amiodarone on cellular proliferation has been described in human lymphocytes (Fromenty et al., 1993). Lymphocytes were more sensitive to glycolytic drugs than AS-30D cells, possibly due to their higher dependence on glycolysis for ATP supply (Wu and Greene, 1992).

Antitumor activity of rhodamine 6G and casiopeina II-gly in AS-30D hepatoma-bearing animals

The survival of tumor-bearing rats was analyzed, in order to test that the drug inhibitory effects on the energy metabolism observed in suspensions or cultures of tumor cells may be extended to a more complex and realistic model.

The survival time of AS-30D hepatoma-bearing rats was 7 days after i.p. tumor implantation, with a median survival time of 6 days. Administration of rhodamine 6G or casiopeina II-gly prolonged the survival of AS-30D-bearing rats (Fig. 3). These drugs were non-toxic for non-tumor-bearing animals, since they did not induce mortality at the doses assayed or at higher concentrations (100 µM casiopeina II-gly) (data not shown). To extend the animal survival time (data not shown), 1–2 extra-doses of each drug were administered on days 9 and 11; the effect of extra-dose administration after day 11 was not examined. Both drugs showed a further increase in the median survival time to 2 (rhod 6G) and 8 (casio II) days, respectively (Fig. 3A).

The tumor progression brought about a 20 and 25-fold increase in the ascites volume and the total cellular density, respectively, of untreated AS-30D-bearing rats (Fig. 3B). In turn, after day 7, both drugs diminished the ascites tumor volume and cellular density of AS-30D hepatoma by 58 ± 10% and 70 ± 12%, respectively.

Discussion

Metabolic changes induced by the presence of different carbon sources

Proliferation of AS-30D and HeLa cells was higher in the presence of glucose and glutamine than in the presence of only one of these carbon sources. Glutamine utilization provides mitochondrial ATP (Table 1) and amines required for purine and pyrimidine synthesis, whereas glucose provides cytosolic ATP,

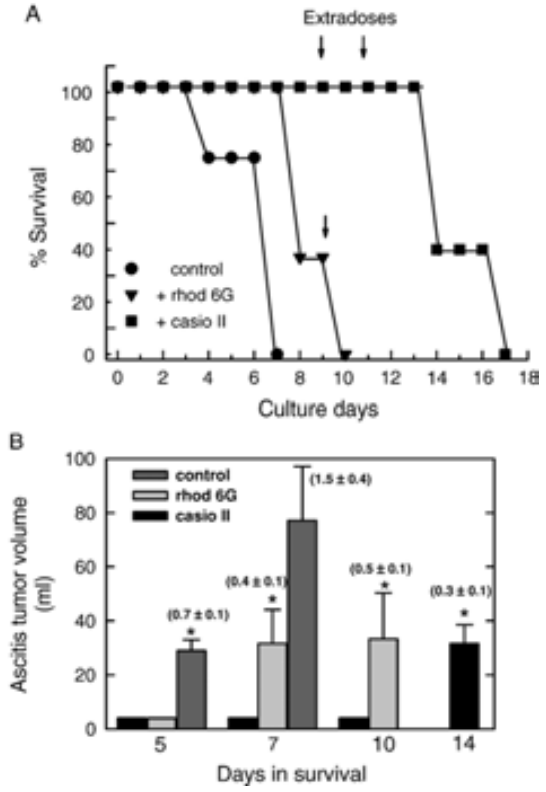

Fig. 3. (A) Survival of AS-30D hepatoma-bearing rats treated with rhodamine 6G or casiopeina II-gly. The drugs (n = 7–10 rats per set) were administered i.p. 30 μg/kg in days 0, 2, 4 and 6; arrows indicate the day when an extra dose was administered. (B) Effects of rhodamine 6G or casiopeina II-gly on the growth (ascitis tumor volume and total cellular density) of AS-30D hepatoma in rats (n = 5). The values shown between parentheses indicate the total cellular number grown ($\times 10^{10}$). *P < 0.005 vs. day 7 column without drugs (n = 10 rats).

reducing equivalents, and glycolytic intermediaries required for biosynthesis of amino acids, phospholipids and ribose phosphate. Differences in the proliferation rate of HeLa cells, grown in glucose or glutamine- and galactose-rich medium, have been previously described (Rossignol et al., 2004). In that study, the presence of glutamine resulted in an enhancement of respiratory rate (50%), cytochrome *c* oxidase activity (30%) and mitochondrial protein expression (respiratory chain complexes I–V and citrate synthase), suggesting that glutamine promoted the de novo biosynthesis of mitochondrial components (Rossignol et al., 2004).

In turn, AS-30D and HeLa cells grown in the presence of glutamine exhibited a significantly higher rate of OxPhos and higher cellular ATP content than cells grown with gln + gluc. When glucose was present, OxPhos of AS-30D and HeLa cells was partially inhibited (Crabtree effect) (Melo et al., 1998; Rodríguez-Enríquez et al., 2001), although most of the cellular ATP was still derived from mitochondria (cf. Table 2).

The severe diminution in the ATP concentration attained in the presence of glucose suggests (a) the inactivation of some ATP-dependent enzymes such as the cyclin-dependent kinases, which are involved in the progression from phase G_1 to phase S (Km_{ATP} = 1 mM) (Schwacha and Bell, 2001); (b) the active degradation of ATP to AMP, and hence the inhibition of P-ribose-PP synthetase (Mazurek et al., 1997); and (c) a strong regulatory function of glycolysis on mitochondrial ATP production (Biswas et al., 1997).

Diminution of growth in HeLa cells and AS-30D hepatoma by oxidative metabolism inhibition

Data of the present work on growth, glycolysis, OxPhos and ATP levels suggest that AS-30D and HeLa tumor cells have an oxidative type of metabolism, which implies that mitochondria play a central role in supporting the proliferation process. Therefore, a strategy to diminish the proliferation of these tumor lines would be the use of drugs that specifically block oxidative metabolism. The addition of typical inhibitors of OxPhos, such as oligomycin or rotenone, at relatively low doses, abolished the tumor proliferation and viability of HeLa cells and AS-30D hepatoma (cf. Table 3). Although both drugs are potent inhibitors of OxPhos, rotenone more drastically diminished the proliferation rate of both tumor lines. This might be due to a much slower binding of oligomycin to the ATP synthase, in comparison to rotenone binding to the respiratory chain complex I; however, the lengthy incubation of cells with the inhibitors might invalidate this explanation. Alternatively, the respiratory complex I could exert a higher flux control on OxPhos than the ATP synthase in both cell types (Rodríguez-Enríquez et al., 2000), bringing about a higher sensitivity to rotenone. Moreover, it has been reported that, in the lymphoma cell line WP and in a human osteosarcoma-derived line 143 B, low doses of rotenone (0.1 and 0.5–1 μM, respectively) arrest the cell cycle at G2/M and affect the microtubule assembly, leading to apoptosis (Armstrong et al., 2001).

Thus, the results of the present work support the proposal that the inhibition of the OxPhos pathway may be a suitable strategy for growth diminution in tumor lines with a predominantly oxidative type of metabolism. The effect of typical inhibitors of OxPhos on HeLa cell growth has already been reported (Izyumov et al., 2004): these inhibitors combined with 2-deoxyglucose induce cell death. However, the effect of these drugs on OxPhos was evaluated in the absence of exogenous energy substrates (cf. Table 2); in addition, these typical inhibitors can also affect non-tumorigenic cells. Hence, it would be of higher clinical relevance to test drugs that do not alter the physiology of healthy host cells (Lampidis et al., 1983; Fearon et al., 1987). Thus, the most appropriate strategy would probably be the use of lipophilic cationic drugs such as rhodamines, which preferentially accumulate and retain for longer periods in tumor cells than in normal tissues (Davis et al., 1985), promoting inhibition of mitochondrial function.

Several drugs that affect mitochondrial metabolism (i.e., 3-BrPA, clofazimine, ceramide) or glycolysis (lonidamine, cyclophosphamide or clotrimazol) have been considered as potent antitumor drug candidates (Sri-Pathmanathan et al., 1994; Gudz et al., 1997; Vivi et al., 1997; Ko et al., 2001; Penso and Beitner, 2002; Schimmel et al., 2004). However, some of them have been used at very high concentration (up to 5 mM) and have inhibitory effects over other cellular processes (De Martino et al., 1987; Pulselli et al., 1996; Penso and

Beitner, 2002). In contrast, rhodamine 123 at low doses (1 and 10 μg/ml, i.e., 2.6 and 26 μM) diminishes the colony formation of human tumors such as CRL 1420 and MCF-7 cells by 80–100%; a higher concentration (130 μM) does not affect growth of normal fibroblasts (Lampidis et al., 1983).

The addition of the glycolytic inhibitors iodoacetate, arsenite or gossypol did not significantly disturb the proliferation of AS-30D and HeLa cells (cf. Table 2). These observations suggested that glycolysis was not essential for cell proliferation, as long as OxPhos remained active in the cells. Although it has been documented that gossypol inhibits mitochondrial succinate dehydrogenase in PC3 (prostate cancer cells) (Jiang et al., 2002), respiration of AS-30D hepatoma and HeLa cells was not altered by this drug. It has been reported that the IAA concentration used in the present study for AS-30D cells (100 μM) totally inhibits glycolysis in intrapulmonary arteries, Muller cells and human retinal epithelial cells (Leach et al., 2001; Winkler et al., 2003). However, IAA could inhibit other enzymes (cysteine proteases) (Choi et al., 1998) and cellular processes (microtubule assembly) at concentrations above 100 μM (Luduena et al., 1994).

The ATP supply is not the only cellular process affected by the addition of the glycolytic or oxidative drugs. Targeting mitochondria induces either apoptosis, necrosis or blockage of cellular progression at low inhibitor concentrations in leukemia cells, HL-60 cells and Jurkat cells (Linsinger et al., 1999; Li et al., 2003; Pelicano et al., 2003). Therefore, the use of this kind of compounds may be effective against tumor cells by virtue of their toxic effect at several cellular levels, not only affecting ATP availability. Interestingly, rhodamines and casiopeina II-gly, at low doses, proved to be potent antineoplastic agents abolishing in vitro proliferation of both tumor cell types without affecting viability and proliferation of a non-tumorigenic line (cf. Table 3). These observations suggest that rhodamine 123, rhodamine 6G and casiopeina II-gly might be employed as an alternative metabolic therapy.

Rhodamine 6G has already been used in other in vivo models such as Walker 256 carcinosarcoma (Fearon et al., 1987). However, the effect of rhodamine 6G was only effective after adding 3-mercaptopicolinic acid, in agreement with the observation that Walker 256 depends on both ATP-producing pathways (Fearon et al., 1987). Indeed, the concentrations of rhodamine 6G and casiopeina II-gly, used in the present study to diminish tumor growth in vivo, were much lower than those of the same (0.8 mg/kg) or other metabolic drugs (1–128 mg/kg) used in other studies (Gold, 1971; Fearon et al., 1987; Sri-Pathmanathan et al., 1994; Weisberg et al., 1996). Rhodamine 6G and casiopeina II were not fully effective in preventing the hepatoma growth in animals. Thus, further studies with higher drug concentrations and with glycolytic drugs in combination with the oxidative drugs have to be carried out. Each type of cancer has different DNA mutations and perturbations of the intermediary metabolism; however, the ATP supply continues to depend solely on glycolysis and OxPhos. In the present study, we demonstrated in an in vivo model (cf. Figs. 3A, B) that low (micromolar) doses of only one drug, that affects the prevalent energy metabolism in rodent and human tumor lines, sufficed to delay and reduce the tumor growth. Furthermore, these results suggest that selective inhibition of prevalent tumor energy metabolism through metabolic therapy is a potential novel approach to cancer treatment.

The changes in tumor energy metabolism have been already applied to diagnose and monitor cancer through PET (positron emission tomography) or a combination of PET with computed tomography of a glucose derivative (Seemann, 2004). By assuming that tumor cells have a higher glucose utilization (and hence higher glucose uptake) than normal cells, it has been possible to localize a variety of primary tumors and metastases (Patronas et al., 1985; Wagner, 1993; Schiepers and Hoh, 1998) although, unfortunately, the PET technique has been unsuccessful in detecting others (Lassen et al., 1999). Perhaps the assumption that cancer cells exhibit higher glucose utilization does not apply to all tumor cell lines and, as shown in the present work, many tumor cells may have an oxidative type of metabolism. It follows that once the type of energy metabolism in a tumor cell line is established, it might be possible to apply PET with a probe directed towards mitochondria in those tumors which are presumably non-glycolytic but oxidative.

Moreover, acquired or inherent drug resistance in tumor cells, which is a recurrent problem in treatment therapies, seems closely related to the presence of partially uncoupled mitochondria that preferentially oxidize fatty acids and over-express uncoupling protein 2 (Harper et al., 2002). But lipophilic cation drugs such as rhodamines and casiopeinas might not be highly effective to kill this type of tumor cells, since the lower mitochondrial membrane potential would not preferentially accumulate cationic drugs. However, by understanding this particular tumor type of metabolism, it seems feasible to design drugs that specifically block mitochondrial fatty acid oxidation or uncoupling protein activity.

Acknowledgments

The present work was partially supported by grants SALUD-2002-C01-7677 and 43811-Q from CONACyT-México. The authors thank Lidia Barron for her expert technical assistance in the isolation of lymphocytes.

References

Armstrong, J.S., Hornung, B., Lecane, P., Jones, D.P., Knox, S.J., 2001. Rotenone-induced G2/M cell cycle arrest apoptosis in a human B lymphoma cell line PW. Biochem. Biophys. Res. Commun. 289, 973–978.

Baggetto, L.G., 1992. Deviant energetic metabolism of glycolytic cancer cells. Biochimie 74, 959–974.

Bergmeyer, H.U., 1983. Metabolites 1, carbohydrates. In: Bergmeyer, H.U. (Ed.), Methods of Enzymatic Analysis. Weinheim Verlag Chemie, Germany, p. 671.

Bergmeyer, H.U., Bernt, E., 1974. Metabolites, carbohydrate metabolism. In: Bergmeyer, H.U. (Ed.), Methods of Enzymatic Analysis. Academic Press, Orlando, FL, p. 174.

Biswas, S., Ray, M., Misra, S., Dutta, D.P., Ray, S., 1997. Selective inhibition of mitochondrial respiration and glycolysis in human leukaemic leucocytes by methylglyoxal. Biochem. J. 323, 343–348.

Cariati, R., Zancai, P., Righetti, E., Rizzo, S., De Rossi, A., Boiocchi, M.l., Dolcetti, R., 2003. Inhibition of oxidative phosphorylation underlies the

antiproliferative and proapoptotic effects of mofarotene (Ro 40-8757) in Burkitt's lymphoma cells. Oncogene 22, 906–918.

Choi, M.H., Park, W.J., Park, Y.J., Chai, J.Y., Lee, S.H., 1998. Isolation and characterization of a 40 kDa cysteine protease from *Gymnophalloides seoi* adult worms. Korean J. Parasitol. 36, 133–141.

Davis, S., Weiss, M.J., Wong, J.R., Lampidis, T.J., Chen, L.B., 1985. Mitochondrial and plasma membrane potentials cause unusual accumulation and retention of rhodamine 123 by human breast adenocarcinoma-derived MCF-7 cells. J. Biol. Chem. 260, 13844–13850.

De Martino, C., Malorni, W., Accinni, L., Rosati, F., Nista, A., Formisano, G., Silvestrini, B., Arancia, G., 1987. Cell membrane changes induced by lonidamine in human erythrocytes and T lymphocytes, and Ehrlich ascites tumor cells. Exp. Mol. Pathol. 46, 15–30.

Dixon, H.B.F., 1997. The biochemical action of arsenic acids, especially as phosphate analogues. Adv. Inorg. Chem. 44, 191–227.

Eigenbrodt, E., Fister, P., Reinacher, M., 1985. New perspectives on carbohydrate metabolism in tumor cells. In: Reitner, R. (Ed.), Regulation of Carbohydrate Metabolism. CRC Press, Boca Raton, FL, pp. 141–179.

Fanciulli, M., Valentini, A., Bruno, T., Citro, G., Zupi, G., Floridi, A., 1996. Effect of the antitumor drug lonidamine on glucose metabolism of adriamycin-sensitive and -resistant human breast cancer cells. Oncol. Res. 8, 111–120.

Fantin, V.R., Berardi, M.J., Scorrano, L., Korsmeyer, S.J., Leder, P., 2002. A novel mitochondriotoxic small molecule that selectively inhibits tumor cell growth. Cancer Cell 2, 29–42.

Fearon, K.C.H., Plumb, J.A., Burns, H.J.G., Calman, K.C., 1987. Reduction of the growth rate of the Walker 256 tumor in rats by rhodamine 6 G together with hypoglycemia. Cancer Res. 47, 3684–3687.

Ferrari, D., Stepczynska, A., Los, M., Wesselborg, S., Schulze-Osthoff, K., 1998. Differential regulation and ATP requirement for Caspase-8 and Caspase-3 activation during CD95- and anticancer drug-induced apoptosis. J. Exp. Med. 18, 894–979.

Fromenty, B., Letteron, P., Fisch, C., Berson, A., Deschamps, D., Pessayre, D., 1993. Evaluation of human blood lymphocytes as a model to study the effects of drugs on human mitochondria. Effects of low concentrations of amidarone on fatty acid oxidation, ATP levels and cell survival. Biochem. Pharmacol. 46, 421–432.

Geschwind, J.F.H., Ko, Y.H., Torberson, M.S., Magee, C., Pedersen, P.L., 2002. Novel therapy for liver cancer: direct intraarterial injection of a potent inhibitor of ATP production. Cancer Res. 62, 3013–3909.

Gold, J., 1971. Inhibition of Walker 256 intramuscular carcinoma in rats by administration of hydrazine sulfate. Oncology 25, 66–71.

Gudz, T.I., Tserng, K.Y., Hoppel, C.L., 1997. Direct inhibition of mitochondrial respiratory chain complex III by cell-permeable ceramide. J. Biol. Chem. 272, 24154–24160.

Hagen, T., D'Amico, G., Quintero, M., Palacios-Callender, M., Hollis, V., Lam, F., Moncada, S., 2004. Inhibition of mitochondrial respiration by the anticancer agent 2-methoxyestradiol. Biochem. Biophys. Res. Commun. 322, 923–929.

Harper, M.E., Antoniou, A., Villalobos-Menuey, E., Russo, A., Trauger, R., Vendemelio, M., George, A., Bartholomew, R., Carlo, D., Shaikh, A., Kupperman, J., Newell, E.W., Bespalov, I.A., Wallace, S.S., Liu, Y., Rogers, J.R., Gibbs, G.L., Leahy, J.L., Camley, R.E., Melamede, R., Newell, M.K., 2002. Characterization of a novel metabolic strategy used by drug-resistant tumor cells. FASEB J. 16, 1550–1557.

Ikehara, T., Yamaguchi, H., Hosokawa, K., Sakai, T., Miyamoto, H., 1984. Rb^+ influx in response to changes in energy generation: effect of the regulation of the ATP content of HeLa cells. J. Cell Physiol. 119, 273–282.

Izyumov, D.S., Avetisyan, A.V., Pletjushkina, O.Y., Sakharov, D.V., Wirtz, K. W., Chernyak, B.V., Skulachev, V.P., 2004. "Wages of fear": transient threefold in intracellular ATP level imposes apoptosis. Biochim. Biophys. Acta 1658, 141–147.

Jaroszewski, J.W., Kaplan, O., Cohen, J.S., 1990. Action of gossypol and rhodamine 123 on wild type and multidrug-resistant MCF-7 human breast cancer cells: 31P nuclear magnetic resonance and toxicity studies. Cancer Res. 50, 6936–6943.

Jiang, J., Ghosh, P.K., Kulp, S.K., Sugimoto, Y., Liu, S., Czekajewski, J., et al., 2002. Effects of gossypol on O_2 consumption and CO_2 production in prostate cancer cells. Anticancer Res. 22, 1491–1496.

Jing, X., Ueki, N., Cheng, J., Imanishi, H., Hada, T., 2002. Induction of apoptosis in hepatocellular carcinoma cell lines by emodin. Jpn. J. Cancer Res. 93, 874–882.

Ko, Y.H., Pedersen, P.L., Geschwind, J.F., 2001. Glucose catabolism in the rabbit VX2 tumor model for liver cancer: characterization and targeting hexokinase. Cancer Lett. 173, 83–91.

Lampidis, J.J., Bernal, S.D., Summerhayes, I.C., Chen, L.B., 1983. Selective toxicity of rhodamine 123 in carcinoma cells in vivo. Cancer Res. 43, 716–720.

Lassen, U., Daugaard, G., Eigtved, A., Damgaard, K., Friberg, L., 1999. 18F-FDG whole body positron emission tomography (PET) in patients with unknown primary tumours (UPT). Eur. J. Cancer 35, 1076–1082.

Leach, R.M., Hill, H.M., Snetkov, V.A., Robertson, T.P., Ward, J.T.P., 2001. Divergent roles of glycolysis and the mitochondrial electron transport chain in hypoxic pulmonary vasoconstriction of the rat: identity of the hypoxic sensor. J. Physiol. 536, 211–224.

Li, N., Ragheb, K., Lawler, G., Sturgis, J., Rajwa, B., Melendez, J.A., Robinson, J.P., 2003. Mitochondrial complex I inhibitor rotenone induces apoptosis through enhancing mitochondrial reactive oxygen species production. J. Biol. Chem. 278, 8516–8525.

Linsinger, G., Wilhelm, S., Wagner, H., Hacker, G., 1999. Uncouplers of oxidative phosphorylation can enhance a Fas death signal. Mol. Cell Biol. 19, 3299–3311.

Luduena, R.F., Roach, M.C., Epstein, D.L., 1994. Interaction of ethacrynic acid with bovine brain tubulin. Biochem. Pharmacol. 47, 1677–1681.

Marín-Hernández, A., Gracia-Mora, I., Ruíz-Ramírez, L., Moreno-Sánchez, R., 2003. Toxic effect of copper-based antineoplastic drugs (casiopeinas) on mitochondrial functions. Biochem. Pharmacol. 65, 1979–1989.

Mazurek, S., Boschek, C.B., Eigenbrodt, E., 1997. The role of phosphometabolites in cell proliferation, energy metabolism, and tumor therapy. J. Bioenerg. Biomembr. 29, 315–330.

Medina, M.A., Sánchez-Jimenes, F., Márquez, F.J., Pérez-Rodriguez, J., Quesada, A.R., Nunez de Castro, I., 1988. Glutamine and glucose as energy substrates for Ehrlich ascites tumour cells. Biochem. Int. 16, 339–347.

Melo, R.F., Stevan, F.R., Campello, A.P., Carnieri, E.G.S., Martinelli-De Oliveira, M.B., 1998. Occurrence of the Crabtree effect in HeLa cells. Cell Biochem. Funct. 16, 99–105.

Moreno-Sánchez, R., Bravo, C., Vásquez, C., Ayala, G., Silveira, L., Martínez-Lavín, M., 1999. Inhibition and uncoupling of oxidative phosphorylation by nonsteroidal anti-inflammatory drugs: study in mitochondria, submitochondrial particles, cells, and whole heart. Biochem. Pharmacol. 57, 743–752.

Nakashima, R.A., Paggi, M.G., Pedersen, P.L., 1984. Contributions of glycolysis and oxidative phosphorylation to adenosine 5′-triphosphate production in AS-30D hepatoma cell. Cancer Res. 44, 5702–5706.

Osthus, R.C., Shim, H., Kim, S., Li, Q., Reddy, R., Mukherjee, M., Xu, Y., Wonsey, D., Lee, L.A., Dang, C.V., 2000. Deregulation of glucose transporter 1 and glycolytic gene expression by c-Myc. J. Biol. Chem. 275, 21797–21800.

Park, S.J., Wu, C.H., Gordon, J.D., Zhong, X., Emami, A., Safa, A.R., 2004. Taxol induces caspase-10-dependent apoptosis. J. Biol. Chem. 279, 51057–51067.

Patronas, N.J., Di Chiro, G., Kufta, C., Bairamian, D., Kornblith, P.L., Simon, R., Larson, S.M., 1985. Prediction of survival in glioma patients by means of positron emission tomography. J. Neurosurg. 62, 816–822.

Pedersen, P.L., 1978. Tumor mitochondria and the bioenergetics of cancer cells. Prog. Exp. Tumor Res. 22, 190–274.

Pelicano, H., Feng, L., Zhou, Y., Carew, J.S., Hileman, E.O., Plunkett, W., Keating, M.J., Huang, P., 2003. Inhibition of mitochondrial respiration: a novel strategy to enhance drug-induced apoptosis in human leukemia cells by a reactive oxygen species-mediated mechanism. J. Biol. Chem. 278, 37832–37839.

Penso, J., Beitner, R., 2002. Detachment of glycolytic enzymes from cytoskeleton of Lewis lung carcinoma and colon adenocarcinoma cells induced by clotrimazole and its correlation to cell viability and morphology. Mol. Genet. Metab. 76, 181–188.

Poptani, H., Bansal, N., Jenkins, W.T., Blessington, D., Mancuso, A., Nelson, D. S., Feldman, M., Delikatny, E.J., Chance, B., Glickson, J.D., 2003. Cyclophosphamide treatment modifies tumor oxygenation and glycolytic

rates of RIF-1 tumors: 13C magnetic resonance spectroscopy, Eppendorf electrode, and redox scanning. Cancer Res. 63, 8813–8820.
Pulselli, R., Amadio, L., Fanciulli, M., Floridi, A., 1996. Effect of lonidamine on the mitochondrial potential in situ in Ehrlich ascites tumor cells. Anticancer Res. 16, 419–423.
Qian, S.Z., Wang, Z.G., 1984. Gossypol: a potential antifertility agent for males. Annu. Rev. Pharmacol. Toxicol. 24, 329–360.
Reitzer, L.J., Wice, B.M., Kenell, D., 1979. Evidence that glutamine, not sugar, is the major energy source for cultured HeLa cells. J. Biol. Chem. 254, 2669–2676.
Rodríguez-Enríquez, S., Torres-Márquez, M.E., Moreno-Sánchez, R., 2000. Substrate oxidation and ATP supply in AS-30D hepatoma cells. Arch. Biochem. Biophys. 375, 21–30.
Rodríguez-Enríquez, S., Juárez, O., Rodríguez-Zavala, J.S., Moreno-Sanchez, R., 2001. Multisite control of the Crabtree effect in ascites hepatoma cells. Eur. J. Biochem. 268, 2512–2519.
Rossignol, R., Gilkerson, R., Aggeler, R., Yamagata, K., Remington, S.J., Capaldi, R.A., 2004. Energy substrate modulates mitochondrial structure and oxidative capacity in cancer cells. Cancer Res. 64, 985–993.
Schiepers, C., Hoh, C.K., 1998. Positron emission tomography as a diagnostic tool in oncology. Eur. Radiol. 8, 1481–1494.
Schimmel, K.J., Richel, D.J., Van den Brink, R.B., Guchelaar, H.J., 2004. Cardiotoxicity of cytotoxic drugs. Cancer Treat. Rev. 30, 181–191.
Schwacha, A., Bell, S.P., 2001. Interactions between two catalytically distinct MCM subgroups are essential for coordinated ATP hydrolysis and DNA replication. Mol. Cell 8, 1093–1104.
Seemann, M.D., 2004. PET/CT: fundamental principles. Eur. J. Med. Res. 9, 241–246.
Shim, H., Chun, Y., Lewis, B.C., Dang, C.V., 1997. A unique glucose-dependent apoptotic pathway induced by c-Myc. Proc. Natl. Acad. Sci. U.S.A. 95, 1511–1516.
Sri-Pathmanathan, R.M., Plumb, J.A., Fearon, K.C., 1994. Clofazimine alters the energy metabolism and inhibits the growth rate of a human lung-cancer cell line in vitro and in vivo. Int. J. Cancer 56, 900–905.
Stahl, A., Frick, A., 1978. Enzymic micro-assay for blood glutamine. Clin. Chem. 24, 1730–1733.
Storch, A., Kaftan, A., Burkhardt, K., Schwarz, J., 2000. 1-Methyl-6,7-dihydroxy-1,2,3,4-tetrahydroisoquinoline (salsolinol) is toxic to dopaminergic neuroblastoma SH-SY5Y cells via impairment of cellular energy metabolism. Brain Res. 855, 67–75.
Vivi, A., Tassin, M., Ben-Horin, H., Navon, G., Kaplan, O., 1997. Comparison of action of the anti-neoplastic drug lonidamine on drug-sensitive and drug-resistant human breast cancer cells: 31P and 13C nuclear magnetic resonance studies. Breast Cancer Res. Treat. 43, 15–25.
Wagner, H.N., 1993. Oncology: a new engine for PET/SPECT. J. Nucl. Med. 34, 13N–29N.
Weisberg, E.L., Koya, K., Modica-Napolitano, J., Li, Y., Chen, L.B., 1996. In vivo administration of MKT-077 causes partial yet reversible impairment of mitochondrial function. Cancer Res. 56, 551–555.
Winkler, B.S., Sauer, M.W., Starnes, C.A., 2003. Modulation of the Pasteur effect in retinal cells: implication for understanding compensatory metabolic mechanism. Exp. Eye Res. 76, 715–723.
Wu, G., Greene, L.W., 1992. Glutamine and glucose metabolism in bovine blood lymphocytes. Comp. Biochem. Physiol. B 103, 821–825.
Zu, X.L., Guppy, M., 2004. Cancer metabolism: facts, fantasy, and fiction. Biochem. Biophys. Res. Commun. 313, 459–464.

the FEBS Journal

Determining and understanding the control of glycolysis in fast-growth tumor cells

Flux control by an over-expressed but strongly product-inhibited hexokinase

Alvaro Marín-Hernández[1], Sara Rodríguez-Enríquez[1], Paola A. Vital-González[1], Fanny L. Flores-Rodríguez[1], Marina Macías-Silva[2], Marcela Sosa-Garrocho[2] and Rafael Moreno-Sánchez[1]

1 Instituto Nacional de Cardiología, Departamento de Bioquímica, Juan Badiano no. 1, Colonia Sección XVI, México, Mexico
2 Instituto de Fisiología Celular, Departamento de Biología Celular, Universidad Nacional Autónoma de México, Mexico

Keywords
elasticity coefficient; flux-control coefficient; hexokinase type 2; metabolic control analysis; phosphofructokinase type 1

Correspondence
R. Moreno-Sánchez, Instituto Nacional de Cardiología, Departamento de Bioquímica, Juan Badiano no. 1, Col. Sección XVI, Tlalpan, México 14080, Mexico
Fax: 52 55 55730926
Tel: 52 55 55732911 ext. 1422, 1298
E-mail: rafael.moreno@cardiologia.org.mx, morenosanchez@hotmail.com

(Received 17 October 2005, revised 21 February 2006, accepted 3 March 2006)

doi:10.1111/j.1742-4658.2006.05214.x

Control analysis of the glycolytic flux was carried out in two fast-growth tumor cell types of human and rodent origin (HeLa and AS-30D, respectively). Determination of the maximal velocity (V_{max}) of the 10 glycolytic enzymes from hexokinase to lactate dehydrogenase revealed that hexokinase (153–306 times) and phosphfructokinase-1 (PFK-1) (22–56 times) had higher over-expression in rat AS-30D hepatoma cells than in normal freshly isolated rat hepatocytes. Moreover, the steady-state concentrations of the glycolytic metabolites, particularly those of the products of hexokinase and PFK-1, were increased compared with hepatocytes. In HeLa cells, V_{max} values and metabolite concentrations for the 10 glycolytic enzyme were also significantly increased, but to a much lesser extent (6–9 times for both hexokinase and PFK-1). Elasticity-based analysis of the glycolytic flux in AS-30D cells showed that the block of enzymes producing Fru(1,6)P_2 (i.e. glucose transporter, hexokinase, hexosephosphate isomerase, PFK-1, and the Glc6*P* branches) exerted most of the flux control (70–75%), whereas the consuming block (from aldolase to lactate dehydrogenase) exhibited the remaining control. The Glc6*P*-producing block (glucose transporter and hexokinase) also showed high flux control (70%), which indicated low flux control by PFK-1. Kinetic analysis of PFK-1 showed low sensitivity towards its allosteric inhibitors citrate and ATP, at physiological concentrations of the activator Fru(2,6)P_2. On the other hand, hexokinase activity was strongly inhibited by high, but physiological, concentrations of Glc6*P*. Therefore, the enhanced glycolytic flux in fast-growth tumor cells was still controlled by an over-produced, but Glc6*P*-inhibited hexokinase.

It is well documented that fast-growth tumor cells have higher rates of lactate formation even under aerobic conditions than nontumorigenic cells. For instance, different types of hepatoma (Reuber, Morris, Dunings LC18) and fibrosarcoma 1929 exhibit rates of 0.2–2.7 μmol lactate·h^{-1}·(mg protein)$^{-1}$, whereas normal liver and kidney cells have rates of 0.05 μmol lactate·h^{-1}·(mg protein)$^{-1}$ [1,2].

The increase in tumor glycolysis has been associated with the activation of several oncogenes (*c-myc*, *ras* and *src*) or with the expression of the hypoxia-inducible factor (HIF-1α) in transformed human lymphoblastoid

Abbreviations
DHAP, dihydroxyacetone phosphate; G6PDH, glucose-6-phosphate dehydrogenase; GAPDH, glyceraldehyde-3-phosphate dehydrogenase; GluT, glucose transporter; LDH, lactate dehydrogenase; PFK-1, phosphofructokinase type 1.

and human U87 glioma [3,4]. As a result of oncogene activation and expression, the over-expression of several genes encoding eight glycolytic proteins, including the glucose transporter (GluT), takes place [5]. The over-expression of a plasma membrane H^+-ATPase in rat fibroblasts, to alter the cytosolic pH regulation, and presumably enhance ATP consumption, also promotes a sevenfold stimulation of glycolysis, in addition to inducing malignant transformation [6].

In comparison with hepatocytes, in several fast-growth tumor cells (AS-30D, Novikoff) there is over-expression of hexokinase-II [7,8], due to the activation of its own promoter, through a demethylation process [9] or through protein p53 activation (an abundant protein in fast-growth tumor cells) [10].

Binding of tumoral hexokinase-II to the mitochondrial outer membrane apparently changes its kinetic properties, compared with the cytosolic isoenzyme, i.e. mitochondrial hexokinase-II shows lower sensitivity ($\approx 30\%$) to inhibition by its product Glc6*P* [7]. The close vicinity of hexokinase-II to the adenine nucleotide translocase in tumor mitochondria ensures that mitochondrial ATP is preferentially used for hexose phosphorylation [8]. It has also been reported that hexokinase-II plays an important role in preventing apoptotic events, such as cytochrome *c* release in HeLa cells, by interfering with the binding of the pro-apoptotic protein Bax to the outer mitochondrial membrane [11].

In normal tissues, citrate and ATP are potent allosteric inhibitors of phosphofructokinase type 1 (PFK-1) [12], where it is mainly constituted by M subunits, but this does not occur when the predominant subunit is L or C [13]. The tumoral isoenzyme is less sensitive to the inhibitory effect of these two allosteric effectors [13,14]. In this regard, it has been observed that the subunit L or C content of tumor PFK-1 increases, whereas that of subunit M decreases, which explains the smaller effect of its negative modulators [15–17]. It has also been reported that the content of Fru(2,6)P_2 (a potent PFK-1 activator [12]) in HeLa cells, Ehrlich ascites cells and HT29 human colon adenocarcinoma is much higher than in normal hepatocytes [20–80 versus 6 pmol·(mg protein)$^{-1}$, respectively] [18–21]. These observations suggest that PKF-1 is highly active in tumors cells [13,20].

In mammalian nontumorigenic systems, such as human erythrocytes and rat perfused heart, glycolytic flux is mainly controlled by hexokinase (60–80%) and PFK-1 (20–30%) [22,23]. In tumor cells, an expected consequence of the over-expression of several glycolytic enzymes and glucose transporters, and kinetic changes in hexokinase and PFK-1, is a large modification of the regulatory mechanisms and fuctioning of the pathway. Hence, the assumption that control of the glycolytic flux in tumor cells is similar to that of normal cells is apparently not well supported. Therefore, to identify the flux-controlling sites of tumoral glycolysis, we firstly determined the V_{max} of each glycolytic enzyme from hexokinase to lactate dehydrogenase (LDH) in AS-30D and HeLa cells. Measurement of enzyme activity under V_{max} conditions ensures the determination of the content of active enzyme and allows the degree of over-expression compared with normal cells to be established. Secondly, we determined the steady-state concentrations of several intermediate metabolites to identify enzymes that may impose limitations on the glycolytic flux, although such inferences do not always hold, particularly for intermediates involved in more than two reactions.

To evaluate quantitatively flux control in tumoral glycolysis, we used the theory of the metabolic control analysis [24] by applying an elasticity analysis. This consists of the experimental determination of the sensitivity of segments of the pathway towards a common intermediate. Once we had identified the main sites of flux control, we performed experiments to determine which biochemical mechanisms are involved in establishing why some enzymes exert significant control and others do not.

Results

Maximal activities of glycolytic enzymes in hepatocytes and fast-growth tumor cells

In normal freshly isolated hepatocytes, the enzymes with lower activity (and hence less content) were hexokinase < PFK-1 < aldolase, enolase (Table 1). This activity pattern is in agreement with that found in hepatocytes by other authors [7,15]. In whole liver, the activities of all glycolytic enzymes were very similar, except for pyruvate kinase, which was 3 times lower than that obtained in isolated hepatocytes (data not shown). In an attempt to establish a proliferating, non-tumorigenic cell system, to make a more rigorous comparison with the tumor cell lines used in this work, we also isolated hepatocytes from regenerating rat liver; organ regeneration was induced by prior treatment with CCl_4 [0.39 g·(kg body weight)$^{-1}$] for 12 or 24 h. In two different cell preparations, the V_{max} values of the glycolytic enzymes were essentially identical with those found for normal isolated hepatocytes (data not shown).

In rat AS-30D hepatoma cells, the enzymes with lower activity were hexokinase, PFK-1 and aldolase, a

Table 1. Maximal activity of glycolytic enzymes in hepatocytes and tumor cells. AS-30D, HeLa and hepatocytes (65 mg protein·mL^{-1}) were incubated in lysis buffer as described in Experimental procedures. Activities of all enzymes were determined in the cytosolic-enriched fraction at 37 °C. Specific activities are expressed in U·(mg protein)$^{-1}$. The values shown represent the mean ± SD with the number of different preparations assayed in parentheses. HK, hexokinase; HPI, hexosephosphate isomerase; TPI, triosephosphate isomerase; GAPDH, glyceraldehyde-3-phosphate dehydrogenase; PGK, phosphoglycerate kinase; PGAM, phosphoglycerate mutase; PYK, pyruvate kinase; LDH, lactate dehydrogenase; G6PDH, glucose-6-phosphate dehydrogenase; α-GPDH, α-glycerophosphate dehydrogenase; PGM, phosphoglucomutase; ND, not detected.

Enzymes	Hepatocytes	AS-30D	AS-30D/ hepatocytes	HeLa
HK	0.003 ± 0.002 (3)	0.46 ± 0.1** (7)	153	0.02 ± 0.006†† (4)
HPI [a]	0.4 ± 0.05 (3)	1.6 ± 0.7* (4)	4	3.0 ± 1.7 (4)
PFK-1 [b]	0.01 ± 0.002 (3)	0.21 ± 0.1* (4)	22	0.09 ± 0.02 †(5)
Aldolase	0.09 ± 0.02 (3)	0.23 ± 0.07* (4)	2.7	0.2 ± 0.05 (5)
TPI [a]	15.6 ± 5.6 (3)	56 ± 15* (4)	3.6	42 ± 13 (3)
GAPDH	0.32 ± 0.07 (3)	1 ± 0.28* (3)	2.7	2 ± 0.74 (5)
GAPDH [a]	0.66 ± 0.23 (3)	0.9 (2)	1.4	2.5 ± 0.8 (5)
PGK	8.2 ± 5.8 (3)	27 ± 10* (4)	3.3	13 ± 6† (5)
PGAM	11 ± 2 (3)	20 ± 5* (4)	2.3	1.4 ± 1 (4)
Enolase	0.11 ± 0.03 (3)	0.51 ± 0.13* (3)	4.3	0.36 ± 0.15 (5)
PYK	0.8 ± 0.36 (3)	6.6 ± 1.5** (4)	8.1	3 ± 1.3 † (4)
LDH	4.4 ± 1.9 (3)	6.4 ± 3.7 (4)	1.5	1.7 ± 0.6 (3)
G6PDH	0.03 ± 0.003 (3)	0.05 ± 0.02 (3)	1.4	0.22 ± 0.08†† (5)
PGM [c]	0.37 (2)	0.21 ± 0.06 (5)	0.6	0.42 ± 0.13 (4)
α-GPDH [d]	0.11 (2)	0.002 ± 0.001 (3)	0.05	ND

*P < 0.05 versus hepatocytes, **P < 0.005 versus hepatocytes, †P < 0.05 versus AS-30D, ††P < 0.005 versus AS-30D. Student's t-test for nonpaired samples. [a] Activity in the reverse reaction. [b] Activity determined in the presence of 16–20 mM NH_4^+. [c] The PGM activity was determined in the absence of glucose-1,6- bisphosphate. [d] The reaction was started by adding DHAP.

pattern that also agrees with that reported for the same cells [7] and for other tumor cell types [25]. The AS-30D/hepatocyte activity ratio revealed that hexokinase and, to a lesser extent, PFK-1 were the enzymes that were most over-expressed in tumor cells; all other glycolytic enzymes, including glucose-6-phosphate dehydrogenase (G6PDH), were also over-expressed in AS-30D tumor cells (Table 1).

In HeLa cells, all glycolytic enzymes, except phosphoglycerate mutase, also exhibited a higher activity than that shown by hepatocytes. However, in these human tumor cells neither hexokinase nor PFK-1 were highly over-expressed as they were in rodent AS-30D cells. In HeLa cells, hexosephosphate isomerase, PFK-1, triosephosphate isomerase and pyruvate kinase, together with G6PDH, showed greater over-expression compared with hepatocytes (Table 1). V_{max} for phosphoglycerate mutase in HeLa cells was 14 and 8 times lower than that found in AS-30D cells and hepatocytes, respectively; such low phosphoglycerate mutase activity has also been observed by other authors [25]. Negligible α-glycerophosphate dehydrogenase activity was found in both tumor cell types. A similar observation has been described for the Morris hepatomas 3924A, 5123D, 7793 and 44 [26], which are fast or moderate-growth tumor lines [27].

Glycolytic flux and intermediary concentrations

As expected from the general increase in glycolytic enzymes, steady-state generation of lactate in the presence of 5 mM glucose was markedly higher in AS-30D and HeLa cells (9–13 times) than in hepatocytes (Table 2). In the absence of added glucose, the glycolytic flux diminished drastically in both tumor cell types, being negligible in AS-30D cells. The difference between the rates of lactate formation with and with-

Table 2. Glycolysis in hepatocytes and tumor cells. AS-30D and HeLa cells (15 mg protein·mL^{-1}) and hepatocytes (30 mg protein·mL^{-1}) were incubated in Krebs–Ringer medium as described in Experimental procedures. Under these conditions, the rate of lactate formation in AS-30D cells was constant after 2 min and up to 10 min from glucose addition (i.e. steady-state glycolysis). The intracellular concentration of Fru(1,6)P_2 was also invariant between the 2- and 10-min points, after the addition of glucose (data not shown). Glycolytic fluxes are expressed in nmol·min^{-1}·(mg cell protein)$^{-1}$. The values shown represent the mean ± SD with the number of different preparations assayed in parentheses. The negative flux value indicates lactate consumption.

Condition	Hepatocytes	AS-30D	HeLa
+ Glucose	2.4 ± 1.7 (6)	21 ± 9 (40)	32 ± 10 (8)
– Glucose	– 0.4 ± 1 (6)	– 2.2 ± 2.6 (17)*	7 ± 9 (6)

out added glucose indicates that net glycolytic flux depends on external glucose, which was 8–9 times higher in AS-30D and HeLa cells than in hepatocytes.

The elevated glycolytic flux in HeLa cells in the absence of added glucose was probably sustained by endogenous sources, i.e. glycogen degradation. The content of glycogen was apparently not depleted in HeLa cells by the 10 min preincubation at 37 °C. In contrast, the total dependence of the glycolytic flux on external glucose in AS-30D cells suggests depletion of glycogen induced by the 10 min preincubation at 37 °C. The glycolytic flux values reported in this work are in the same range as reported for other tumor cell types [2].

The steady-state concentrations of all glycolytic metabolites in AS-30D tumor cells also significantly increased, except for phosphoenolpyruvate and pyruvate (Table 3). In particular, Fru(1,6)P_2 increased 250 times and dihydroxyacetone phosphate (DHAP) 16.6 times. The cytosolic pyridine nucleotide redox state ($NADH/NAD^+$), estimated from the lactate/pyruvate ratio, was more reduced in AS-30D cells, a situation that favors flux through biosynthetic pathways. The concentration of ATP was also higher in AS-30D cells than in hepatocytes; however, the ATP/ADP ratio was similar (2.3 and 2.4). The latter values are similar to those previously reported [28] for normal organs such as rat heart (5.7) and liver (4.9), as well as mouse Erhlich ascites cells (2.3) and 3924A hepatoma cells (1.2).

Table 3. Steady-state concentrations (mM) of glycolytic intermediates in normal rat hepatocytes and hepatoma cells. See legend to Table 2 and Experimental procedures for experimental details. Values shown are the mean ± SD. The number of experiments is shown in parentheses. ND, not detected; NM, not measured; DHAP, dihydroxyacetone phosphate; G3P, glyceraldehyde 3-phosphate; PEP, phosphoenolpyruvate; Lac, lactate; Pyr, pyruvate.

Metabolite	Hepatocytes	AS-30D	HeLa
Glucose	NM	6.2 ± 1 (3)	NM
Glc6*P*	0.96 ± 0.16 (3)	5.3 ± 2.6**(23)	0.6 ± 0.16††(4)
Fru6*P*	0.4 ± 0.03 (3)	1.5 ± 0.7**(22)	0.22 ± 0.09†† (4)
Fru(1,6)P_2	0.1 ± 0.05 (3)	25 ± 7.6**(19)	0.29 ± 0.06†† (4)
DHAP	0.6 ± 0.1 (3)	10 ± 2.3**(14)	0.93 ± 0.07†† (3)
G3P	0.09 ± 0.01 (3)	0.9 ± 0.4*(7)	ND
PEP	0.1 (2)	0.1 ± 0.02 (3)	0.32 (2)
Pyr	1.6 ± 0.7 (3)	2.1 ± 1 (7)	8.5 ± 3.6†† (5)
Lac [a]	9.6 ± 1.3 (3)	27 ± 11* (3)	33 (2)
ATP	3.6 ± 0.24 (3)	5.6 ± 1.2* (9)	9.2 ± 1.9† (4)
ADP	1.6 ± 0.6 (4)	2.4 ± 0.7 (7)	2.7 ± 1.3 (3)
Lac/Pyr ratio	6.3	12.9	3.9

[a] L-Lactate was intracellularly located. *$P < 0.05$ versus Hepatocytes, **$P < 0.005$ versus Hepatocytes, †$P < 0.05$ versus AS-30D, ††$P < 0.005$ versus AS-30D.

In contrast with AS-30D cells, the steady-state concentrations of Glc6*P*, Fru6*P*, Fru(1,6)P_2 and DHAP in HeLa cells were similar to those observed in hepatocytes, whereas the ATP and pyruvate concentrations were 1.6 and 4 times higher than in AS-30D cells (Table 3).

Determination of flux control coefficients for glycolysis in hepatoma cells

Metabolic control analysis establishes how to determine quantitatively the degree of control (named flux control coefficient, C^{J}_{Ei}) that each enzyme Ei exerts over the metabolic flux J [24]. In the oxidative phosphorylation pathway, C^{J}_{Ei} values can be determined by titrating the flux with specific inhibitors [24,29,30]. However, there are no specific, permeable inhibitors for each glycolytic enzyme.

An alternative approach called elasticity analysis [31–34] consists of experimental determination of the sensitivity of enzyme blocks towards a common intermediate metabolite m. By applying the summation and connectivity theorems of metabolic control analysis (see Eqns 1 and 2 in Experimental procedures), the C^{J}_{Ei} values can be calculated. Variations in the steady-state activity of the enzyme blocks can be attained by adding different concentrations of the initial substrate or inhibitors of either block, which do not have to be specific for only one enzyme but they do have to inhibit only one block. The block of enzymes that generates the common intermediate is named the producer block, whereas the block of enzymes consuming that metabolite is named the consumer block.

For glycolysis, and other pathways, any metabolite may be used as the common intermediate that connects producer and consumer branches. However, to reach consistent results, it is more convenient to use, as common intermediates, metabolites that are present at relatively high concentrations and that are only connected to the specific pathway, such as Fru(1,6)P_2. Although other metabolites such as Glc6*P*, Fru6*P* and DHAP may be present at high concentrations, they are connected with other pathways (glycogen synthesis and degradation, pentose phosphate cycle, glycerol and triacylglycerol synthesis). However, this last group of metabolites may still be used in elasticity-based analysis as long as the flux through the other pathways is low (or it is assumed to be negligible) [33,35,36] or by actually determining the effect of the branching pathways on the main flux and on the concentration of the connecting metabolite [23].

To determine the elasticity coefficients of the consumer block for the common metabolite (ε^{Ei}_{m}), we

incubated hepatoma cells with different glucose concentrations (4–6 mM) or with the hexosephosphate isomerase inhibitor 2-deoxyglucose (0.5–10 mM), which induced variations in flux and in the steady-state concentrations of the metabolite. The elasticity of the producer block was determined by titrating flux with the LDH inhibitor, oxalate (0.5–2 mM), or the glyceraldehyde-3-phosphate dehydrogenase inhibitor, arsenite (5–100 μM). Thus, the glycolytic flux (measured as the rate of lactate formation) and the concentration of several intermediates [Glc6*P*, Fru6*P*, Fru(1,6)P_2 and DHAP] were determined under both conditions. The tangents to the curves, or the straight lines, taken at the reference, control points (100%) in the normalized plots of flux versus [metabolite] obtained with glucose and oxalate, or 2-deoxyglucose and arsenite, represent the elasticities towards the intermediate metabolite of the consumer and producer blocks, respectively.

We are aware that the experimental points in the flux versus [metabolite] plot should be fitted to a hyperbolic curve rather than to a straight line, as most of the glycolytic enzymes and transporters follow a Michaelis–Menten kinetic pattern; a near-linear relation between rate and substrate concentration might be attained when the product concentration varies concomitantly. However, the lack of sufficient experimental points near the reference, unaltered state may generate high, unrealistic slope values ($\gg 2$) for the estimation of elasticity coefficients (Fig. 1) either by fitting to hyperbolic or linear equations. The definitions of the elasticity and flux control coefficients as well as the theorems of metabolic control analysis are based on differentials. However, it was not easy to produce small changes (and much less infinitesimal changes) of flux and metabolite concentration by using the experimental protocols described. In consequence, slope values were calculated with both approximations, nonlinear hyperbolic fitting and linear regression. In general, similar elasticity coefficients resulted from either approximation, although less dispersion was attained with the linear regression (see legend to Table 4 for values).

Titration of the glycolytic flux with exogenous glucose and oxalate (Fig. 1A), or with 2-deoxyglucose and arsenite (Fig. 1B), induced changes in flux and the Fru(1,6)P_2 concentration. Analysis of both segments showed that the Fru(1,6)P_2 consumer block (formed by enzymes from aldolase to LDH) showed a higher elasticity than the producer block (comprising GluT to PFK-1). In the first case (with glucose or 2-deoxyglucose), the slope had a positive value because Fru(1,6)P_2 is a substrate for the consumer block. On the other hand, with oxalate or arsenite titration, the slope had a negative value because Fru(1,6)P_2 is a product of the producer block, i.e. Fru(1,6)P_2 accumulation inhibits the producer activity.

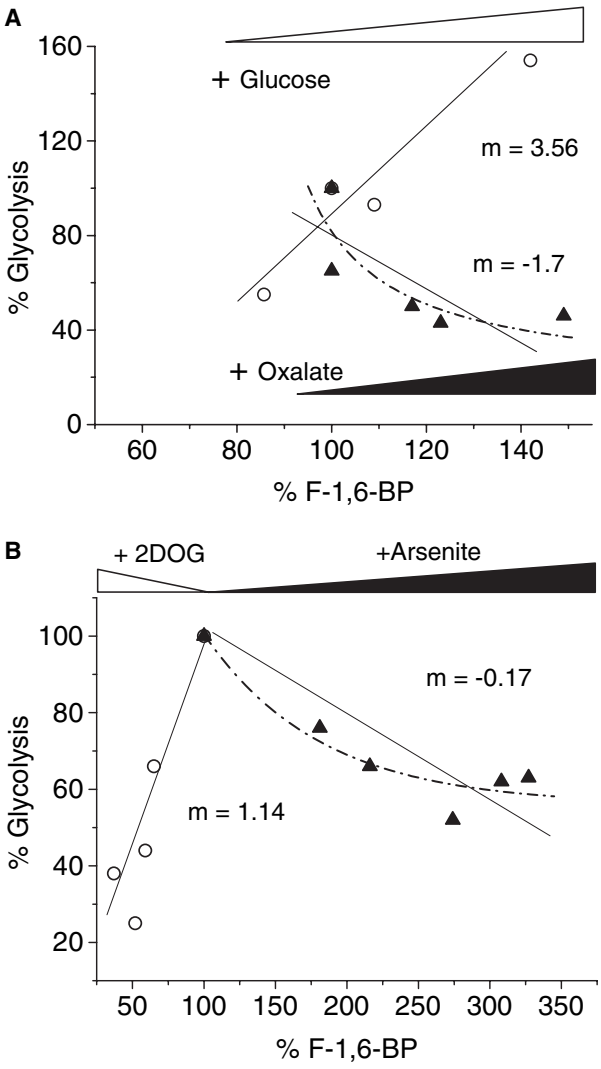

Fig. 1. Experimental determination of elasticity coefficients for glycolytic intermediates in tumor cells. AS-30D hepatoma cells (15 mg protein·mL^{-1}) were incubated in Krebs–Ringer medium at 37 °C. After 10 min, different concentrations of glucose (○, 4–6 mM) and oxalate (▲, 0.5–2 mM) in (A), or 2-deoxyglucose (○, 0.5–10 mM) and arsenite (▲, 5–100 μM) in (B), were added to the cell suspension. When a glycolytic inhibitor was added, glucose was kept constant at 5 mM. The hexokinase and PFK-1 activities, which are part of the Fru(1,6)P_2-producing block, were not affected by 10 mM oxalate or 1 mM arsenite (data not shown). Thus, the effect of these two inhibitors on flux was due to their interaction with enzymes of the Fru(1,6)P_2-consuming block, most likely LDH [66] (data not shown) and glyceraldehyde-3-phosphate dehydrogenase [67]. The values of the straight lines, or the tangents to the curves, at 100% Fru(1,6)P_2 (m), which are the elasticity coefficients in these normalized plots, are shown on the traces.

Table 4. Control (C) and elasticity (ε) coefficients values of AS-30D hepatoma cells. Control coefficients were calculated from elasticity coefficients, derived from data such as those shown in Fig. 1, and applying summation and connectivity theorems (Eqns 1 and 2; see Experimental procedures). $\varepsilon^{p}{}_{m}$, elasticity of producer block; $\varepsilon^{c}{}_{m}$, elasticity of consumer block; $C^{J}{}_{p}$, control coefficient of producer block; $C^{J}{}_{c}$, control coefficient of consumer block. All the elasticity coefficients shown in the table were calculated by using slope values derived from linear regression, although similar values were attained by nonlinear regression. For instance, the nonlinear regression for the titrations with 2-deoxyglucose and arsenite gave $\varepsilon^{C}{}_{FBP}$ and $\varepsilon^{P}{}_{FBP}$ of 1.99 ± 0.79 and −1.5 ± 1.6, which yielded the $C^{J}{}_{c}$ and $C^{J}{}_{P}$ of 0.39 ± 0.24 and 0.61 ± 0.24, respectively. The number of experiments is shown in parentheses, and values are mean ± SD. DHAP, Dihydroxyacetone phosphate.

Metabolite	$\varepsilon^{C}{}_{m}$	$C^{J}{}_{C}$	$\varepsilon^{P}{}_{m}$	$C^{J}{}_{P}$
	+ Glucose		+ Oxalate	
Glc6*P*	2.1 ± 1.7 (6)	0.29 ± 0.17 (3)	− 0.86 ± 0.41 (3)	0.71 ± 0.17 (3)
Fru6*P*	1.2 ± 0.45 (4)	0.31 ± 0.14 (3)	− 0.67 ± 0.43 (3)	0.69 ± 0.14 (3)
Fru(1,6)P_2	2.2 ± 0.95 (5)	0.44 ± 0.08 (5)	− 1.35 ± 0.66 (6)	0.62 ± 0.08 (5)
DHAP	1.27 ± 0.47 (5)	0.49 ± 0.18 (5)	− 1.5 ± 1 (5)	0.51 ± 0.18 (5)
	+ 2-Deoxyglucose		+ Arsenite	
Fru(1,6)P_2	0.93 ± 0.2 (3)	0.24 ± 0.06 (3)	− 0.25 ± 0.1 (3)	0.75 ± 0.05 (3)
	+ Glucose		+ Arsenite	
DHAP	1.18 ± 0.2 (3)	0.37 ± 0.15 (3)	− 0.5 ± 0.1 (3)	0.63 ± 0.14 (3)

It is worth emphasizing that, owing to the multitude of variables involved in determining flux and intermediary concentrations, which have to be kept constant during the experimental determination of elasticities towards one metabolite, the dispersion of the experimental points can be considerable in some cell preparations. This can be appreciated in Fig. 1 and in the values shown in Table 4. Nonetheless, it is possible to reach relevant conclusions about which steps exert significant flux control of glycolysis and which steps have low or negligible control (Table 5).

The elasticity coefficients, estimated from experiments such as those shown in Fig. 1, are summarized in Table 4. The flux control coefficients derived from the elasticity coefficients are also shown. These data clearly established that the main control of the glycolytic flux in AS-30D cells resides in the upstream part of the pathway. The experiments with glucose and oxalate show a high value for the flux control coefficient of the Glc6*P* producer block [$C^{J}{}_{P(Glc6P)}$], which indicates that GluT, hexokinase and perhaps the degradation of glycogen, steps that lead to the formation of Glc6*P*, were the sites that exerted most of the flux control. In turn, the experiments with 2-deoxyglucose and arsenite revealed that the producer block of Fru(1,6)P_2 exerted most of the control, which indicates that flux control was mainly located in GluT, hexokinase and glucogenolysis together with hexosephosphate isomerase and PFK-1.

Table 5. Distribution of control of glycolysis in AS-30D cells. GluT, Glucose transporter; HK, hexokinase; HPI, hexosephosphate isomerase; TPI, triosephosphate isomerase; GAPDH, glyceraldehyde-3-phosphate dehydrogenase; PGAM, phosphoglycerate mutase; PYK, pyruvate kinase; LDH, lactate dehydrogenase.

Enzymes or branches	$C^{J}{}_{Ei}$
GluT + HK	0.71
Pentose phosphate cycle + HPI + glycogen synthesis	−0.02
PFK-1	0.06
Aldolase, TPI, GAPDH, PGAM, enolase, PYK, LDH, Pyr branches, ATP demand	0.25
$\Sigma C^{J(glycolysis)}{}_{Ei}$ =	1.00

The same conclusion may be drawn from the high $C^{J}{}_{P(Fru6P)}$ value (Table 4). However, the glycolytic flux was negligible in the absence of added glucose (Table 2), indicating that Glc6*P* and Fru6*P* formation from glycogen degradation was not significant in AS-30D cells. Hence, from the difference between the values of $C^{J}{}_{P(Glc6P)}$ and $C^{J}{}_{P(Fru6P)}$, which were determined under the same experimental conditions with glucose and oxalate, it was possible to calculate a specific flux control value of −0.02 for the Glc6*P* branches, pentose phosphate cycle and glycogen synthesis (Table 4).

Because of the less than perfect match of $C^{J}{}_{C}$ and $C^{J}{}_{P}$ values estimated from three different experimental protocols (Table 4), it was difficult to obtain a reliable flux control coefficient for the DHAP consumer branch. With 2-deoxyglucose and arsenite, the $C^{J}{}_{P(Fru(1,6)P2)}$ value of 0.75 suggests that the rest of the pathway (from aldolase to LDH) exerts a flux control of 0.25 (Table 5). However, the $C^{J}{}_{C(DHAP)}$ values with glucose and oxalate or with glucose and arsenite were 0.49 and 0.37, respectively, which revealed some discrepancy with the 2-deoxyglucose and arsenite protocol. If the total summation of $C^{J}{}_{Ei}$ values was higher than 1.0, then branching in the middle and lower segments of glycolysis might be significant, bringing about negative flux control coefficients.

The flux control coefficient of PFK-1 (Table 5) was estimated from the $C^{J}_{P(Fru(1,6)P2)}$ value attained with 2-deoxyglucose and arsenite minus the $C^{J}_{P(Glc6P)}$ value attained with external glucose and oxalate (Table 4). Only positive differences between C^{J}_{P} values are to be taken into account for elucidating flux control for specific enzymes. With negative differences [for instance, with $C^{J}_{P(Fru(1,6)P2)}$ minus $C^{J}_{P(Fru6P)}$ both attained with glucose and oxalate], the explanation is that there is a pathway branch at the measured metabolite concentration, or that the experimental dispersion masks small differences, or that indeed there is no difference between the enzyme blocks analyzed.

Kinetic analysis of tumoral hexokinase and PFK-1

To understand why hexokinase retained a significant degree of control on glycolytic flux, despite its high over-expression, and why PFK-1 control became negligible, the kinetic properties of the two enzymes were analyzed in cell extracts. The affinity of hexokinase for glucose and ATP in both the cytosolic and mitochondrial fractions (Table 6) was in the same range as reported by Wilson [37] for hexokinase from nontumorigenic mammalian tissues. Hexokinase was equally distributed between the cytosol and mitochondria in AS-30D hepatoma cells. Both hexokinase isoenzymes, cytosolic and mitochondrial, were 81–93% inhibited by 1 mM Glc6*P* (Fig. 2A).

The PFK-1 in the cytosolic-enriched fraction from AS-30D cells exhibited K_m and $K_{0.5}$ values for ATP and Fru6*P* (Table 6) similar to those reported for PFK-1 from other tumor cell lines [13,15]. In the absence of added effectors, the PFK-1 kinetic pattern was sigmoidal with respect to Fru6*P* [although $\approx$8–12 mM $(NH_4)_2SO_4$ coming from the coupling enzymes was present], and hyperbolic with respect to low concentrations of ATP (0.01–1 mM). At high concentrations (> 1 mM), ATP was inhibitory for PFK-1 activity. Citrate was also inhibitory at relatively low (< 1 mM) Fru6*P* concentrations. However, when 1.5 mM Fru6*P* (physiological concentration) or higher concentrations were used, citrate was innocuous, even at concentrations as high as 10 mM (data not shown), in the presence of 8–10 mM $(NH_4)_2SO_4$. Fru(2,6)P_2 was the most potent activator of tumoral PFK-1, followed by AMP and NH_4^+ (Table 6).

The mean ± SD intracellular concentrations of AMP and citrate determined under glycolytic steady-state conditions in AS-30D cells were 3.3 ± 1.4

Table 6. Tumoral hexokinase and PFK-1 kinetic parameters. The activities of hexokinase and PFK-1 were determined at 37 °C as described in Experimental procedures. For hexokinase, the K_m value for ATP was determined in the presence of 5 mM glucose, whereas that for glucose was determined with 10 mM ATP. For PFK-1, the K_m value for ATP was determined in the presence of 10 mM Fru6*P*, whereas the $K_{0.5}$ value for Fru6*P* was determined with 0.25 mM ATP. The ammonium concentration in the assay mixture, proceeding from the coupling enzymes, was 16–20 mM. The $K_{0.5}$ values for NH_4^+, AMP and Fru(2,6)P_2 were determined in the presence of 2 mM Fru6*P* and 0.8 mM ATP, and with lyophilized coupling enzymes (i.e. in the absence of contaminating ammonium). The number of independent experiments is shown in parentheses. Units of K_m and $K_{0.5}$ are μM; V_{max}, U·(mg protein)$^{-1}$.

	ATP		Glucose	
Hexokinase	K_m	V_{max}	K_m	V_{max}
Mitochondrial	696 ± 180 (3)	1.96 ± 0.4 (3)	146 ± 12 (3)	1.65 ± 0.18 (3)
Cytosolic	990 ± 50 (3)	0.52 ± 0.1 (3)	180 ± 40 (3)	0.44 ± 0.1 (3)
Type I [a]	500		30	
Type II [a]	700		300	
Type III [a]	1000		3	
	ATP		Fru6*P*	
PFK-1	K_m	V_{max}	$K_{0.5}$	V_{max}
	14 ± 2 (3)	0.2 ± 0.09 (3)	200 (2)	0.2 (2)
	NH_4^+		AMP	
	$K_{0.5}$	V_{max}	$K_{0.5}$	V_{max}
	1400 ± 800 (3)	0. 51 ± 0.2 (3)	100 ± 50 (4)	0.58 ± 0.14(4)
	Fru(2,6)P_2			
	$K_{0.5}$	V_{max}		
	0.96 ± 0.3 (3)	0.52 ± 0.16 (3)		

[a] Values taken from [37].

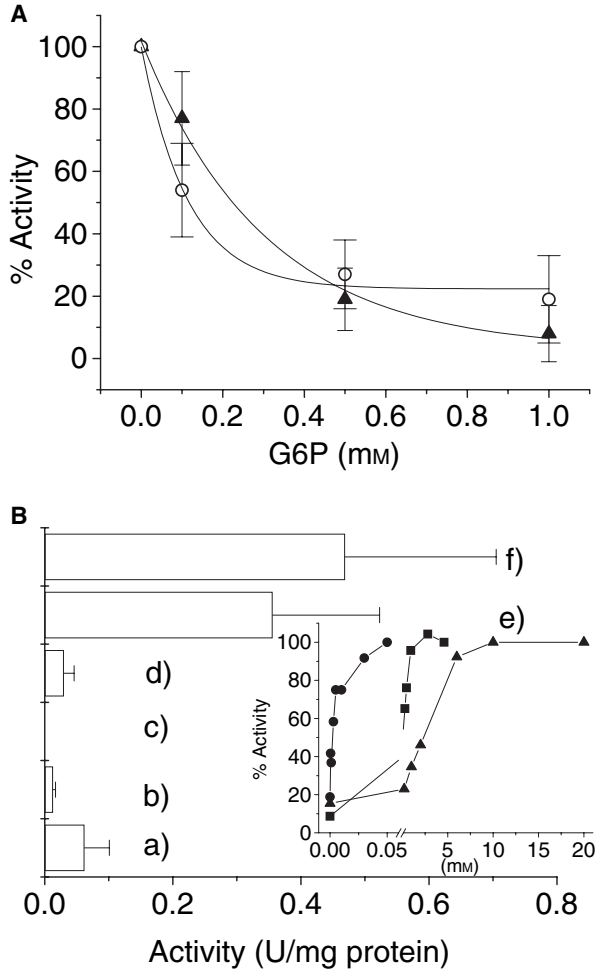

Fig. 2. Effect of modulators on tumoral hexokinase and PFK-1. (A) Inhibition of mitochondrial bound (○) and cytosolic hexokinase (▲) by Glc6*P*. Values shown represent the mean ± SD from three different preparations assayed, except for the experiments with cytosolic hexokinase at 0 and 1 mM Glc6*P*, in which nine different preparations were analyzed. (B) Effect of modulators of PFK-1. PFK-1 activity was determined in the presence of 1.5 mM Fru6*P* and (a) 0.8 mM ATP; (b) 3.9 mM ATP; (c) 3.9 mM ATP +1.7 mM citrate; (d) 3.9 mM ATP +1.7 mM citrate + 3.2 mM AMP; (e) 3.9 mM ATP + 1.7 mM citrate + 3.2 mM AMP + 5 μM Fru(2,6)P_2; and (f) 3.9 mM ATP + 1.7 mM citrate + 3.2 mM AMP + 50 μM Fru(2,6)P_2. Values shown represent the mean ± SD from three different preparations assayed. Inset: Activation of PFK-1 by different concentrations of Fru(2,6)P_2 (●), AMP (■) and NH_4^+ (▲), in the presence of 2 mM Fru6*P* and 0.8 mM ATP.

($n = 10$) and 1.7 ± 0.7 mM ($n = 6$), respectively. Thereafter, the PFK-1 activity was determined in the presence of the intracellular concentrations of its substrates (ATP, Fru6*P*), inhibitors (ATP, citrate) and activators [AMP, Fru(2,6)P_2]. PFK-1 activity was fully inhibited in the presence of ATP and citrate; this activity was only partially restored by AMP (Fig. 2B). The potent ATP + citrate inhibition was totally overcome, or even surpassed, by Fru(2,6)P_2 at concentrations found in tumor cells [18–21].

Discussion

Distribution of glycolytic flux control

Metabolic control analysis has been applied to determine the control structure of glycolysis in several normal mammalian systems, such as human erythrocytes, rat heart and mouse skeletal muscle extracts [22,23,38]. With this quantitative framework, hexokinase and PFK-1 have been identified as the main controlling steps. Fast-growth tumor cells develop a nontypical metabolism [39,40], which includes an accelerated glycolytic flux. As glycolysis in different tumor lines has been considered to be an extremely fast pathway [39], the identification of which enzyme(s) controls glycolytic flux becomes clinically relevant.

The 10 enzymes of the AS-30D hepatoma glycolytic pathway showed higher activity than in normal rat hepatocytes. Despite showing the greatest over-expression, hexokinase and PFK-1, together with aldolase, had the lowest V_{max} values (Table 1). Other groups have described a similar pattern for AS-30D [7] and other tumor cell types [25]. However, in all previous papers [7,15,25,41,42] it was difficult to establish a strict activity sequence order, as not all glycolytic activities were determined; moreover, the activity assays were performed at nonphysiological pH (> 7) and temperature (< 37 °C). Indeed, determining V_{max} under near-physiological conditions establishes the true content of active enzyme, which is not possible when mRNA, or protein, is measured.

The tumoral hexokinase and PFK-1, enzymes that in normal tissues control the flux (100% in human erythrocytes, 59% in isolated rat heart, and 100% in rat skeletal muscle reconstituted pathway) [22,23,38], exhibited the highest activity enhancement (306-fold and 22–56-fold increase versus hepatocytes; Table 1). In addition, the cytosolic concentrations of Glc6*P* and Fru(1,6)P_2, which are products of hexokinase and PFK-1, respectively, increased by fivefold and 250-fold (Table 3). The upper limits of activity increment were established by taking into account both the cytosolic and mitochondrial hexokinase activities (Table 6), and the PFK-1 maximal activity attained in the presence of the activator Fru(2,6)P_2 (Fig. 2B inset).

The flux control coefficients calculated from elasticities are, to a great extent, determined by the definition of producing and consuming blocks [24,43,44]. Elasticity-based analysis requires that (a) the metabolic

pathway reaches a quasi-steady-state (see legend to Table 2 for experimental details on how the glycolytic steady-state flux was established), and (b) the intermediates that link the blocks are not significantly affected by other pathways. However, some of the glycolytic intermediates used in this work for the estimation of elasticity coefficients such as Glc6*P*, Fru6*P* and DHAP are indeed connected to other pathways, and hence changes in the flux of glycogen synthesis and degradation, pentose phosphate cycle, and glycerol and triacylglycerol synthesis might affect the concentrations of these metabolites.

Another important assumption (c) in this elasticity-based analysis is that producing and consuming blocks affect each other only through the common metabolite. However, the glycolytic segments analyzed in this work may also interact through the moiety-conserved pools of ATP–ADP–AMP and NAD(P)H–NAD(P)$^+$. The discrepancy in the calculated flux control coefficients for producing and consuming blocks of DHAP and Fru(1,6)P_2, by using different experimental protocols (Table 4), might partly be due to variation in the nicotinamide nucleotide redox state and adenine nucleotide energy state, respectively.

Furthermore, the elasticity-based analysis might be flawed, and the control distribution reported might be erroneous, if the concentrations of adenine nucleotides also varied in the titration experiments. It is worth mentioning that several other studies involving elasticity-based analysis have not taken into account the potential interactions between producing and consuming blocks mediated by the pool of adenine nucleotides [23,33–36,45]. Therefore, the variation in the concentrations of ATP, ADP and AMP was determined under the conditions of the experiments shown in Fig. 1. The results indicate that none of the adenine nucleotides changed significantly ($n = 4$) on varying either glucose (from 4.5 to 5.5 mM) or oxalate (from 0 to 1 mM); with 2 mM oxalate, a 10–30% increase in ATP, ADP and AMP was observed. Thus, these findings support the control distribution of glycolysis (Table 5) derived from the elasticity-based analysis shown in Table 4.

DHAP is certainly connected with nonglycolytic reactions that involve NAD$^+$ such as α-glycerophosphate dehydrogenase, which was however, negligible in AS-30D cells (Table 1). Likewise, Fru(1,6)P_2 formation may affect the ATP/ADP ratio, which in turn establishes communication with glycolytic downstream reactions (phosphoglycerate kinase, pyruvate kinase) and with other energy-dependent reactions (adenylate kinase, ATPases, biosynthetic pathways). Moreover, PFK-1 is activated by AMP (Table 6 and Fig. 2B), which connects with the adenylate kinase reaction. Therefore, the connectivity theorem used here for the calculation of the flux control coefficients from elasticities towards some intermediates [Eqn 2 in Experimental procedures] was apparently incomplete and too simplistic to describe all interactions, and it may be necessary to consider more complicated relationships [24,43,44].

Notwithstanding the above arguments, the elasticity-based analysis, as used here, revealed that the Glc6*P*-producing block (GluT and hexokinase) exerted the main control of flux. The finding that the intracellular concentration of free glucose was high and saturating for hexokinase (Table 3) suggests that most of the control exerted by the Glc6*P*-producing block might reside in hexokinase. Moreover, high over-expression of GluT has been documented for HeLa cells and other human tumor cell types [46,47]. However, before we can conclude that hexokinase is the main controlling step, we should further examine the content and activity of the GluT under physiological conditions, as product inhibition of the GluT activity has not been explored [48].

In HeLa cells, all glycolytic enzymes except LDH were also over-expressed compared with hepatocytes. However, it should be noted that to achieve a more rigorous comparison, a normal proliferating endothelial cell line should be used instead of hepatocytes. The over-expression in HeLa cells was much less than that in AS-30D cells (Table 1); however, the glycolytic rates were similar (Table 2). This was probably due to a high rate of degradation of glycogen (high lactate formation in the absence of added glucose; Table 2) and amino acids (elevated concentration of pyruvate; Table 3), the products of which bypass hexokinase, the presumed main controlling step, to enter the glycolytic pathway.

In HeLa cells, the control of glycolytic flux may also reside in hexokinase, as in normal hepatocytes and AS-30D cells, as well as in PFK-1, because the two enzymes have the lowest V_{max} values, and they are not highly over-expressed. The eightfold lower concentration of Glc6*P* in HeLa cells, compared with AS-30D cells, is expected to exert a low or negligible inhibition of hexokinase. The low Glc6*P* concentration in HeLa cells may be related to a higher activity of the Glc6*P* branches, glycogen synthesis and pentose phosphate cycle. Indeed, G6PDH activity was 4–7 times higher in HeLa cells than in hepatocytes and AS-30D cells (Table 1).

A higher ATP concentration in HeLa cells than in AS-30D cells suggests a lower activity of ATPases and other ATP-dependent cell processes or, alternatively, that ATP production by oxidative phosphorylation

was faster. Indeed, the rate of oligomycin-sensitive respiration, which reflects the rate of oxidative phosphorylation [40,49], in the presence of 5 mM glucose + 0.6 mM glutamine was 43 ± 4 ng-atoms oxygen·min^{-1}·10^{-7} cells ($n = 4$) in AS-30D cells and 92 ± 16 ng-atoms oxygen·min^{-1}·10^{-7} cells ($n = 6$) in HeLa cells. As the enzymatic assay of ADP determines total but not free ADP, the ATP/ADP ratio was not highly reliable as an indicator of the cellular energy status.

There are two α-glycerophosphate dehydrogenase isoenzymes in mammalian cells, one bound to the mitochondrial inner membrane and another in the cytosol, which regulate the cytosolic NADH/NAD$^+$ ratio and are involved in the synthesis of triacylglycerols [50]. The activity of the cytosolic isoenzyme decreases or becomes negligible in fast-growth hepatomas [26,27] and AS-30D and HeLa cells (Table 1), which may induce DHAP accumulation (Table 3). An alternative route for triacylglycerol synthesis has been described that does not require α-glycerophosphate. This pathway starts with the acylation of DHAP, in a reaction catalyzed by DHAP acyltransferase, which is present in rat liver, kidney, spleen and adipose tissue; at the subcellular level, this enzyme is localized in the mitochondrial and microsomal fractions [51]. Such a route might be operating in tumor cells.

Biochemical mechanisms underlying the evaluated distribution of flux control

It should be emphasized that the analysis of V_{max} values only (i.e. cellular content of active enzyme) to reach conclusions on the metabolic pathway control is certainly incomplete, as the enzymatic activities are determined in the absence of their physiological activators and inhibitors, at saturating substrate concentrations, and in the absence of products; these factors discard the role of the reversibility of reactions under physiological conditions on control of flux [52].

Accumulation of products may decrease the forward reaction. In this regard, it is well documented that Glc6*P* is a potent inhibitor of hexokinase-I, hexokinase-II and hexokinase-III [37]. In consequence, the increased hexokinase activity might be counterbalanced by stronger Glc6*P* inhibition. One way to circumvent this blockade is to over-express hexokinase-III, an isoenzyme with a higher K_i for Glc6*P* (0.1 mM). Alternatively, hexokinase binding to mitochondria may protect it against Glc6*P* inhibition [7,53]. However, the Glc6*P* inhibition was strong and similar for both mitochondrial and cytosolic hexokinase isoenzymes (Figure 2A), when the activity was assayed under near-physiological conditions of pH (7.0) and temperature (37 °C) and high concentrations of glucose (> 1 mM) and Glc6*P* (≥ 1 mM). On the other hand, Nakashima *et al.* [7] and Bustamante *et al.* [53] determined Glc6*P* inhibition of mitochondrial hexokinase at 22–30 °C, pH 7.9, and in a hypotonic medium with nonphysiological concentrations of glucose (< 1 mM) and Glc6*P* (< 1 mM). The presence of this Glc6*P* regulatory mechanism in tumoral hexokinase supports an essential role for this enzyme in the control of flux.

Four hexokinase isoenzymes have been identified in mammalian cells: Type-I, II, III and IV (glucokinase), from which the first three are Glc6*P*-sensitive [37]. Hexokinase-I and hexokinase-II may bind to the outer mitochondrial membrane, as they have a specific hydrophobic N-terminal segment [54]. Hexokinase-I is predominantly located in brain, kidney, retina and breast, whereas hexokinase-II is abundant in skeletal muscle and adipose tissue [8]. In tumor cells, hexokinase-II is apparently the main over-expressed isoenzyme [7,8,37], except for brain tumors, in which hexokinase-I is over-expressed [8].

Analysis of the hexokinase kinetic properties and subcellular redistribution towards mitochondria suggested that the isoenzyme over-expressed in AS-30D cells was type II, as previously suggested using a similar analysis [7]. The amount of mitochondrial hexokinase in AS-30D (50%) and HeLa cells (70%; data not shown) was also similar to that observed for Novikoff and AS-30D ascites tumor cells of 50–80% [55,56]. This observation explains, at least in part, the enhanced glycolytic flux (Table 2, [8]) and the resistance to apoptosis [11] in these tumor cells.

The kinetic analysis of PFK-1 revealed that the isoenzyme present in AS-30D cells was completely insensitive to the usual allosteric inhibitors, ATP and citrate, in the presence of a low, physiological concentration of Fru(2,6)P_2, and that it was highly sensitive to the activators NH_4^+, AMP and Fru(2,6)P_2. The high, physiological concentration of AMP in AS-30D did not suffice to potently activate PFK-1 in the presence of ATP and citrate. The expression of a PFK-2 isoenzyme with a low fructose-2,6-bisphosphatase activity in several human tumor lines has been described [57,58], which ensures a high concentration of Fru(2,6)P_2. Indeed, Fru(2,6)P_2 was the most potent activator of PFK-1 and blocked the inhibition by ATP and citrate (Fig. 2B and Table 6, and also [12]).

Therefore, its kinetic properties predict that PFK-1 activity cannot impose a flux limitation on glycolysis in AS-30D cells. Under near-physiological conditions, the estimated elasticity coefficient of PFK-1 for Fru6*P* was high ($\varepsilon^{\text{PFK-1}}_{\text{Fru6}P} = 1.2$), which provides the bio-

chemical mechanism for its low flux control coefficient (Table 5). The PFK-1 elasticity and kinetic properties also provide a biochemical basis for understanding the diminished Pasteur effect observed in AS-30D [49] and other tumor cell types [39].

Experimental procedures

Chemicals

Hexokinase, G6PDH, hexosephosphate isomerase, aldolase, α-glycerophosphate dehydrogenase, triosephosphate isomerase, glyceraldehyde-3-phosphate dehydrogenase, pyruvate kinase and LDH were purchased from Roche Co. (Mannheim, Germany). Recombinant enzymes enolase, pyruvate phosphate dikinase and phosphoglycerate kinase from *Entamoeba histolytica* were kindly provided by E Saavedra, Instituto Nacional de Cardiología, México. Glucose, Glc6*P*, Fru(1,6)P_2, glyceraldehyde 3-phosphate, 2-phosphoglycerate, phosphoenolpyruvate, Fru(2,6)P_2, pyruvate, citrate, ATP, AMP, ADP, GTP, dithiothreitol, cysteine, NADH, NAD^+, NADP and oxalate were from Sigma Chemical (St Louis, MO, USA). Fru6*P* and 3-phosphoglycerate were from Roche (Indianapolis, IN, USA). Methoxy[^{3}H]inulin was from Perkin–Elmer Life Sci (Boston, MA, USA). All other reagents were of analytical grade from commercial sources.

Isolation of tumor and liver cells

AS-30D hepatoma cells [(2–4) × 10^8 cells·mL^{-1}) were propagated in female Wistar rats (200 g) by intraperitoneal transplantation. Hepatoma cells were isolated as described elsewhere [59].

HeLa cells (1.5×10^4 cells·mL^{-1}) were grown in Dulbecco's minimal essential medium (Gibco Life Technologies, Rockville, MD, USA), supplemented with 10% fetal bovine serum (Gibco), 10 000 U·mL^{-1} streptomycin/penicillin, and fungizone (amphotericin B; Gibco) in 175-cm^2 flasks (Corning, New York, NY, USA) at 37 °C in 5% CO_2/95%O_2. Hepatocytes were isolated by perfusion of isolated liver with collagenase IV (Worthington, Lakewood, NJ, USA) from fed Wistar rats [60]. The cellular viability assayed by trypan blue exclusion was 80–85%. Experimental manipulation of human and rodent cells and animal specimens were carried out following the Instituto Nacional de Cardiología de Mexico guidelines in accordance with the Declaration of Helsinki and the US NIH guidelines for care and use of experimental animals.

Determination of steady-state concentrations of metabolites

Cells (15 mg protein·mL^{-1}) were incubated in Krebs-Ringer medium with orbital shaking (150 r.p.m.) at 37 °C in a plastic flask. After 10 min, 5 mM glucose was added to the cell suspension. The reaction was stopped 3 min later with ice-cold perchloric acid (3%, v/v, final concentration). For the determination of the intracellular L-lactate, an aliquot (1 mL) of the cell suspension was rapidly withdrawn and centrifuged at 20 800 ***g*** for 10–15 s at room temperature. The supernatant was discarded, and the pellet rinsed with fresh Krebs–Ringer medium and then resuspended in 3% perchloric acid. The samples were neutralized with 3 M KOH/0.1 M Tris. The concentrations of Glc6*P*, Fru6*P*, Fru(1,6)P_2, DHAP, glyceraldehyde 3-phosphate, phosphoenolpyruvate, pyruvate, ATP, ADP, AMP, citrate and L- lactate were determined by standard enzymatic assays [61].

Protein was determined by the biuret method using BSA as standard [62].

Determination of intracellular glucose

AS-30D cells (15 mg·mL^{-1}) were preincubated for 10 min in the absence of exogenous substrates at 37 °C. Exogenous glucose was added after 10 min, and the cells were incubated for 3 min more. Afterwards, an aliquot (0.5 mL) was carefully poured into microcentrifuge tubes containing, from bottom to top, 30% (v/v) perchloric acid (0.3 mL), 1-bromododecane (0.3 mL) and fresh Krebs–Ringer medium (0.3 mL). The sample was centrifuged for 2–3 min in a refrigerated Microfuge (Eppendorf centrifuge 5804 R, Eppendorf, Hamburg, Germany) at 20 800 ***g***. The bottom layer was collected and neutralized with 10% NaOH. Glucose was determined by enzymatic analysis [61].

To correct for the presence of exogenous glucose from the incubation medium in the cellular pellet, the content of external water was evaluated by using methoxy[^{3}H]inulin. An aliquot of cells (5–30 mg protein·mL^{-1}) was incubated in 0.5 mL Krebs–Ringer medium with [^{3}H]inulin (0.15 mg·mL^{-1}, specific radioactivity 5200 c.p.m.·μg^{-1}) for 15 s. Thereafter, the cell suspension was carefully layered into microcentrifuge tubes prepared as described above. The radioactivity of the bottom layer was measured in a liquid scintillation analyzer (Packard Instruments/Canberra, Meriden, CT, USA). The concentration of glucose carried from the extracellular milieu was 1.28 mM. This value was subtracted from the original intracellular concentration.

Determination of glycolytic flux in liver and tumor cells

Cells (15 mg protein·mL^{-1}) were incubated in 3 mL Krebs–Ringer medium with orbital stirring (150 r.p.m.) at 37 °C in a plastic flask. After 10 min, 5 mM glucose was added to the cells; the reaction was stopped with cold 3% perchloric acid 0 and 3 min later. The samples were neutralized with 3 M KOH/0.1 M Tris. L-Lactate generated was determined by enzymatic analysis [61].

Cell extracts of tumor and liver cells

Cells (65 mg protein·mL^{-1}) were resuspended in 25 mM Tris/HCl buffer, pH 7.6, with 1 mM EDTA, 5 mM dithiothreitol and 1 mM phenylmethanesulfonyl fluoride. The cell suspension was frozen in liquid nitrogen and thawed in a water bath at 37 °C; this procedure was repeated three times. Cell lysates were centrifuged at 39 000 ***g*** for 20 min and 4 °C. Afterwards, the supernatant was collected for determination of enzyme activity. Activities of hexokinase, hexosephosphate isomerase, PFK-1, triosephosphate isomerase, aldolase, glyceraldehyde-3-phosphate dehydrogenase, phosphoglycerate kinase, phosphoglycerate mutase, enolase, pyruvate kinase, LDH, α-glycerophosphate dehydrogenase, phosphoglucomutase and G6PDH were determined spectrophotometrically by standard assays [63,64]. The incubation buffer was 50 mM Mops, pH 7, at 37 °C. Phosphoglycerate kinase activity was determined in 50 mM potassium phosphate, pH 7, at 37 °C. To assay mitochondrial hexokinase, isolated mitochondria were prepared as described elsewhere [59]. The assays for both cytosolic and mitochondrial hexokinase isoenzymes were carried out at 37 °C in 1 mL KME buffer (100 mM KCl, 50 mM Mops, 0.5 mM EGTA, pH 7.0) plus 2 U G6PDH, 1 mM $NADP^+$, 5 mM $MgCl_2$, glucose (from 0.05 to 10 mM) and 1 μM oligomycin. The reaction was started by the addition of ATP (0.05–5 mM) after 2 min incubation.

Assay for hexokinase inhibition by Glc6*P* was carried out in 3 mL of KME buffer at 37 °C, in the presence of 3 mM ATP, 5 mM $MgCl_2$, 1 μM oligomycin and 0.2–1 mM Glc6*P*. Owing to the high unspecific oxidation of added NADH by the cytosolic-enriched and mitochondrial fractions (despite the addition of rotenone), the activity was calculated from the ADP generated, which was determined by a standard assay [61]. The hexokinase activity was corrected for the ADP formed in the absence of added glucose. Bound and free isoenzymes were preincubated for 2 min, and then the hexokinase reaction was started by adding 3 mM glucose. After 30 s, the reaction was stopped with ice-cold perchloric acid (3%, v/v, final concentration). The samples were neutralized with 3 M KOH/0.1 M Tris. The control activities for both hexokinase isoenzymes were comparable to those determined by the G6PDH coupling assay.

For PFK-1 activity, freshly prepared extracts were incubated at 37 °C in 50 mM Mops, pH 7. The reaction assay contained 0.15 mM NADH, 5 mM $MgCl_2$, 1 mM EDTA, Fru6*P* (from 0.01 to 10 mM) and ammonium sulfate suspensions of the following coupling enzymes: 0.36 U aldolase, 9 U triosephosphate isomerase, and 3.1 U α- glyceraldehyde-3-phosphate dehydrogenase. The reaction was started by the addition of exogenous ATP (from 0.01 to 2 mM). For the determination of $K_{0.5}$ for NH_4^+, AMP and Fru(2,6)P_2, as well as for the effect of activators and inhibitors, lyophilized (ammonium-free) coupling enzymes were used in KME buffer.

Determination of flux control coefficients

The flux control coefficients (C^J_{Ei}) were determined by using the elasticity-based analysis [31,34,45,65,]. This approach quantifies the sensitivity of a given enzyme or block of enzymes to variations in its substrate or product when the steady-state flux is modified. Glycolysis was stimulated by exogenous glucose (4–6 mM) or inhibited by oxalate (0.5–2 mM), 2-deoxyglucose (0.5–10 mM) or arsenite (5–100 μM). Under these conditions, the variation in the glycolytic flux and in several intermediates was determined. Flux control coefficients were estimated using the connectivity (Eqn 1) and summation theorems (Eqn 2) [24],

$$C^J_{E1}\varepsilon^{E1}_m + C^J_{E2}\varepsilon^{E2}_m = 0 \quad (1)$$

$$C^J_{E1} + C^J_{E2} = 1 \quad (2)$$

in which J is the glycolytic flux (rate of lactate formation), E1 is the enzyme block that produces the intermediate (m) and E2 is the enzyme block that consumes m.

Acknowledgements

This work was partially supported by grant no. 43811-Q from CONACyT-México.

References

1 Warburg O (1956) On respiratory impairment in cancer cells. *Science* **124**, 269–270.
2 Zu XL & Guppy M (2004) Cancer metabolism: facts, fantasy, and fiction. *Biochem Biophys Res Commun* **313**, 459–465.
3 Dang C & Semenza GL (1999) Oncogenic alterations of metabolism. *Trends Biochem Sci* **24**, 68–72.
4 Lu H, Forbes RA & Verma A (2002) Hypoxia-inducible factor 1 activation by aerobic glycolysis implicates the Warburg effect in carcinogenesis. *J Biol Chem* **277**, 23111–23115.
5 Osthus RC, Shim H, Kim S, Li Q, Reddy R, Mukherjee M, Xu Y, Wonsey D, Lee LA & Dang C (2000) Deregulation of glucose transporter 1 and glycolytic gene expression by c-Myc. *J Biol Chem* **275**, 21797–21800.
6 Gillies RJ, Martinez-Zaguillan R, Martinez GM, Serrano R & Perona R (1990) Tumorigenic 3T3 cells maintain an alkaline intracellular pH under physiological conditions. *Proc Natl Acad Sci USA* **87**, 7414–7418.
7 Nakashima R, Paggi M, Scott LJ & Pedersen PL (1988) Purification and characterization of a bindable form of mitochondrial bound hexokinase from the highly glycolytic AS-30D rat hepatoma cell line. *Cancer Res* **48**, 913–919.
8 Pedersen PL, Mathupala S, Rempel A, Geschwind JF & Hee Ko Y (2002) Mitochondrial bound type II

hexokinase: a key player in the growth and survival of many cancers and an ideal prospect for therapeutic intervention. *Biochim Biophys Acta* **1555**, 14–20.
9 Goel A, Mathupala SP & Pedersen PL (2003) Glucose metabolism in cancer. Evidence that demethylation events play a role in activating type II hexokinase gene expression. *J Biol Chem* **278**, 15333–15340.
10 Mathupala SP, Heese C & Pedersen PL (1997) Glucose catabolism in cancer cells. The type II hexokinase promoter contains functionally active response elements for the tumor suppressor p53. *J Biol Chem* **272**, 22776–22780.
11 Pastorino JG, Shulga N & Hoek JB (2002) Mitochondrial binding of hexokinase II inhibits Bax-induced cytochrome *c* release and apoptosis. *J Biol Chem* **277**, 7610–7618.
12 Depré C, Rider MH & Hue L (1998) Mechanisms of control of heart glycolysis. *Eur J Biochem* **258**, 277–290.
13 Staal GEJ, Kalff A, Heesbeen EC, Van Veelen CWM & Rijksen G (1987) Subunit composition, regulatory properties, and phosphorylation of phosphofructokinase, from human gliomas. *Cancer Res* **47**, 5047–5051.
14 Meldolesi MF, Macchia V & Lacceti P (1976) Differences in phosphofructokinase regulation in normal and tumor rat thyroid cells. *J Biol Chem* **251**, 6244–6251.
15 Oskam R, Rijksen G, Staal GEJ & Vora S (1985) Isozymic composition and regulatory properties of phosphofructokinase from well-differentiated and anaplastic medullary thyroid carcinomas of the rat. *Cancer Res* **45**, 135–142.
16 Vora S, Halper JP & Knowles DM (1985) Alterations in the activity and isozymic profile of human phosphofructokinase during malignant transformation *in vivo and in vitro*: transformation-and progression-linked discriminants of malignancy. *Cancer Res* **45**, 2993–3001.
17 Sánchez-Martínez C & Aragón JJ (1997) Analysis of phosphofructokinase subunits and isozymes in ascites tumor cells and its original tissue, murine mammary gland. *FEBS Lett* **409**, 86–90.
18 Denis C, Paris H & Murat JC (1986) Hormonal control of fructose-2,6-bisphosphate concentration in the HT29 human colon adenocarcinoma cell line. *Biochem J* **239**, 531–536.
19 Mojeda M, Bosca L & Hue L (1985) Effect of glutamine on fructose-2,6-biphosphate and on glucose metabolism in HeLa cells and in chick-embryo fibroblasts. *Biochem J* **232**, 521–527.
20 Loiseau AM, Rousseau GG & Hue L (1985) Fructose-2,6-bisphosphate and the control of glycolysis by glucocorticoids and by other agents in rat hepatoma cells. *Cancer Res* **45**, 4263–4269.
21 Nissler K, Petermann H, Wenz I & Brox D (1995) Fructose-2,6-bisphosphate metabolism in Ehrlich ascites tumour cells. *J Cancer Res Clin Oncol* **121**, 739–745.
22 Rapoport T, Heinrich R, Jacobasch G & Rapoport S (1974) A linear steady-state treatment of enzymatic chains. A mathematical model of glycolysis of human erytrocytes. *Eur J Biochem* **42**, 107–120.
23 Kashiwaya Y, Sato K, Tsuchiya N, Thomas S, Fell DA, Veech RL & Passonneau JV (1994) Control of glucose utilization in working perfused rat heart. *J Biol Chem* **269**, 25502–25514.
24 Fell D (1997) *Understanding the Control of Metabolism*. Plenum Press, London.
25 Wu R (1959) Regulatory mechanisms in carbohydrate metabolism. V. Limiting factors of glycolysis in HeLa cells. *J Biol Chem* **234**, 2806–2810.
26 Harding JW, Pyeritz EA, Morris HP & White HB (1975) Proportional activities of glycerol kinase and glycerol 3-phosphate dehydrogenase in rat hepatomas. *Biochem J* **148**, 545–550.
27 Pedersen PL (1978) Tumor mitochondria and the bioenergetics of cancer cells. *Prog Exp Tumor Res* **22**, 190–274.
28 Traut TW (1994) Physiological concentrations of purines and pyrimidines. *Mol Cell Biochem* **140**, 1–22.
29 Moreno-Sánchez R & Torres-Márquez ME (1991) Control of oxidative phosphorylation in mitochondria, cells and tissues. *Int J Biochem* **23**, 1163–1174.
30 Groen AK, Wanders RJ, Westerhoff HV, van der Meer R & Tager JM (1982) Quantification of the contribution of various steps to the control of mitochondrial respiration. *J Biol Chem* **257**, 2754–2757.
31 Kacser H (1983) The control of enzyme systems *in vivo*: elasticity analysis of the steady state. *Biochem Soc Trans* **11**, 35–40.
32 Moreno-Sánchez R, Bravo C & Westerhoff HV (1999) Determining and understanding the control of flux. An illustration in submitochondrial particles of how to validate schemes or metabolic control. *Eur J Biochem* **264**, 427–433.
33 Groen AK, van Roermund CW, Vervoom RC & Tager JM (1986) Control of gluconeogenesis in rat liver cells. Flux control coefficients of the enzymes in the gluconeogenic pathway in the absence and presence of glucagon. *Biochem J* **237**, 379–389.
34 Hafner RP, Brown GC & Brand MD (1990) Analysis of the control of respiration rate, phosphorylation rate, proton leak rate and protonmotive force in isolated mitochondria using the 'top-down' approach of metabolic control theory. *Eur J Biochem* **188**, 313–319.
35 Thomas S, Mooney PJ, Burrell MM & Fell DA (1997) Metabolic control analysis of glycolysis in tuber tissue of potato (*Solanum tuberosum*): explanation for the low control coefficient of phosphofructokinase over respiratory flux. *Biochem J* **322**, 119–127.
36 Ainscow EK & Brand MD (1999) Top-down control analysis of ATP turnover, glycolysis and oxidative phosphorylation in rat hepatocytes. *Eur J Biochem* **263**, 671–685.
37 Wilson JE (2003) Isozymes of mammalian hexokinase: structure, subcellular localization and metabolic function. *J Exp Biol* **206**, 2049–2057.

38 Jannaschk KD, Burgos M, Centerlles JJ, Ovadi J & Cascante M (1999) Application of metabolic control analysis to the study of toxic effects of copper in muscle glycolysis. *FEBS Lett* **445**, 144–148.
39 Eigenbrodt E, Fister P & Reinacher M (1985) New perspectives in carbohydrate metabolism in tumor cells. In. *Regulation of Carbohydrate Metabolism* (Reitner, R, ed.), vol. 2, pp 141–179. CRC Press, Boca Raton, FL.
40 Rodríguez-Enríquez S & Moreno-Sánchez R (1998) Intermediary metabolism of fast-growth tumor cells. *Arch Med Res* **29**, 1–12.
41 Mazuret S, Eigenbrodt E, Failing K & Steinberg P (1999) Alterations in the glycolytic and glutaminolytic pathways after malignant transformation of rat liver oval cells. *J Cell Physiol* **181**, 136–146.
42 Mazuret S, Michel A & Eigenbrod E (1997) Effect of extracellular AMP on cell proliferation and metabolism of breast cancer cell lines with high and low glycolytic rates. *J Biol Chem* **272**, 4941–4952.
43 Shuster S, Kahn D & Westerhoff HV (1993) Modular analysis of control of complex metabolic pathways. *Biophys Chem* **48**, 1–17.
44 Ainscow EK & Brand MD (1998) Control analysis of systems with reaction blocks that 'cross-talk'. *Biochim Biophys Acta* **1366**, 284–290.
45 Brown GC, Lakin-Tomas L & Brand MD (1990) Control of respiration and oxidative phosphorylation in isolated rat liver cells. *Eur J Biochem* **192**, 355–362.
46 Kitagawa T, Tsuruhara Y, Hayashi M, Endo T & Stanbridge EJ (1995) A tumor-associated glycosylation change in the glucose transporter GLUT1 controlled by tumor suppressor function in human cell hybrids. *J Cell Sci* **108**, 3735–3743.
47 Macheda ML, Rogers S & Best JD (2005) Molecular and cellular regulation of glucose transporter (GLUT) proteins in cancer. *J Cell Physiol* **202**, 654–662.
48 Colville C, Seatter MJ, Jess TJ, Gould GW & Thomas HM (1993) Kinetic analysis of the liver-type (GLUT2) and brain-type (GLUT3) glucose transporters in *Xenopus oocytes*: substrate specificities and effects of transport inhibitors. *Biochem J* **290**, 701–706.
49 Rodríguez-Enríquez S, Juárez O, Rodríguez-Zavala JS & Moreno-Sánchez R (2001) Multisite control of the Crabtree effect in ascites hepatoma cells. *Eur J Biochem* **268**, 2512–2519.
50 Houstek J, Cannon B & Lindberg O (1975) Glycerol-3-phosphate shuttle and its funtion in intermediary metabolism of hamster brow-adipose tissue. *Eur J Biochem* **54**, 11–18.
51 Hajra AK (1997) Dihydroxyacetone phosphate acyltransferase. *Biochim Biophys Acta* **1348**, 27–34.
52 Mendoza-Cozatl DG & Moreno-Sanchez R (2006) Control of glutathione and phytochelatin synthesis under cadmium stress. Pathway modeling for plants. *J Theor Biol* **238**, 919–936.
53 Bustamante E & Pedersen PL (1977) High aerobic glycolysis of rat hepatoma cells in culture: role of mitochondrial hexokinase. *Proc Natl Acad Sci USA* **74**, 3735–3739.
54 Smith TAD (2000) Mammalian hexokinases and their abnormal expression in cancer. *Br J Biomed Sci* **57**, 170–178.
55 Arora KK & Pedersen PL (1988) Functional significance of mitochondrial bound hexokinase in tumor cell metabolism. *J Biol Chem* **263**, 17422–17428.
56 Parry DM & Pedersen PL (1983) Intracellular localization and properties of particulate hexokinase in the Novikoff ascites tumor. *J Biol Chem* **258**, 10904–10912.
57 Atsumi T, Chesney J, Metz C, Leng L, Donnelly S, Makita Z, Mitchell R & Bucala R (2002) High expression of inducible 6-phosphofructo-2-kinase/fructose-2,6-bisphosphatase (iPFK-2; PFKFB3) in human cancers. *Cancer Res* **62**, 5881–5887.
58 Chesney J, Mitchell R, Benigni F, Bacher M, Spiegel L, Al-Abed Y, Han JH, Metz C & Bucala R (1999) An inducible gene product for 6-phosphofructo-2-kinase with an AU-rich instability element: role in tumor cell glycolysis and the Warburg effect. *Proc Natl Acad Sci USA* **96**, 3047–3052.
59 López-Gómez F & Torres-Márquez & Moreno-Sánchez R (1993) Control of oxidative phosphorylation in AS-30D hepatoma mitochondria. *Int J Biochem* **25**, 373–377.
60 Berry MN & Friend DS (1969) High-yield preparation of isolated rat liver parenchymal cells. A biochemical and fine structural study. *J Cell Biol* **43**, 506–520.
61 Bergmeyer HU (ed.) (1974) *Methods of Enzymatic Analysis*. Verlag Chemie, Weinheim.
62 Gornall AG, Bardwill CJ & David MM (1949) Determination of serum proteins by means of biuret reaction. *J Biol Chem* **177**, 751–766.
63 Bergmeyer HU (ed.) (1983) *Methods of Enzymatic Analysis*. Verlag Chemie, Weinheim.
64 Saavedra E, Encalada R, Pineda E, Jasso-Chávez R & Moreno-Sánchez R (2005) Glycolysis in *Entamoeba histolytica*. Biochemical characterization of recombinant glycolytic enzymes and flux control analysis. *FEBS J* **272**, 1767–1783.
65 Tager JM, Wanders JA, Groen AK, Kunz W, Bohnensack R, Küster U, Letko G, Böhme G, Duszynski J & Wojtczak L (1983) Control of mitochondrial respiration. *FEBS Lett* **151**, 1–9.
66 Simpson RJ, Brindle KM, Brown FF, Campbell ID & Foxall DL (1982) Studies of lactate dehydrogenase in the purified state and in intact erythrocytes. *Biochem J* **202**, 581–587.
67 Meunier JC & Dalziel K (1978) Kinetics studies of glyceraldehyde-3-phosphate dehydrogenase from rabbit muscle. *Eur J Biochem* **82**, 483–492.